SCUOLA DI DOTTORATO

UNIVERSITÀ DEGLI STUDI DI MILANO-BICOCCA

Dipartimento di / Department of

SCUOLA DI MEDICINA E CHIRURGIA/SCHOOL OF MEDICINE AND SURGERY

Dottorato di Ricerca in / PhD program NEUROSCIENZE/NEUROSCIENCE Ciclo / Cycle XXXI

Curriculum in (se presente / if it is) NEUROSCIENCE SPERIMENTALI/EXPERIMENTAL NEUROSCIENCE

NERVE EXCITABILITY TESTING IN ANIMAL MODELS OF OXALIPLATIN INDUCED PERIPHERAL NEUROTOXICITY: *ION CHANNEL DYSFUNCTION AS A POSSIBLE PATHOGENETIC MECHANISM.*

Cognome / Surname ALBERTI Nome / Name PAOLA

Matricola / Registration number 064514

Tutore / Tutor: PROF. GUIDO ANGELO CAVALETTI, MD

Coordinatore / Coordinator: PROF. GUIDO ANGELO CAVALETTI, MD

ANNO ACCADEMICO / ACADEMIC YEAR 2017/2018

UNIVERSITY OF MILANO-BICOCCA

SCHOOL OF MEDICINE AND SURGERY

PhD PROGRAM IN NEUROSCIENCE

NERVE EXCITABILITY TESTING IN ANIMAL MODELS OF OXALIPLATIN INDUCED PERIPHERAL NEUROTOXICITY:

ION CHANNEL DYSFUNCTION AS A POSSIBLE PATHOGENETIC MECHANISM.

Mentor: Professor Guido Cavaletti, MD

Mentee:

Paola Alberti, MD

ID. 064514

PhD Cycle: XXXI

Academic Year 2017/2018

"In art, as in science, reductionism does not trivialize our perception - of color, light, and perspective - but allows us to see each of these components in a new way."

Eric R. Kandel (1929-)

1 INTRODUCTION 7
1.1 OXALIPLATIN INDUCED PERIPHERAL NEUROTOXICITY (OIPN) 7
1.1.1 OXALIPLATIN AND ITS CLINICAL INDICATION 7
1.1.2 CHEMOTHERAPY INDUCED PERIPHERAL NEUROTOXICITY (CIPN) 8
1.1.3 OXALIPLATIN INDUCED PERIPHERAL NEUROTOXICITY (OIPN): FROM BED-SIDE TO BENCH-SIDE AND VICEVERSA 9
1.2 ANIMAL MODELS TO UNRAVEL OIPN ISSUES 11
1.2.1 STANDARD NEUROPHYSIOLOGY: NERVE CONDUCTION STUDIES AND ELECTROMYOGRAPHY 12
1.2.2 ADVANCED NEUROPHYSIOLOGY: NERVE EXCITABILITY TESTING 13
1.3 TOPIRAMATE: PROOF-OF-CONCEPT FOR OIPN PREVENTION 24
2 AIMS 25
3 OUTLINE OF THE PROJECT 26
4 MATERIALS AND METHODS 27
4.1 ANIMALS AND HOUSING 27
4.2 DRUG ADMINISTRATION 27
4.3 STANDARD NEUROPHYSIOLOGY: NERVE CONDUCTION STUDIES AND EMG TESTING AT REST 27
4.4 ADVANCED NEUROPHYSIOLOGY: NET 31
4.5 BEHAVIORAL TESTS 34
4.6 NEUROPATHOLOGY 34
4.7 STATISTICAL ANALYSIS 35
5 STUDY DESIGN 36
5.1 TASK 1 - PROOF OF CONCEPT: EMG AT REST AS AN *IN VIVO* INDIRECT EVIDENCE OF AXONAL HYPER-EXCITABILITY 36
5.1.1 Groups and treatment plan 36
5.1.2 Time points and variables collected 36
5.2 TASK 2 - ACUTE SETTING: NET RECORDINGS IN RATS AFTER A SINGLE OHP ADMINISTRATION 37
5.2.1 Groups and treatment plan 37
5.2.2 Time points and variables collected 37
5.3 TASK 3 - CHRONIC SETTING: NET RECORDINGS IN RATS IN THE CONTEXT OF CHRONIC OHP ADMINISTRATION 38
5.3.1 Groups and treatment plan 38
5.3.2 Time points and variables collected 38
5.4 TASK 4 - REFINEMENT OF THE CHRONIC SETTING – A DOSE FINDING STUDY IN OHP TREATED RATS 39
5.4.1 Groups and treatment plan 39
5.4.2 Time points and variables collected 39
5.5 TASK 5 - TOPIRAMATE (TPM) AS A NEUROPROTECTANT AGENT AGAINST ACUTE OIPN IN RATS 40
5.5.1 Groups and treatment plan 40
5.5.2 Time points and variables collected 40
5.7 TASK 6 - TOPIRAMATE (TPM) AS A NEUROPROTECTANT AGENT AGAINST CHRONIC OIPN IN RATS 41

5.7.1 Groups and treatment plan 41
5.7.2 Time points and variables collected 41
6 RESULTS 42
6.1 TASK 1 - PROOF OF CONCEPT: EMG AT REST AS AN *IN VIVO* INDIRECT EVIDENCE OF AXONAL HYPER-EXCITABILITY 42
6.1.1 Baseline data 42
6.1.2 Data after single drug administration 44
6.1.3 Data at 7 days after administration 45
6.1.4 Summary of inferences from TASK 1 45
6.2 TASK 2 - ACUTE SETTING: NET RECORDINGS IN RATS AFTER A SINGLE OHP ADMINISTRATION 46
6.2.1 Baseline data 46
6.2.2 Data after single OHP administration 49
6.2.3 Summary of inferences from TASK 2 51
6.3 TASK 3 - CHRONIC SETTING: NET RECORDINGS IN RATS IN THE CONTEXT OF CHRONIC OHP ADMINISTRATION 52
6.3.1 Baseline data 52
6.3.2 Data after 1st administration 56
6.3.3 End of treatment data 58
6.3.4 Data at 1 week after treatment. 62
6.3.5 Data at 6 weeks after treatment 64
6.3.6 Summary of inferences from TASK 3 68
6.4 TASK 4 - REFINEMENT OF THE CHRONIC SETTING – A DOSE FINDING STUDY IN OHP TREATED RATS 69
6.4.1 Baseline data 69
6.4.2 Data after the 1st administration 72
6.4.3 End of treatment data 75
6.4.4 Summary of inferences from TASK 4 82
6.5 TASK 5 - TOPIRAMATE (TPM) AS A NEUROPROTECTANT AGENT AGAINST ACUTE OIPN IN RATS 83
6.5.1 Baseline data 83
6.5.2 Data at 24 hours 84
6.5.3 Data at 48 hours 88
6.5.4 Data at 72 hours 91
6.5.5 Summary of inferences from TASK 5 95
6.6 TASK 6 - TOPIRAMATE (TPM) AS A NEUROPROTECTANT AGENT AGAINST CHRONIC OIPN IN RATS 96
6.6.1 Baseline data 96
6.6.2 End of treatment data 99
6.6.3 Summary of inferences from TASK 6 108
7 DISCUSSION 109
7.1 DEVISING THE APPROPRIATE ANIMAL MODEL 109

7.2 PATHOPHYSIOLOGICAL CONSIDERATIONS THANKS TO NET 112
7.3 NEUROPROTECTION FINDINGS 114
8 FUTURE DEVELOPMENTS 123
9 BIBLIOGRAPHY 124
10 ACKNOWLEDGEMENTS 130

1 INTRODUCTION

1.1 OXALIPLATIN INDUCED PERIPHERAL NEUROTOXICITY (OIPN)

1.1.1 OXALIPLATIN AND ITS CLINICAL INDICATION

Oxaliplatin (OHP) is a third-generation platinum complex, i.e., a platinum compound with a 1,2-diaminocyclohexane (DACH) carrier ligand; it was first introduced in clinical practice in 1996 in France. Subsequently, in 1999, its use was extended in whole Europe and in 2002 in the USA: initially, it was indicated only for metastatic colorectal cancer (CRC) treatment; later it was also recommended to treat CRC in the adjuvant setting, in combination with 5-fluorouracil and leucovorin[1]. Nowadays, the major indication for OHP is CRC and it is administered in combination with 5-fluoruracil and folinic acid; it is also active against other gastro-enteric neoplasms, such as biliary tract and pancreatic tumor[2].

OHP was originally developed with the intent of overcoming major limitations of older platinum drugs, cisplatin and carboplatin. Despite the impressive antitumor activity of these two compounds against ovarian, bladder, head and neck, and lung cancers, there were, in fact, some relevant issues: they showed consistent side effects (nausea/vomiting, nephrotoxicity, ototoxicity and peripheral neuropathy for cisplatin and myelosuppression for carboplatin) and intrinsic resistance against some more common tumor types, such as colorectal and pancreatic cancers; moreover, they were not able to confer long-lasting remissions in responding tumor types, due to the emergence of acquired resistance, especially ovarian cancer[3]. Additionally, the analysis of dose intensification with either cisplatin or carboplatin suggested a plateau in their efficacy, but a marked increase in toxicity with a limited therapeutic index, thus making necessary to look for a new agent of the same class[4,5]. However, even though OHP it was develop to ameliorate cisplatin and carboplatin profile, it was efficacious in a completely different clinical setting; it gained the indication to treat CRC[6], a malignancy for which cisplatin displayed no activity, and was not efficacious to treat lung and ovarian cancers, the major indications of cisplatin and carboplatin. Moreover, differently from its predecessors, OHP maximum efficacy was obtained only in synergistic combination with fluoropyrimidines, 5-fluorouracil [7] and capecitabine[8]; low activity was instead obtained with OHP administration as a single drug[9].

Despite these differences, all platinum complexes share a common mechanism of action against cancer cells: they form intra-strand and inter-strand cross-links on DNA, being thus alkylating agents. The unique efficacy and toxicity OHP profile can be explained taking into account some distinguishing features compared to cis- and carboplatin: transport and metabolism; effect of DNA platination due to the larger OHP size; mechanisms involved in repair of DNA adducts and in sensing DNA damage through the DNA mismatch repair system; transduction of DNA damage signals such as activation of apoptosis or immunogenic cell death[10].

All platinum drugs are associated with peripheral neurotoxicity development, even though some are more neurotoxic than others: cisplatin has been reported to be neurotoxic in about 60% of patients, when receiving at least 225-500 mg/m^2; OHP have been associated with a rate up to 75% of neurosensory symptoms in patients treated with FOLFOX or XELOX regimen; carboplatin, instead, is significantly less neurotoxic than other two platinum compounds[11].

1.1.2 CHEMOTHERAPY INDUCED PERIPHERAL NEUROTOXICITY (CIPN)

Chemotherapy Induced Peripheral Neurotoxicity (CIPN) is not a clinical entity related only to platinum compound administration. In last decades, this "new" side effect has gained the attention of health care professional who are in charge of cancer patients: CIPN is, in fact, a toxicity second only to hematological ones[12]. It is not of short duration; it is one of the so-called "chronic or late toxicities", toxic effects persistent more than 12 months or presenting 12 months after the end of chemotherapy[12]. It is a rather common adverse event related to widely used anticancer drugs: platinum drugs, taxanes, vinca alkaloids, proteasome inhibitors, epothilones and thalidomide[11,13]. Growing awareness of CIPN has promoted its recognition and concerns about its duration, both in children[14-16] and in adults[17-20]. Nowadays, in fact, cancer patients have – thankfully - become a long surviving population, as a result of advances in diagnosis and treatment; worldwide, it has been estimated there are 28 million cancer survivors since cancer-related mortality, adjusted for age, dramatically decreased in pediatric and adult population in the 1950-2010 period[12].

CIPN persistence is a clinically relevant issue due to its negative impact on Quality of Life (QoL) in cancer survivors, as it is clear considering its clinical spectrum. CIPN is mainly a sensory, length-dependent neuropathy/neuronopathy; rarely, motor, autonomic impairment or cranial nerve involvement have been observed[21]. Different drugs are related to slightly different and rather specific neurological alterations, even respect to sensory alterations[11,13,22]. However, some features are quite constant among different compounds. Sensory alterations can be negative and/or positive. "Negative" signs/symptoms are impairment in touch, pin and vibration perception; in the case of the latter, if there is a consistent loss of large fiber modalities, the patient can develop a consistent disability, even though the motor function is preserved, due to sensory ataxia. This condition can cause imbalance and increased fall risk[23,24] as well as difficulty in manipulating small objects, the so called loss of "composite functions"[22]. "Positive" symptoms are mainly related to damage of small fibers, with development of paresthesia/dysesthesia and neuropathic pain. Alterations develop initially at limb extremities and then they have a distal-to-proximal progression, according to the pathophysiology of a length-dependent neuropathy. Initial manifestations and worsening is usually dose-dependent during chemotherapy administration[21]; however, all platinum drugs are related also to a peculiar temporal pattern in neurological deterioration: neuropathy can worsen for a few months after chemotherapy suspension, the so called "coasting phenomenon"[11].

CIPN relevance is also due to lack of an efficacious treatment once it ensues, as accurately pointed out in a meta-analysis published by American Society for Clinical Oncology (ASCO) in 2014[25]: only duloxetine has been recognized as moderately efficacious as a symptomatic option[25,26]. Despite the great effort that the scientific community is making to solve this issue, even in 2018 we are far from being able to adequately treat CIPN patients, as pointed out by Cavaletti and Marmiroli[27]: we have still an uncomplete knowledge on CIPN pathophysiology and there is a need to improve the translation of these warranted preclinical results into clinical setting.

1.1.3 OXALIPLATIN INDUCED PERIPHERAL NEUROTOXICITY (OIPN): FROM BED-SIDE TO BENCH-SIDE AND VICEVERSA

All considerations made so far are, of course, true also for Oxaliplatin Induced Peripheral Neurotoxicity (OIPN). However, in this case neurological toxicity is even more challenging: it is not only a common side effect but is one of the dose limiting-toxicities. OHP is cornerstone drug for CRC, one of the most common tumor types in both sexes, so OIPN is a constant and relevant issue in any Oncologist daily practice. OIPN pathogenesis is still unclear, even though many hypotheses have been generated at the "bench-side", which are common to all platinum-drugs: oxidative stress and mitochondrial damage, altered calcium-signaling, apoptosis[11,28]. An even more intriguing mechanism, specific only for OHP, could be sought for considering OIPN peculiar clinical profile: it is not only associated with the above mentioned chronic and cumulative peripheral nervous system damage (we will name it "chronic OIPN"), but it is also associated with an "acute" and transient toxicity, lasting mainly 24-72 hours after OHP i.v. administration (we will name it "acute OIPN"). Acute OIPN is reported by patients as cold-induced, transient, paresthesia/dysesthesia (located mainly at limb extremities, at pharynx/larynx, and at mouth/lips). Jaw-spasm and cramps/muscle spasms have also been described, even if more rarely[29]. All these phenomena were compared with other condition such as cold-induced acute neuromyotonia-like syndrome, whose hallmark are both motor and sensory nerve hyper-excitability. Neuromyotonia is known to be generated by impairment of voltage-gated ion channels[30]; the acute OIPN clinically resembles neuromyotonia and therefore it could be classified as a channelopathy, because of the interaction between OHP and ion channels located in the cellular membrane. There is growing evidence that OHP may mostly impair voltage-operated sodium channels rather than potassium channels, as demonstrated in *in vitro* studies [31,32] and clinical studies testing nerve excitability in patients treated with OHP[32-34]. Most interestingly, it has been suggested that chronic OIPN may be induced by the decreased cellular metabolism and axoplasmic transport resulting from the accumulation of OHP in dorsal root ganglia (DRG) cells; so, the prolonged activation of Na+ channels, due to acute OIPN, might be a predisposing factor to chronic OIPN, being an adjunctive mechanisms of neuronal damage compared to other platinum compounds, yet mentioned[35,36]. This is not surprising since abnormal kinetics of mutated sodium channels lead to various clinical syndromes, known as sodium channelopathies[37].

Voltage-gated sodium channels consists of a main alpha subunit and one/two beta-subunits; their main features are shown in **Figure 1**.

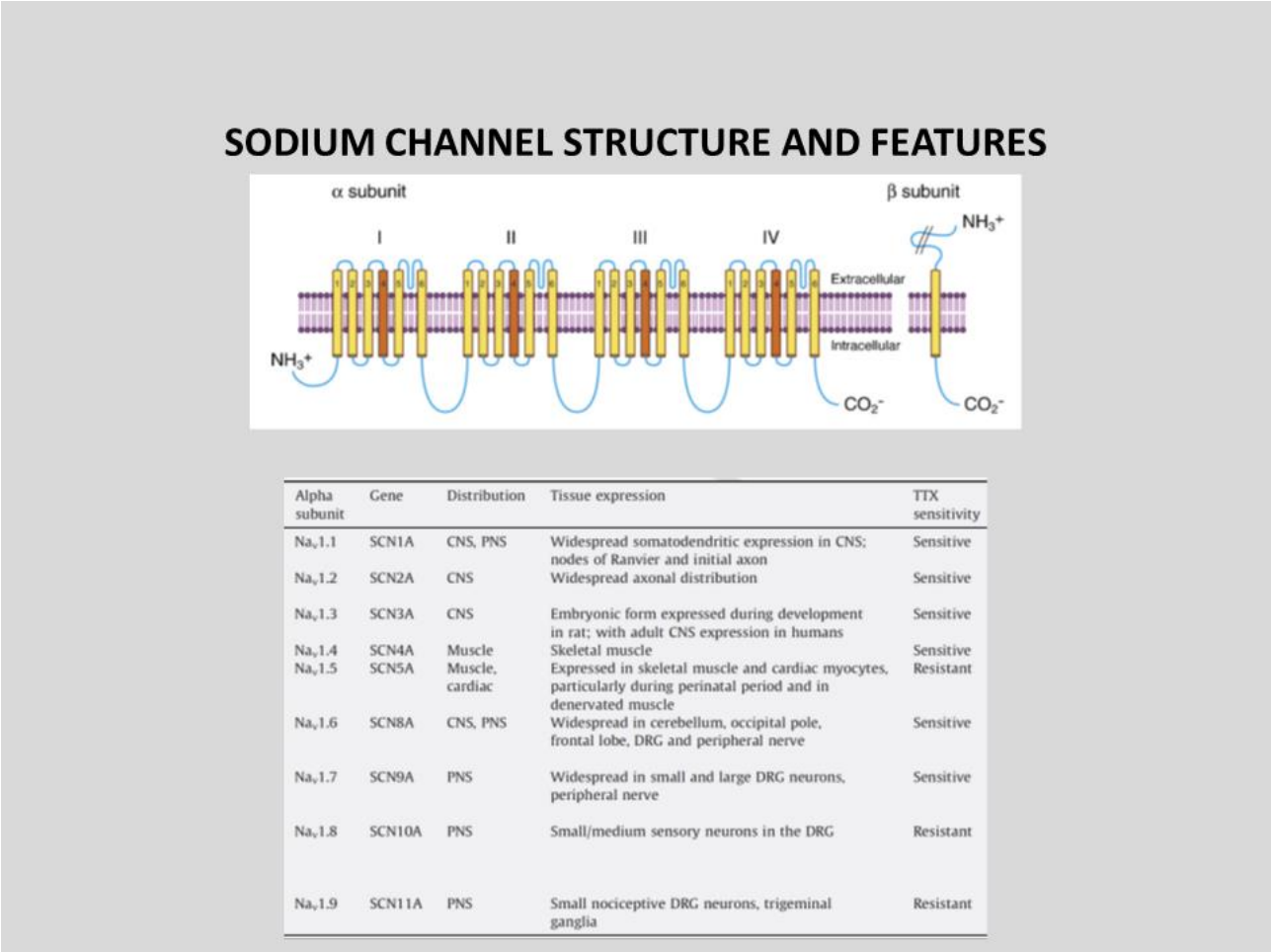

Alpha subunit	Gene	Distribution	Tissue expression	TTX sensitivity
$Na_v1.1$	SCN1A	CNS, PNS	Widespread somatodendritic expression in CNS; nodes of Ranvier and initial axon	Sensitive
$Na_v1.2$	SCN2A	CNS	Widespread axonal distribution	Sensitive
$Na_v1.3$	SCN3A	CNS	Embryonic form expressed during development in rat; with adult CNS expression in humans	Sensitive
$Na_v1.4$	SCN4A	Muscle	Skeletal muscle	Sensitive
$Na_v1.5$	SCN5A	Muscle, cardiac	Expressed in skeletal muscle and cardiac myocytes, particularly during perinatal period and in denervated muscle	Resistant
$Na_v1.6$	SCN8A	CNS, PNS	Widespread in cerebellum, occipital pole, frontal lobe, DRG and peripheral nerve	Sensitive
$Na_v1.7$	SCN9A	PNS	Widespread in small and large DRG neurons, peripheral nerve	Sensitive
$Na_v1.8$	SCN10A	PNS	Small/medium sensory neurons in the DRG	Resistant
$Na_v1.9$	SCN11A	PNS	Small nociceptive DRG neurons, trigeminal ganglia	Resistant

Figure 1. Voltage gated sodium channel features (modified from Krishnan et al. 2009[38]).

On the left the general structure of any Na+ channel is shown. On the right nomenclature, distribution and tissue expression are enlisted.

The alpha subunit is composed by 4 homologous domains (I-IV), divided into 6 membrane-spanning components (S1-S6); the beta subunit possesses a single membra-spanning domain. **In Figure 1** is summarized also the nomenclature and distribution of Na+ channels, based on alpha-subunit features.

Since it is known that missense mutations of the SCNA gene confer liability to cold-induced myotonia as well as also to seizures, due to sodium channel dysfunction and neuronal hyper-excitability[39,40], on the basis of some similarity in the clinical phenotype, polymorphisms in these genes might be suggested as predisposing to acute OIPN development. Consequently, if acute OIPN predisposes to chronic OIPN, these polymorphisms could also play a pivotal role in chronic OIPN development, to be further explored since acute and chronic OIPN pathogenesis have not yet been fully elucidated[12,13]. On the basis of these facts (and lacks) **a longitudinal, observational, non-interventional, international and multicenter trial** ("NON-INTERVENTIONAL INTERNATIONAL MULTICENTRE STUDY WHICH WOULD SOUGH TO DEFINE EARLY

PREDICTORS OF PERIPHERAL NEUROPATHY IN OXALIPLATIN-TREATED PATIENTS WITH COLORECTAL CANCER.")[41] was held in four centers distributed into three countries in Europe (Italy: Monza and Padua; Greece: Patras; Spain: Barcelona); our Center was the coordinating one for Italy. The study closed in 2011, and majority of data has been published. Main findings are reported here, since they were the starting point of the preclinical project here presented.

The whole study primary aim was to evaluate the best available method(s) and biomarker(s) to detect patients at high risk of developing OIPN. Among secondary aims the hypothesis that SCNA polymorphisms, conferring liability to Na+ dysfunction, confer also liability to OIPN was tested. Subjects were evaluated three times: before first OHP cycle, at mid-treatment, soon after chemotherapy termination. Blood samples were collected at base line as a source of reference DNA. Our cohort allowed us to gain many inferences about OIPN development and natural history. Acute OIPN was present in 146 of 170 patients (85.9%); cold-induced perioral (95.2%) or pharyngo-laryngeal (91.8%) dysesthesias were the main symptoms reported. The increased number of acute OIPN symptoms was correlated significantly with both the development and the degree of the chronic OIPN; so we hypothesized that patients who had a more complex combination of acute phenomena, related to axonal hyper-excitability, were those who eventually develop more severe OIPN[42]. The overdominant model (CT vs CC1TT) of the skeletal muscle SCN4A-rs2302237 (i.e. heterozygous subjects had a higher probability to develop OIPN) and the tetrodotoxin-resistant SCN10A-rs1263292 polymorphisms emerged as being significantly associated with an increased incidence of acute OIPN. The overdominant model of SCN4A-rs2302237 was also able to predict the severity of acute OIPN. A weaker association was found between the overdominant model of SCN4A-rs2302237 and the development of cumulative OIPN[43]. Thus, our clinical data supported the novel hypothesis of a possible involvement of Na+ channels in acute OIPN and the fact that acute OIPN, via Na+ channel dysfunction, might also predispose to chronic OIPN development.

These very promising evidences convinced us to pursue further in this direction: the possible relationship between acute and chronic OIPN was explored, for the first time, in a preclinical setting. The final goal was to ascertain if decreasing acute OIPN, chronic phenomena were decreased too, thus demonstrating a causative relationship between acute and chronic condition.

1.2 ANIMAL MODELS TO UNRAVEL OIPN ISSUES

Bench-side was the ideal setting to test the possible relationship between acute and chronic OIPN, since mechanistic hypothesis can be generated and tested; moreover, differently from "bed side", extensive neuropathological analyses are possible. In this project an *in vivo approach* was elected to maintain a condition as similar as possible to clinical setting: behavioral, neuropathological and neurophysiological observations can be obtained. In CIPN field, rodent models has been extensively devised and studied in the

last 20 years[44,45]. In our laboratory a huge expertise in these models have been obtained and OIPN animal model described by Cavaletti et al. was the basis for this project[46,47]. Neuropathologic analysis is possible after animal sacrifice allowing a morphological confirmation of the degree and kind of damage present in the tested animals; in clinical practice this is not possible since the use of nerve biopsy in CIPN patients is limited and not indicated. However, neurophysiology can be performed in animals as in clinical practice: this outcome measure is the link between bench and bed-side; morphological and pathogenetic preclinical observations can be related to the clinical data and QoL issues which are intended to be amended through CIPN cure.

1.2.1 STANDARD NEUROPHYSIOLOGY: NERVE CONDUCTION STUDIES AND ELECTROMYOGRAPHY

Nerve conduction studies (NCS) are considered one of the most objective measures of peripheral nerve function and considered one of the "gold standard" outcome measures for most Regulatory Authorities (FDA, EMA, …). Nerve conduction studies allow peripheral nerve testing, both for sensory and motor components. The *Sensory Nerve Action Potential* (SNAP) is a compound potential, given by the summation of all the individual sensory fiber action potentials. SNAPs can have a biphasic or triphasic morphology. These parameters are measured: onset latency, peak latency, duration, velocity and amplitude. SNAPs record mainly the largest cutaneous sensory fibers of tested nerves. In case of motor recordings, a Compound Muscle Action Potential (CMAP), is obtained by the summation of all underlying individual muscle fiber action potentials, activated stimulating the correspondent nerve. CMAP morphology is biphasic with an initial negativity, or upward deflection from the baseline. Latency, amplitude, duration, velocity and area of the CMAP are measured. Notably, CMAP amplitude depends on the number of depolarized muscle fibers. As OIPN is mainly a distal, sensory, length-dependent axonal polyneuropathy, distal SNAP amplitude is the key parameter to be monitored for early detection of its development[48]. CMAP recordings can be useful to detect rare motor involvement and to rule out other conditions in clinical practice.

In OHP administered patients, EMG recordings have also gained a specific use; in absence of a nerve involvement able to justify it, EMG at rest was demonstrated to be able to detect spontaneous activity, due to the hyper-excitability condition[49,50]. Muscles normally are quiet at rest, except for potentials recordable at the endplate zone. When the needle is quickly inserted or replaced through muscle, it is normal to perceive a brief burst of muscle fiber potentials, typically lasting no longer than 300 ms; "increased insertional activity" is defined as any activity other than endplate potentials that last longer than 300 ms after brief needle movement. Spontaneous activity is instead any activity seen at rest, lasting more than 3 seconds. There are different kinds of spontaneous activity findings that can be recognized by either pattern recognition or analysis of the waveform; for the purpose of this project classification of spontaneous activity alterations was performed according to what is stated in methods section; in fact, EMG at rest is also reproducible in animal models and can be suggested as a first, simple screening tool to verify absence/presence of axonal

hyperexecitability. But, something more refined is required to adequately study this condition as is discussed in the next section.

1.2.2 ADVANCED NEUROPHYSIOLOGY: NERVE EXCITABILITY TESTING

The complex phenomena OHP treated patients experience cannot be fully investigated with conventional neurophysiological techniques. Routine nerve conduction studies can be used to detect the presence of neuropathy, providing mainly information about the number of conducting fibers and conduction velocity of the fastest ones; little information can be gained to ascertain if acute OIPN predisposes to chronic one. In particular, if a channelopathy is hypothesized as *primum movens* of acute OIPN, *in vitro* techniques, such as patch clamp[51], would appear to be the most suitable option. However, in drug discovery to treat OIPN, *in vivo* animal models are required to effectively translate preclinical data from bench to bed-side, as it has yet pointed out; briefly, *in vitro* approaches, in this case, cannot reproduce the complex interactions that take place *in vivo*. This is the reason why there have been attempts to translate these *in vitro* techniques into something that can be applied in the clinical setting. A technique to test axonal excitability, Nerve Excitability Testing (NET), has been developed with success[52-55]. NET detects complementary data respect to nerve conduction studies; in fact, nerve excitability properties reflect many different elements involved during impulse conduction: ion-channels and ion pumps activation and ion exchanges. Of course, it doesn't directly measure axonal membrane potential, but it enables to gain indirect inferences about it thanks to the detection of changes in axonal excitability, which is measured as alterations in current required to obtained a predefined size potential[38].

In the last two decades, NET has been more extensively employed, mainly in a research setting, thanks to a refinement of the software and hardware available and the development of specific data acquisition protocols[38,52,54-56]. Thus, NET could give insights into pathophysiology underling acute OIPN; in small cohorts of OHP treated patients alterations in nerve excitability properties have yet been demonstrated[36]; Heide et al., have even evidenced that altered nerve excitability is related to sodium channel dysfunctions, again in a clinical setting[57]. These findings support the hypothesis of this project and suggest that NET could be the ideal method to test the relationship between acute and chronic OIPN in animal models. Despite being initially developed at the "bed-side", NET has been successfully reproduced at the "bench-side" both in rats[58-61] and in mice[62,63]. So far, in Literature there are no data on NET use in OIPN animal models; our project would give initial insights of the usefulness and potential of NET in this setting.

Threshold tracking technique is the core of NET: stimulus strength is modified to generate a defined target response. For this purpose, "**threshold**" is defined as the threshold current which is necessary to be applied to elicit a compound action potential of a definite size[54]. Usually the target amplitude is set to 30-40% of the supramaximal one; this is set taking into account - on the stimulus-response curve - the area of the steepest slope[54]. In this setting, modification in threshold current, necessary to obtain the target amplitude, are

tracked automatically: tracking steps are proportional to the error that can be calculated between the target amplitude and the one obtained in that specific step. Therefore, different pattern of stimulation can be applied to evaluate changes in threshold current, thus obtaining indirect evidences of excitability and membrane potential. Clearly, a dedicated software is required to allow these steps and calculation. To perform adequately threshold tracking, the ***TROND protocol*** **-** a semi-automated computer controlled one available in the Qtrac® software - is the most suitable option; the name "TROND" comes from the city of Trondheim (Norway): the protocol was developed during a symposium held there in 1999. Since then the TROND protocol has been applied in many peripheral nerve disorders[55,64]. TROND protocol allows to obtain multiple excitability parameters: it enables to measure changes in excitability, after applying specific manoeuvers that modify base-line membrane potential (i.e., hyper-/hypopolarizing conditioning currents).

The following section summarizes NET main features to better clarify its significance and interpretation, but before describing NET a few notes on axonal structure and functioning are in order.

Impulse propagation traditional theory elected nodes of Ranvier as the place where electrical activity was developed, thanks to specific Na+, K+ and leakage currents; little role was given to myelin and internode axolemma which were accounted as passive components. However, microelectrode studies in intact myelinated axons and voltage clamp studies on demyelinated ones, evidenced the important role of nodal, paranodal and internodal regions: there is an electrical interaction among them thanks to the presence of many different ion channels[65,66]. So, even if it is still true that the axon function is a faithful transmission of the impulse, there are different pattern of impulse activity due to differences in membrane organization; **Figure 2** gives a general overview of the components at each different level.

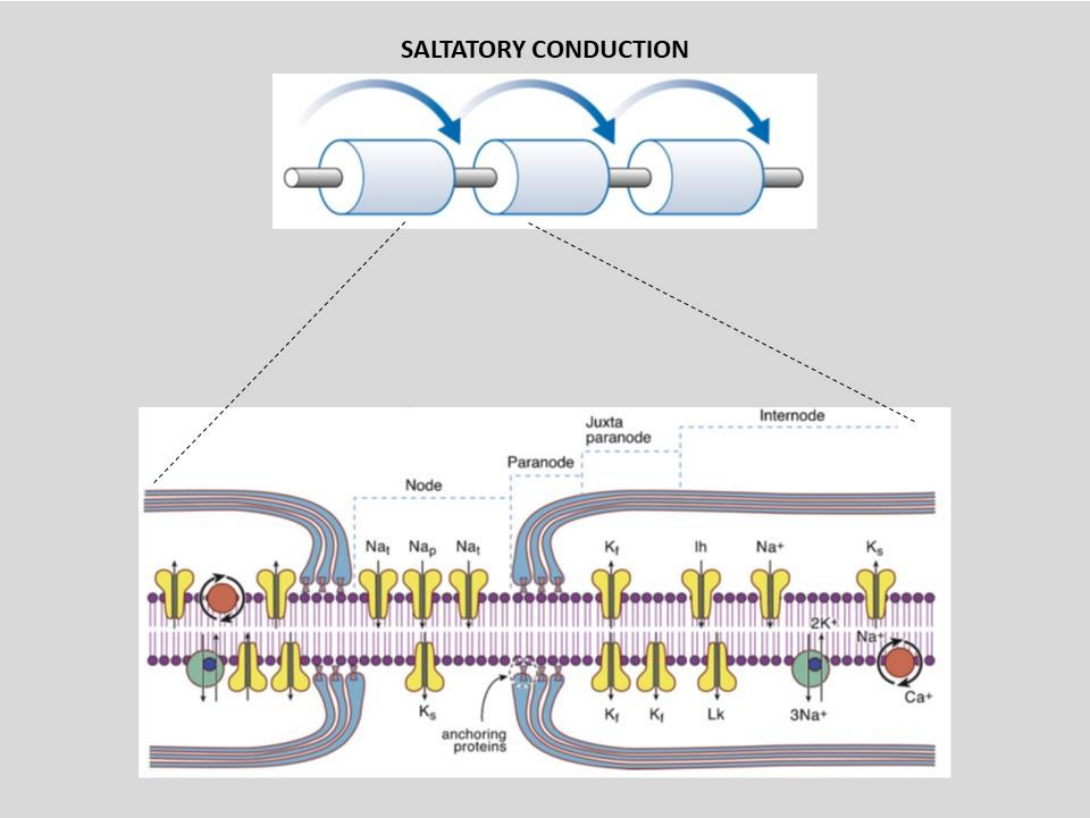

Figure 2 – Saltatory conduction and the role of ion channels/transporters and pumps (modified from Krishnan et al. 2009[38] and Kiernan et al. 2012[67]).

The upper part of the mage shows saltatory conduction which is made possible thanks to the special structure of the axonal membrane showed in the inferior part of the image. I_H=Inward rectifier channels; K_f= fast potassium channels; K_s=slow potassium channels; L_k=potassium voltage-dependent leakage conductances; $Na+_p$= persistent sodium channels; $Na+_t$= transient sodium channels; Na+/Ca+= Na+/Ca2+ exchangers that exports Ca2+ ions and imports Na+ ones driven by electrochemical Na+ gradient; 3Na+/2K+= Na+/K+ ATPase pump.

Action potential can be generated thanks to a rapid exchange of electrolytes across the plasmalemma; intrinsic membrane protein, voltage-gated ion channels, are responsible for this. They have a well-defined three-dimensional structure that establishes an aqueous pore that allows passageway to ions[68]; a selectivity filter is present that is compatible only with a specific ion[38]. This pore is not always in the same condition: its opening or closing state (i.e., the "gating") is determined by the membrane potential – that's why they are named "voltage-operated" or "voltage-gated" channels - and the direction of ion fluxes is strictly dependent on the electrochemical gradient for that ion across the axonal plasmalemma. The different actors specifically involved in the entire process of action potential generation are: Na+ and K+ axonal channels, inward rectification channels and the Na+/K+ pump. See **Figure 3** for an overview of Na+ and K+ current contributions to action potential generation.

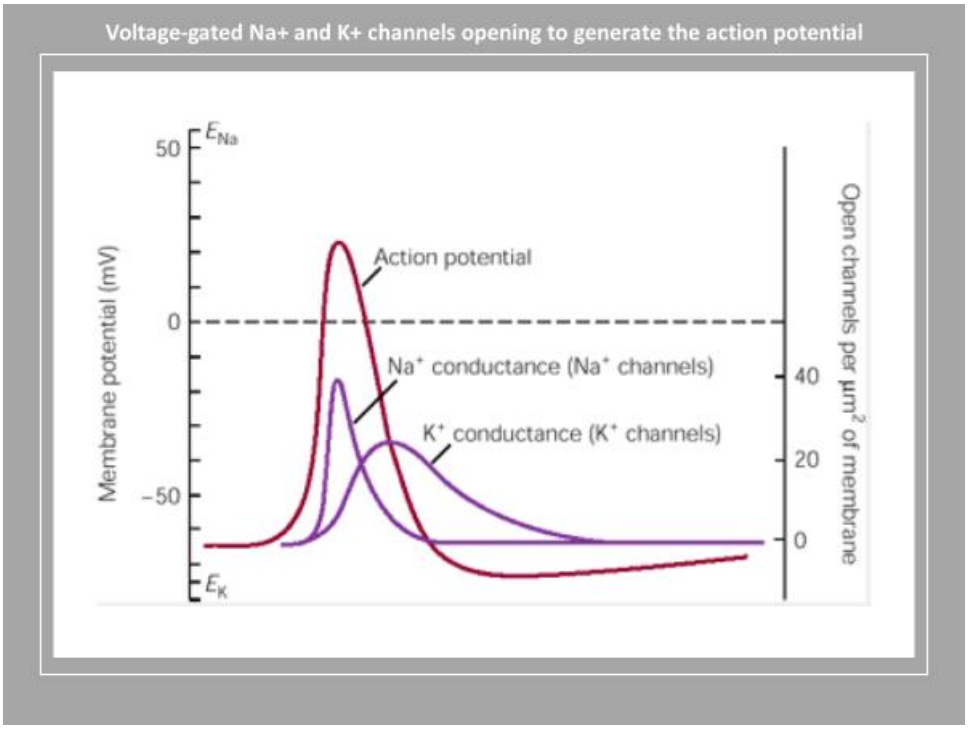

Figure 3. The sequential opening of voltage-gated Na+ and K+ channels that generates the action potential (modified from Kandel et al., 2000[69]).

***E_{Na}** = Na+ equilibrium potential; **E_K** = K+ equilibrium potential.*

Axonal Na+ channels are clustered mainly in the node (density: up to 1000/µm^2), compared to the internode (density: 25/µm^2)[70]. When the nodal membrane is depolarized they allow Na+ ion passage: an inward current is thus generated. This process is voltage-sensitive and regenerative: as depolarization increases, inward current increases too, depolarizing the next node; however, this is not a sustained process since Na+ channels then closes, due to the inactivation (the "gating" mentioned before). The distribution of Na+ channel is quite different between unmyelinated and myelinated axons: they are uniformly distributed in unmyelinated ones and, instead, clustered at nodes of Ranvier in myelinated axons[52,71]. There are two different Na+ channels families, given their distinct functioning: transient Na+ channels and persistent or non-inactivating or slow inactivating Na+ channels. Transient Na+ channels contributes to the 98% of the total current that generates the action potential; they are termed "transient" since they show a fast activation and inactivation kinetics[52,72]. Persistent Na+ channels are activated at a membrane potential more negative than the transient one; so, when the membrane is at the resting potential they have an incomplete voltage-dependent inactivation and give rise to a persistent inward leak of Na+ channels[73].

Axonal K+ channels are the largest and most diverse type of channels[74]. Here a simplified description is presented considering channel kinetics: there are fast and slow K+ channels. Fast K+ channels are clustered almost exclusively in the juxtaparanodal region: they limit the re-excitation of the node after action potential

conduction[75]. Slow K+ channels are, instead, present at high density at the node; they are not responsible for axonal repolarization after the action potential since they are activated quite slowly: they are open at the resting membrane potential cooperating to its maintenance and limiting repetitive firing[75,76].

Axons also possess another "mixed" type of ion channel: inward rectifier ones, which are permeable to both K+ and Na+ ions (they are conventionally referred as "I_H" channels). They are mainly activated as membrane depolarization increases, reaching a maximum at – 110 mV[77]; they are able to limit excessive hyperpolarization allowing the persistence of impulse conduction after a trains of impulses, preventing conduction failure.

Axonal Na+/K+ pump is another key component; Hodgkin and Huxley first demonstrated its electrogenetic properties: it extrudes 3 Na+ ions out of the cell and pumps 2 K+ ions in, at the expense of metabolic energy[78]. It is fundamental to maintain axolemma transmembranic ionic gradients: after action potential conduction it restores Na+ and K+ gradients. It also cooperates to the regulation of the resting membrane potential; a dysfunction of the pump (as can be obtained with oubain or digitalis) results in membrane depolarization[79].

a) Stimulus-response Curve

This is the first curve TROND protocol enables to obtain and it drives all the subsequent steps of the recording; NET is, in fact, determined by stimulus-response property of the axon. In **Figure 4** (curve B), it is shown what happens during this phase: stimulus intensity increases progressively and, consequently, the size of the recorded compound action potential increases until it reaches a maximum peak (supramaximal response). So, the response error (i.e., the difference between actual and target responses) and the slope of the curve can be used to predict the amount needed to change the stimulus, following a modification in the response. For threshold tracking this curve is integral in setting the target submaximal response of interest (this means the target response is located in the steepest part of the curve; in **Figure 4** on Curve B, for example it is located between x-axis intercept and the slope of the curve itself indicated by the number 2); the slope of the curve is used to optimize the subsequent phases of the tracking threshold.

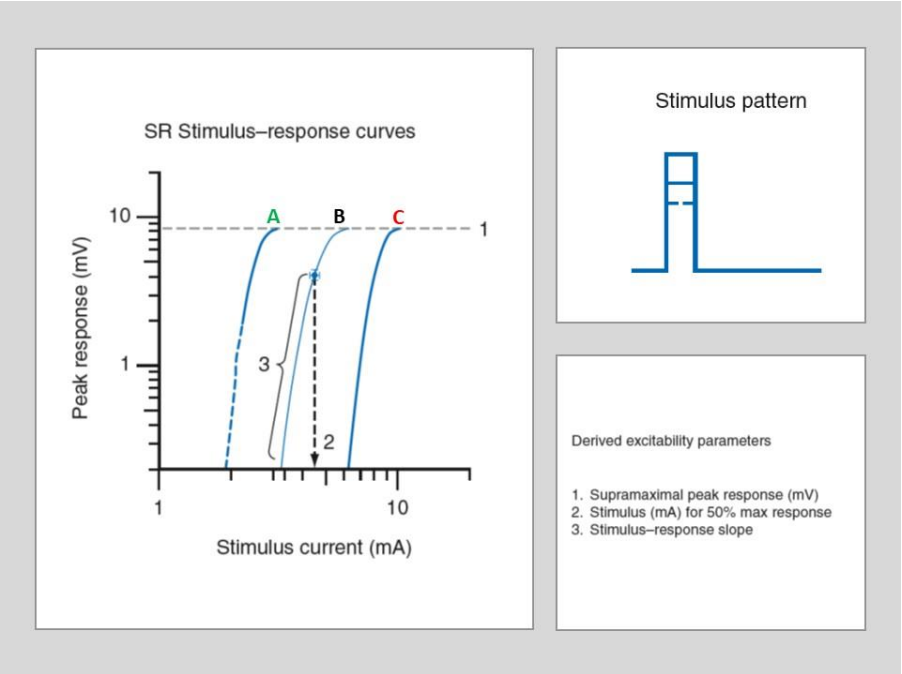

Figure 4 – Stimulus-Response Curve (modified from Kiernan et al. 2012[67]).

On the left the Stimulus-Response relationship can be seen plotted against the current needed to obtain the target response; pattern stimulus is represented in the upper left quadrant of the image. ***Curve B*** *represents the response in base line conditions;* ***Curve A*** *represents changes following a hyperpolarizing conditioning current (the curve is shifted to the right due to the higher stimulus strength required);* ***Curve C*** *represents changes following a depolarizing conditioning current (the curve is shifted to the left due to the lower stimulus strength required).*

b) Strength-Duration Properties

The relationship between strength and stimulus duration is then tested in the subsequent part of the **TROND protocol**. *Duration* of the test stimulus and the *strength* of current needed to elicit a compound action potential – of a given size - have an inverse correlation relationship: as the first increases, the second one decreases. There are two fundamental parameters in this relationship: chronoaxie and rheobase. *Rheobase* is defined as the threshold current (or, better, estimated one in mA) required if the stimulus were of infinite duration; *chronoaxie* is defined as the stimulus duration corresponding to a threshold current which is twice the rheobase (see the right upper quadrant of **Figure 5**). However, instead of chronoaxie, another parameter is usually considered and calculated: the *strength-duration time constant* (*SDTC*). SDTC is an apparent constant of the membrane which has been demonstrated to be equivalent to chronoaxie in human peripheral axons[80,81]; it can be determined analyzing the threshold current and stimulus duration relationship. SDTC measures, as the duration of the stimulus decreases to zero, the rate at which the threshold current instead increases. The SDTC is still remarkably well described by empirical **Weiss's Law**[82], that dates back to 1901[83]:

$$Q = I*t = I_{rh}*(t+STDC)$$

Where: ***Q****= stimulus charge;-* ***I****= stimulus current of duration t;* I_{rh}*= rheobasic current*

Since there is a linear (inverse) relationship between charge and stimulus duration, a charge-stimulus duration plot - with four different stimulus widths (0.2, 0.4, 0.8, 1 msec) – allows SDTC calculation: the x-intercept of the straight line, fitted to the points representing different stimulus widths, corresponds to SDTC; the rheobase is the slope of this linear function. Weiss's Law application is demonstrated on the left graph in **Figure 5**.

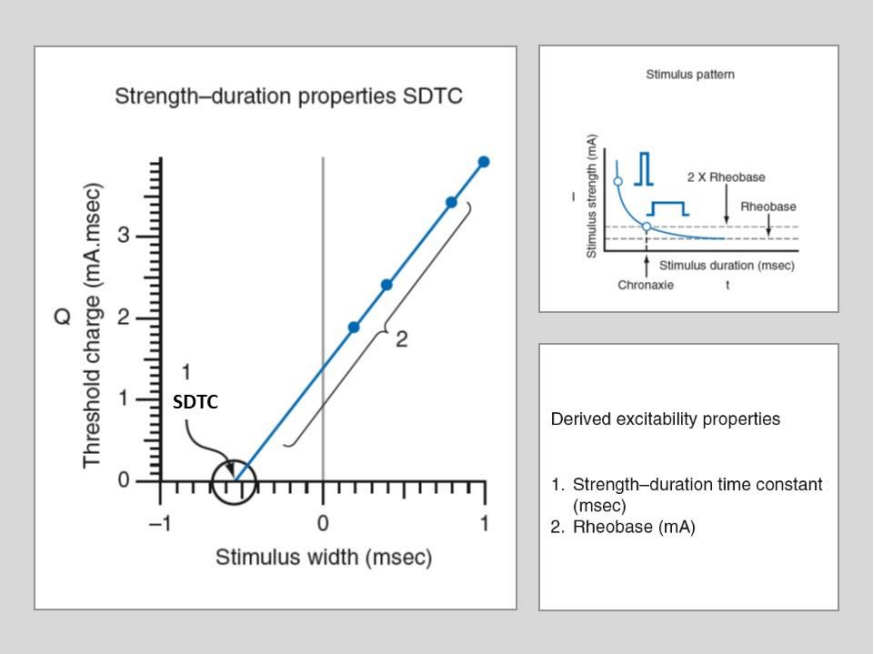

Figure 5 – Strength-duration relationship (modified from Kiernan et al. 2012[67]).

*On the left the Strength-Duration relationship determination through **Weiss's Law** can be seen in the plot of threshold charge versus stimulus width. The upper right quadrant clarifies the concepts of **rheobase** (threshold current required for a stimulus of infinite duration) and **chronoaxie** (the stimulus duration which corresponds to twice the rheobase).*

Rheobase and SDTC reflect nodal membrane parameters; in human peripheral axons SDTC has been found of 0.46 msec in motor axons and of 0.67 in sensory ones[81]. Both parameters reflect Na+ channel (mainly persistent ones) properties[84].

c) Recovery Cycle of Excitability

Recovery cycle is a process composed of definite and reproducible changes in excitability an axon undergoes after the conduction of a single nerve impulse. **Figure 6** summarizes these phases.

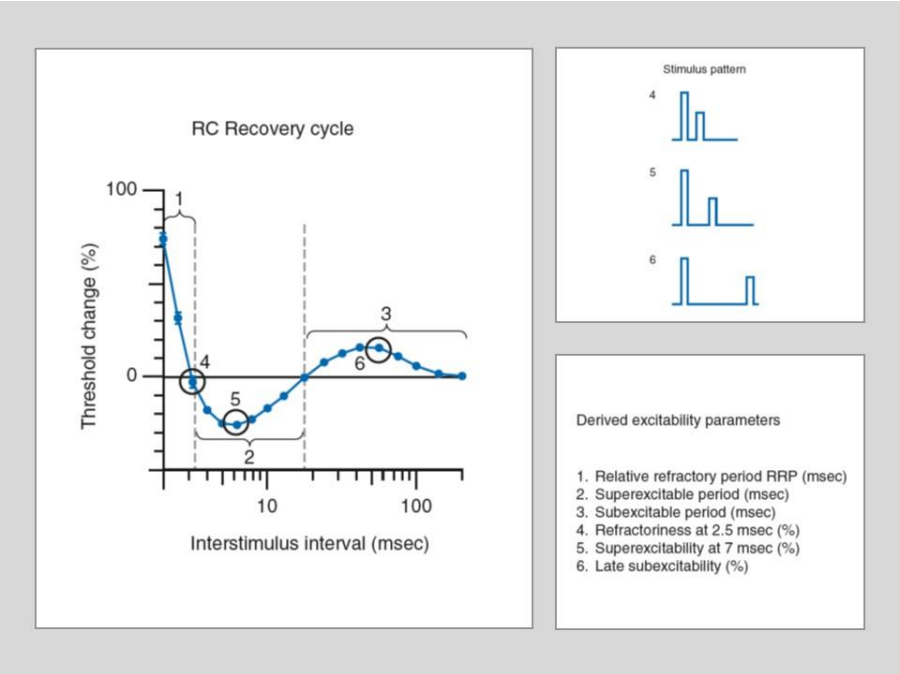

Figure 6 – Recovery cycle of excitability (modified from Kiernan et al. 2012[67]).

On the left Recovery cycle plot is shown: it describes refractory period, superexcitability and subexcitablity. The stimulus pattern necessary to generate this waveform in seen on the left upper quadrant: stimulus number corresponds to the number on the recovery cycle plot curve in relevant points of recovery cycle itself.

Soon after impulse conduction, the membrane potential is altered and passes through four different conditions before settling back to base-line state. At first, axons are completely inexcitable: no stimulus, even one with high strength, can generate an action potential; this is the so-called *absolute refractory period*. After this phase, if a stimulus stronger than the usual threshold is applied, an action potential can be eventually generated; this is termed *relative refractory period*. But, then, axons become more easily excitable – the *superexcitability period* – and even conduction velocity is increased compared to resting state. Then, again, before returning to the original condition, axons develop again a period in which they are less excitable, the *subexcitable or late excitability period*.

Ion channels and transporters are responsible for these phenomena. After the spreading of the action potential, the absolute refractory period is a reflection of the Na+ transient channel inactivation; the subsequent phase, in which they gradually recover from inactivation, corresponds, instead, to relative refractory period[78]. Notably, the relative refractory period duration can be increase from its average value (3ms in human axons) by conditioning depolarizing currents that precedes the action potential, due to Na+ channel voltage dependence[85].

Superexcitability is, instead, the result of the depolarizing afterpotential that follows the impulse conduction. During the action potential there is a larger Na+ efflux than K+ efflux; thus, the whole axon is left with a depolarizing charge that spreads to the internode and node. Thus, the node depolarizes the internode and,

conversely, the internode participate to the node repolarization; in the end, a few millivolts depolarization is present in both sites during the action potential[86]. The internode has a large capacitance; due to this property, after the potential, it can maintain the node depolarized for tens of milliseconds. Superexcitability, in myelinated axons, is greatly influenced by the membrane potential. In case of a subthreshold depolarization that precedes the actual action potential, there is a decrease in Na+ influx and an increase in K+ efflux: the charge imbalance itself during the action potential is thus decrease; moreover, the afterpotential is short-circuited by nodal and internodal K+ channels that open at rest and its duration is decreased[86-88]. On the contrary, superexcitability is increased by hyperpolarization and, in this case, depolarizing after potential has an increased duration. Given these, membrane potential has in superexcitability a useful indicator.

Slow K+ channels at the node of Ranvier are responsible for this last variation in excitability – late subexcitability – since they convey the current that hyperpolarizes the membrane. During the action potential and the subsequent depolarizing action potential they are activated and their inactivation is quite slow[66,89]. Late subexcitability is activity-dependent: it is more pronounced if a brief train of impulses is conducted along the axon; again, nodal slow K+ are responsible for this hypoexcitability[90,91]. However, it should be noted that subexcitability, differently from superexcitability, is not related only to resting membrane potential and it is not a good indicator for it; it is greatly influenced by electrochemical gradient for K+ ions and it can be used to retain information about extracellular K+ levels. If the electrochemical K+ gradient is increased (due to a decrease of extracellular K+ levels), subexcitability is increased too. If, instead, an increase of extracellular K+ levels takes place and determines a depolarization, late excitability is decreased or even abolished, as modelled by the events that take place during ischemia[92].

d) Threshold electrotonus (TE)

This part of the TROND protocol is the only option to test *in vivo* internodal conductances.

These conductances are of a certain interest since there is a specific relationship between the node and the internode for what regards action potential generation and propagation. The internodal capacitance is, in fact, slowly charged by the nodal membrane when the latter changes its potential. So, internodal voltage-dependent channels are affected; although, Na+ channel density is not enough to generation of an action potential at the internode, there is still a change in the internodal membrane so that it can store current and affect consequently the behavior of the node that modified the internodal conductances at first[93].

Electrotonus is defined as membrane potential variations determined by pulses of subthreshold depolarizing or hyperpolarizing current. The **threshold electrotonus** (**TE**) technique evaluates changes of the threshold in consequences of depolarizing or hyperpolarizing subthreshold currents (i.e., which are too weak to generate an action potential); the threshold changes according to electrotonic changes of the membrane potential[54,94].

Figure 7 summarizes changes in response to polarizing currents; polarizing currents are set to have 100-msec duration and an intensity set to the 40% of the unconditioned threshold, obtained with 1-msec test pulses.

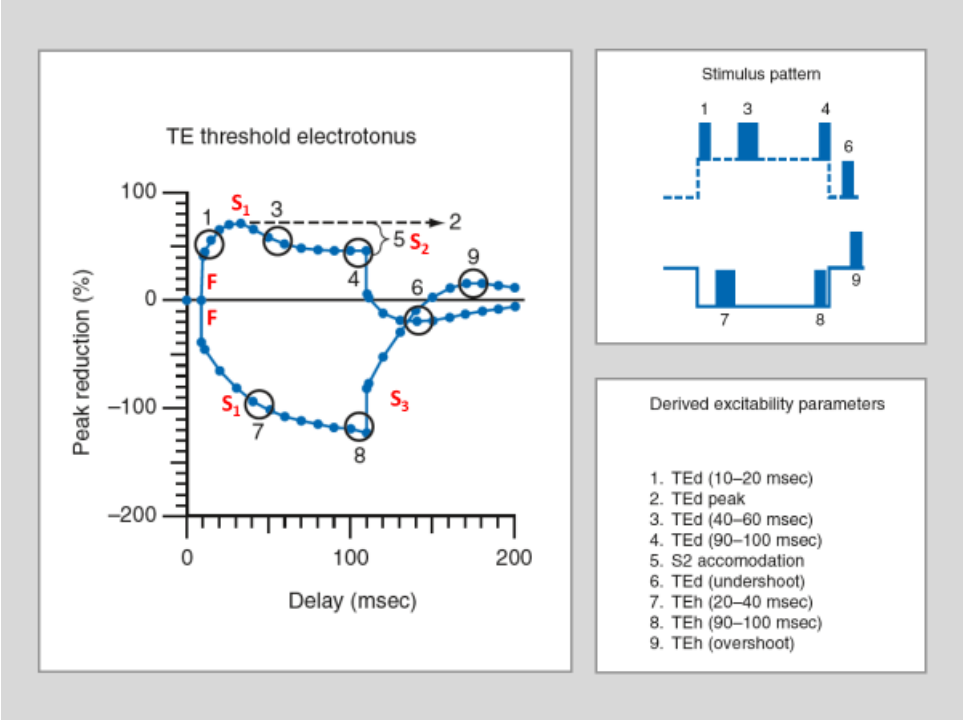

Figure 7 – Threshold electrotonus (modified from Kiernan et al. 2012[67]).

On the left threshold electrotonus (TE) waveform is represented (depolarizing direction is upwards and hyperpolarizing one is downwards): it reproduces the effects of 100 msec subthreshold polarizing currents (+/-40% of the threshold) on axons. The stimuli used to obtain the TE waveform are shown in the upper right quadrant.

Different phases can be recognized on the TE waveform.

In response to subthreshold depolarizing currents (upward response on the graph) the following sequence takes place. There is an initial depolarizing fast phase (F phase); it is proportional to the applied current (a 40% depolarizing current reduces the threshold of 40%): it reflects nodal depolarization. It is followed by a further depolarization phase set in the time frame form 10 to 20 msec after the stimulus is applied [TEd(10-20 msec)]. Then, a first slow depolarizing phase (S1 phase) can be seen: it corresponds to the current spreading and subsequent depolarization of the internode[54,89]. The S1 phase goes on until it reaches a peak [the TE(peak)], but, then, nodal K+ channels are activated and a slow accommodative process ensues (S2 phase) and the threshold returns slowly to the control level [TEd(90-100msec)][54,89,94]. Lastly, as the direct current pulse is terminated, a fast threshold increase can be seen and then the threshold slowly undershoots the control level [TE(undeshoot)], followed again by a return to its original; this occurs since K+ conductances are quite persistent and deactivate slowly[84].

In response to hyperpolarizing currents (downward response on the graph) the following series of events is observed that mirrors greatly what happens after depolarizing ones. At first there is a fast threshold increase

(F phase), proportional to the applied current. As the hyperpolarization spreads to the internode [TEh(10-20 msec)], there is an ongoing threshold increase which goes only slowly (S1 phase). This S1 phase is quite different from the one seen in response to depolarizing stimuli: amplitude and time constant are increased since hyperpolarization deactivates K+ channels (slow nodal, and fast and slow internodal ones) which, thus, are not able to contain the extent of the hyperpolarization itself[54]. S1 phase reaches its peak [TEh(90-100 msec)], and, on termination of the conditioning stimulus, threshold deceases fast and the encounters a slow, depolarizing overshoot [TEh(overshoot)], before returning to the natural condition; these phenomena correspond to inward rectifiers channels (I_H) slow deactivation and slow K+ channels reactivation.

e) Current-Voltage relationship and slope

This current-threshold (I/V) curve is useful to examine inward and outward rectification of the nodal and internodal axolemma[55]. **Figure 8** shows this relationship; long current pulses (i.e., 200-msec) of variable strength are applied to verify variations in threshold current, thus demonstrating inward and outward rectification. Ion conductances activated in response to depolarizing or hyperpolarizing stimuli are responsible for the peculiar shape of the I/V curve[38]. Outward rectification in response to depolarizing currents is the steepening in the upper right quadrant of the left graph in **Figure 8**: fast and slow K+ channel activation is responsible for this component[55]. Inward rectification in response to hyperpolarization is instead seen in bottom left quadrant; the cation conductance, I_H, is responsible for this phenomenon[77]. Resting I/V slope and minimum I/V slope are the two parameters of interest that can be derived from this curve.

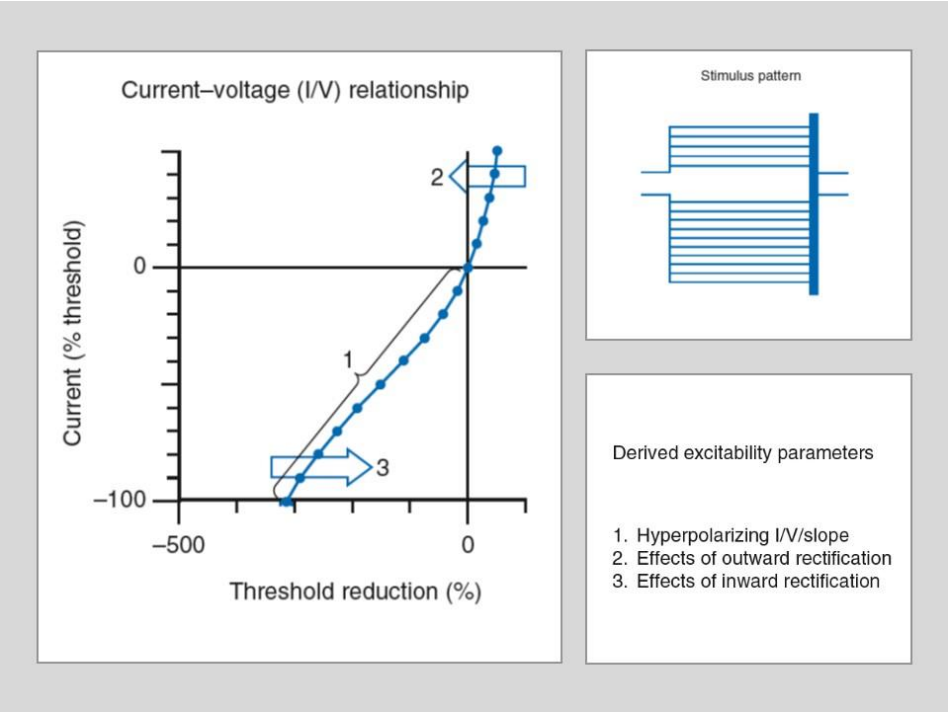

Figure 8 – Current-voltage relationship (modified from Kiernan et al. 2012[67]).

In the right upper panel stimuli required to generate the I/V curve are shown; they consist of 200 msec polarizing ones (range: -/+50% of the threshold current). The I/V curve is shown in the left panel. Outward rectification and inward rectification phenomena are described in the text.

1.3 TOPIRAMATE: PROOF-OF-CONCEPT FOR OIPN PREVENTION

Topiramate was first synthesized as fructose-1,6-diphosphate structural analogous aiming at the enzyme fructose 1,6-bisphosphatase inhibition to treat diabetes, without obtaining satisfactory results[95]. However, it was then noted it showed anticonvulsivant activity in animal models and its development as antiepileptic drug was pursued[96,97]; its main clinical indications are epilepsy and migraine[95,98].

This molecule is highly interesting since it has pleiotropic effects whose result is an increase in neuronal stability; five established pharmacodynamic properties have been described: blockage of voltage-gated sodium channels[99]; reduction of L-type calcium channel activity[100]; inhibition of glutamate activity[101]; enhanced GABAergic neurotransmission activity[101]; and mild inhibition of carbonic anhydrase isoenzymes[96,102,103]. Moreover, a positive modulation of some types of voltage-gated K+ channels has been also suggested as a possible mechanism[101,104].

For the purposes of this project, topiramate was selected as the agent eventually able to contain acute OIPN preventing chronic one; we were in particular interested in its primary ability to modulate sodium channel currents, among all its properties, as demonstrated by Taverna et al. in in vitro studies[99]. However, we were also interested by its other actions since, despite there are robust evidences that acute OIPN is due to sodium channel dysfunction, some other mechanism underling this toxicity have been proposed, involving potassium channels[105]. So, despite keeping the "sodium channel dysfunction hypothesis" as the possible pivotal mechanism for acute OIPN, we aimed at a general hyperexcitability modulation.

Topiramate pharmacokinetics profile is compatible with OHP administration[98]. The dosage used in this project was decided after a review of the preclinical literature in rat models in which a prolonged administration was used; we were in fact required to administer our animals topiramate for nearly 5 weeks. The final elected dosage and schedule was equal to the maximum tolerate dosage for clinical use; the calculation was made keeping as a reference (human) weight 60 Kg[106,107]. This arbitrary decision to use this dosage was taken to ensure a long-lasting and persistent action to stabilize axonal membrane *in vivo* aiming at the decrease acute OIPN, in a proof-of-concept setting.

2 AIMS

The objective of this project was to test if acute OIPN might be able to predispose to chronic OIPN, thus making acute OIPN a target to prevent chronic one. To this aim, Nerve Excitability Testing was elected as the outcome measure to reliably detect acute OIPN in an *in vivo* preclinical setting.

Intermediate objectives were set to gain inferences to verify or reject the working hypothesis:

1. the first step was to verify the presence of acute OIPN phenomena in the animal model and refine the chronic model to induce both acute and chronic phenomena;
2. Once completed the first phase, the second requirement was the identification of a candidate molecule able to decrease the sole acute OIPN in the refined animal model;
3. Then, the last step was to test if the candidate molecule could prevent chronic OIPN reducing acute OIPN; this was the crucial point to verify a possible causative correlation between the two different OIPN toxicities.

In the subsequent section an overview of the Tasks performed is presented.

3 OUTLINE OF THE PROJECT

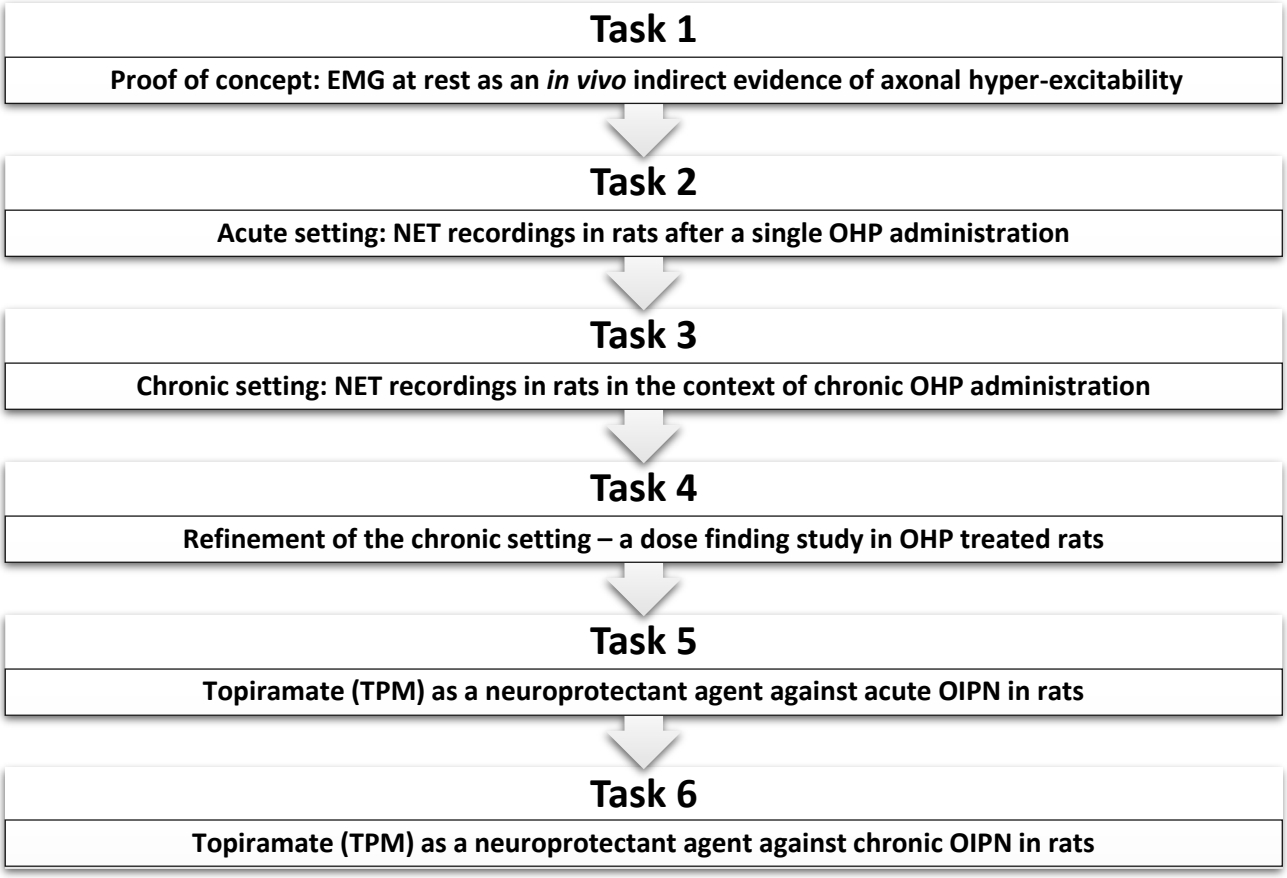

4 MATERIALS AND METHODS

4.1 ANIMALS AND HOUSING

Female Wistar rats, 175-200 grams on arrival (Envigo, Italy) were used in this project. Numerosity for each experiment is described in the "Study Design" section of each individual Task. The care and husbandry of animals were in conformity with the institutional guidelines in compliance with national (D.L. n. 26/2014) and international laws and policies (EEC Council Directive 86/609, OJ L 358, 1, Dec.12, 1987; Guide for the Care and Use of Laboratory Animals, U.S. National Research Council, 1996).

4.2 DRUG ADMINISTRATION

Oxaliplatin (OHP) treated groups received tail vein injections according to the treatment plan (dosage and schedule) as described in the "Study Design" section for each Task. OXALIPLATIN ACCORD 5 mg/mL solution was used; control groups received vehicle injections (5% glucose solution). PACLITAXEL (PTX) ACCORD 6mg/mL solution and CISPLATIN (CDDP) ACCORD 10mg/mL solution were used in TASK1; paclitaxel was administered i.v. and CDDP i.p. according to the dose described in the "Study Design" section for TASK1. Topiramate Accord 100 mg/Kg was administered orally according to the treatment plan as described in the "Study Design" section for each Task, when required. A solution of this drug was freshly prepared before use, dissolving Topiramate Accord 50 mg film-coated tablets in normal saline solution obtaining a 10mg/mL solution (the total volume administered to each animal was not greater than 1.0 mL/100g); a 10 ch nelaton catheter was used (Lofric^{TM}, Rome, Italy) for oral gavage. For iv injections a 22 ch needle was used. For i.p. administrations a 21 ch needle was instead used (Terumo Neolus Needle, Terumo Italy, Rome, Italy).

4.3 STANDARD NEUROPHYSIOLOGY: NERVE CONDUCTION STUDIES AND EMG TESTING AT REST

Nerve conduction studies were performed with the electromyography apparatus Myto2 (ABN Neuro, Firenze, Italy). Stainless steel needle electrodes were used (Subdermal EEG needle, Ambu^{TM}, Ballerup, Denmark). All neurophysiological determinations were performed under standard conditions under deep isofluorane anesthesia; animal body temperature was monitored and kept constant at 37 +/-0.5°C with a thermal pad, electronically connected to a thermal rectal probe (Harvard Apparatus, Holliston, US).

The optimal setting of stimulation for each nerve was reached following the subsequent protocol, as recently published by our group[108-110]:

- Distal caudal nerve SNAP (orthodromic stimulation setting): the active recording electrode was placed at 5 cm from the tip of the tail and the reference recording electrode 6 cm from it; the anode was placed at 1 cm from the tip of the tail and the cathode at 2 cm from it; the ground electrode was placed midway between the cathode and the active recording electrode (see **Figure 9**);

- Proximal caudal nerve SNAP (orthodromic stimulation setting): the reference recording electrode was placed at 1 cm from the base of the tail and the active recording electrode 2 cm from it; the cathode was placed at 5 cm from the base of the tail and the anode at 6 cm from it; the ground electrode was placed midway between the cathode and the active recording electrode (see **Figure 10**);
- Digital nerve SNAP (orthodromic stimulation setting): the reference recording electrode was placed in front of the patellar bone, the active recording electrode close to ankle bone; the cathode was placed at the base of the fourth toe and the anode was positioned at the tip of it; the ground electrode was placed in the sole (see **Figure 11**);
- Caudal nerve CMAP: the reference recording electrode was place at 12 cm from the base of the tail and the active one at 11 cm from it; the ground electrode was placed at 8 cm from the base of the tail; the cathode and anode were placed for the first CMAP recording at the distal stimulation site and then at the proximal one in the following configuration:
    - Distal stimulation site (see **Figure 12**): the cathode was placed at 6 cm from the base of the tail and the anode at 5 cm from it;
    - Proximal stimulation site (see **Figure 13**): the cathode was placed at 2 cm from the base of the tail and the anode at 1 cm from it;

Intensity, duration and frequency of stimulation were set up to obtain optimal results. Averaging technique was applied carefully. For sensory recordings filters were kept between 20 Hz and 3KHz, for motor recordings between 20 Hz and 2 KHz. Sweep was kept at 0,5 msec.

Figure 9. Distal caudal nerve recording set up.

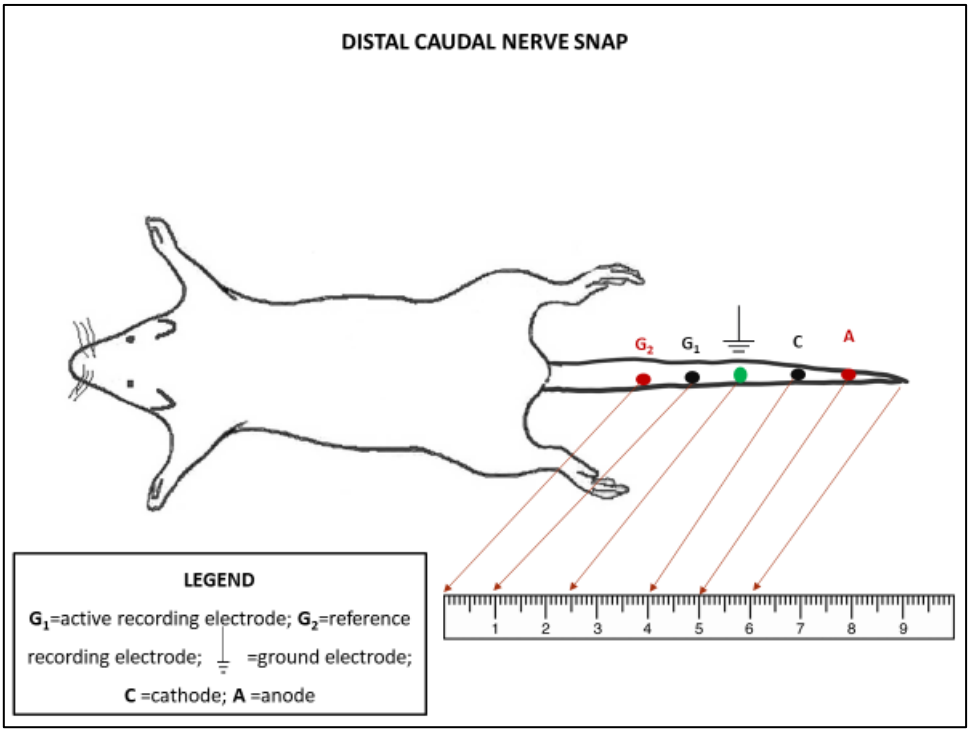

Figure 10. Proximal caudal nerve recording set up.

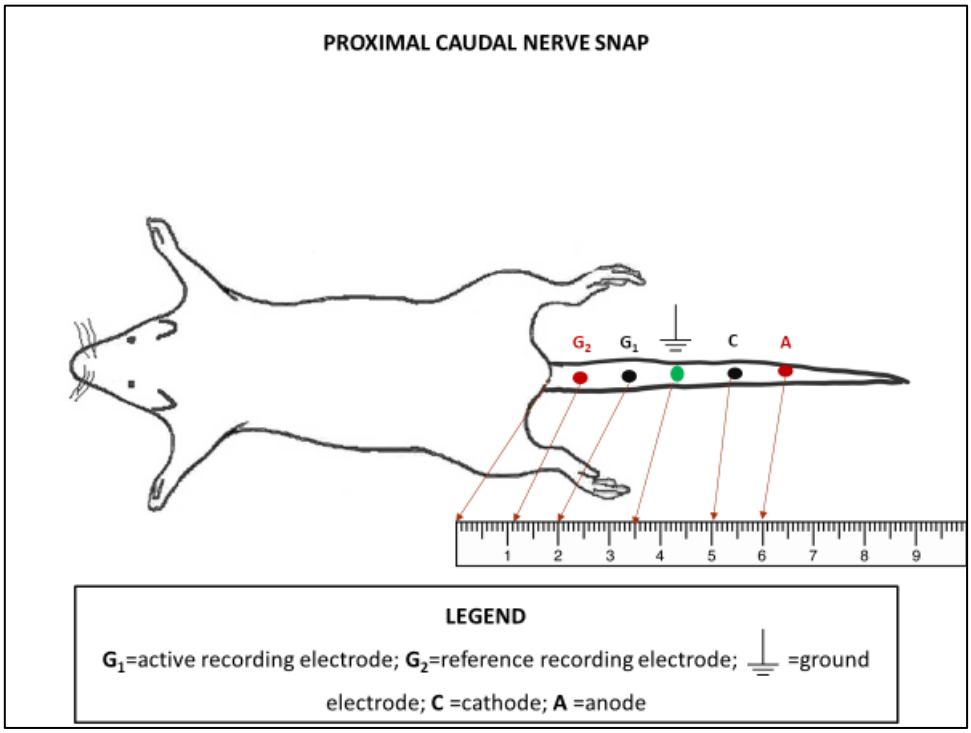

Figure 11. Digital nerve recording set up.

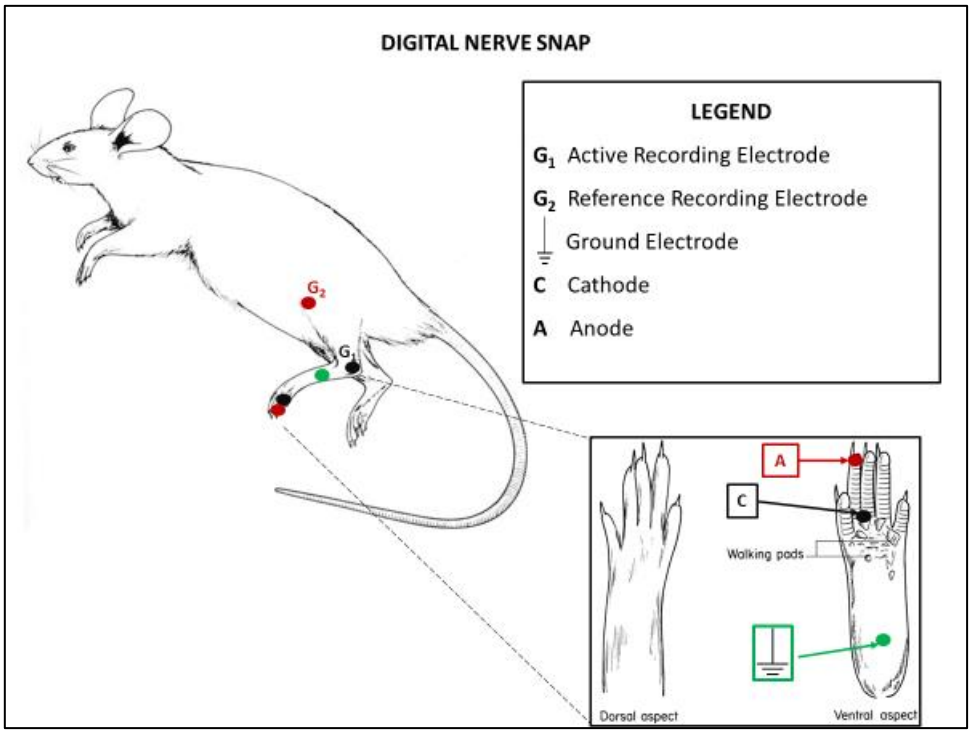

Figure 12. Motor caudal nerve recording set up, distal site of stimulation.

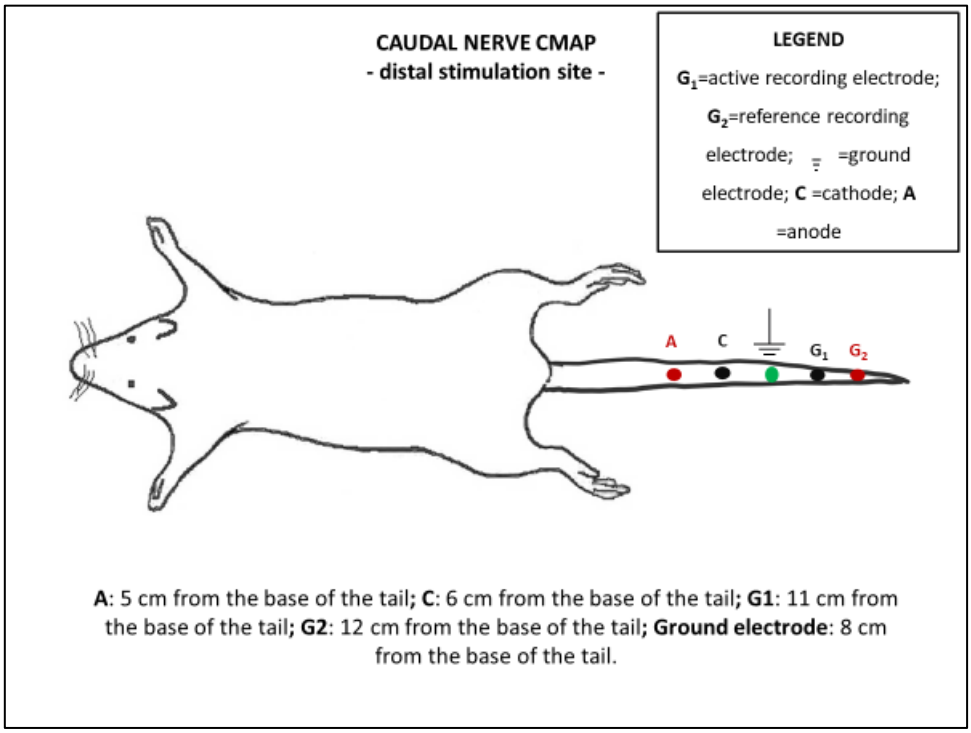

Figure 13. Motor caudal nerve recording set up, proximal site of stimulation.

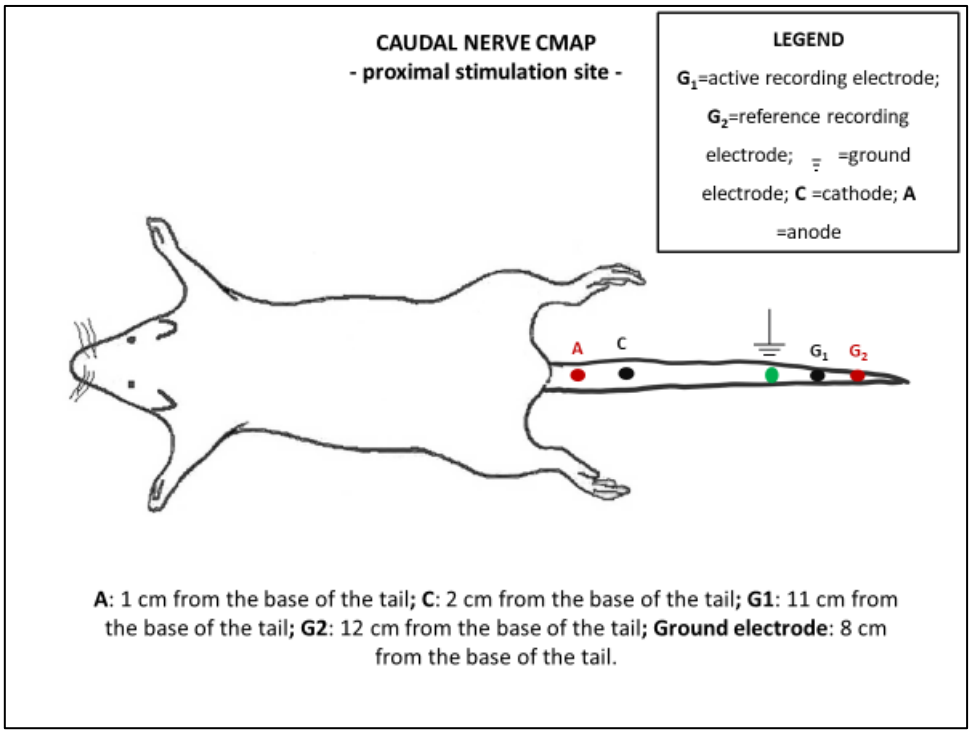

Electromyography (EMG) recordings were performed with a concentric EMG needle (Ambu™, Ballerup, Denmark) to record, at rest, signs of axonal hyper-excitability in the following muscles of the left hind limb: **quadriceps femoris, gastrocnemious, flexor digitorum.** These signs consisted of increased insertional activity

and spontaneous high frequency motor unit activity with muscles at rest; irregular firing at 150-300 Hz for variable time span due to motor unit firing were considered as neuromyotonic discharges[111].

Increased motor unit activity was assessed according to the scoring system proposed by Hill et al. in a cohort of Oxaliplatin treated patients, were the sensitivity and specificity of EMG recordings at rest to detect acute OIPN was demonstrated to be 100% for both indicators[112]:

- Score 0: no abnormal findings at rest;
- Score 1: increased insertional activity;
- Score 2: spontaneous high frequency firing lasting less than 2 seconds;
- Score 3: spontaneous high frequency firing lasting 2-5 seconds;
- Score 4: spontaneous high frequency firing lasting more than 5 seconds.

4.4 ADVANCED NEUROPHYSIOLOGY: NET

Caudal nerve CMAP was tested during NET; the method described by Yang et al. 1999[58] was used. The montage is shown in **Figure 14**. Rats were under deep isofluorane anesthesia during the whole procedure (8-15 minutes per rat); animal body temperature was monitored and kept constant at 37 +/-0.5°C with a thermal pad electronically connected to a thermal rectal probe (Harvard Apparatus, Holliston, US). Disposable Ag-AgCl (i.e., not polarizable) cup electrodes (Ambu™, Ballerup, Denmark) were used for stimulating the caudal nerve in combination with a conductive EEG paste (Ten20 Conductive EEG paste, Weaver and Company, US): the anode was placed on the skin of the left hip - after hair removal with a depilatory cream (Veet™, Slough, UK) - and the cathode was placed on the left side of the tail 1.5 cm from the base. Before placing both electrodes, the skin was gently rinsed with an abrasive gel (Nuprep EEG & ECG Skin Prep Gel, Konan Medical, US) to ensure an adequate cutaneous impedance. Instead, as ground and recording electrodes, stainless steel needle electrodes were used (Subdermal EEG needle, Ambu™, Ballerup, Denmark); the active recording electrode was inserted 6 cm distally to the cathode and the reference electrode was placed 2 cm distally to it. The ground electrode was inserted midway between the cathode and the active recording electrode.

Figure 14. NET montage for caudal nerve recordings (modified from Yang et al., 2000[58])

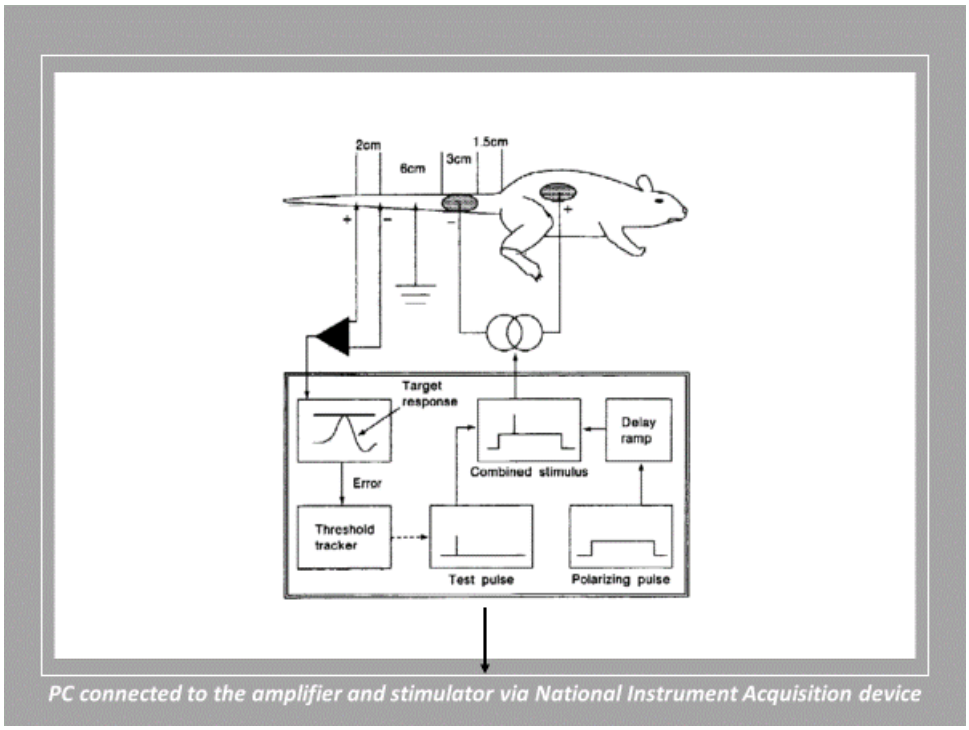

Figure 15. Hardware connections required, in general, to obtain NET recordings.

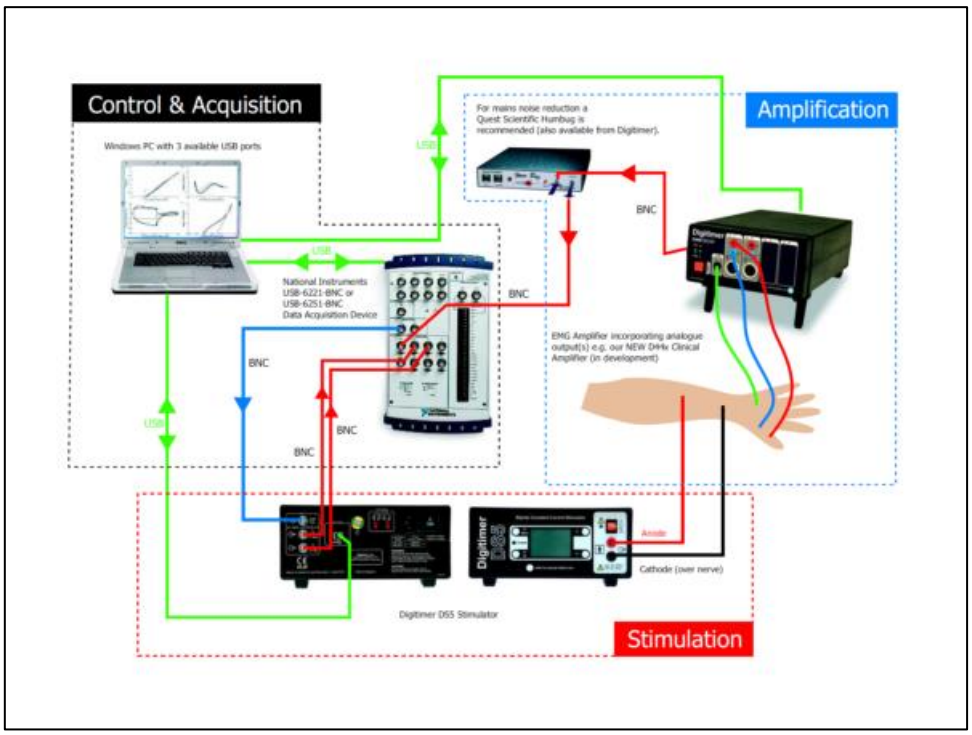

Figure 15 shows how hardware components are connected to obtain a correct NET recording. The setting was adapted and these alternative hardware items were used:

- Stimulator: isolated linear bipolar constant current stimulant (maximal output +/-10mA, DS4, Digitimer, Welwyn Garden City, UK);
- Amplifier: Xcell3 Microelectrode Amplifier (FHC, Bowdoin, US): it was connected to the recording electrodes via a customized probe/adapter specifically designed by FHC for the needs of this PhD project;
- National Instrument USB-6221-BNC Acquisition Device (National Instrument Italy, Assago, Italy).

Axonal excitability recordings were performed using an automated computerized system (Qtrac© Institute of Neurology, Queen Square, UK). TROND protocol was used to acquire multiple excitability parameters as stated in the Introduction, including: threshold electrotonus, internodal conductances and membrane potential, recovery cycle of excitability, current-threshold relationship and rectifying properties[54,55]. The protocol acquired data into a four steps procedure resulting in **4 main curves** summarizing data: **stimulus-response**, **current-threshold**, **threshold electrotonus**, **recovery cycle curves**.

For threshold tracking the target amplitude was set automatically at +/- 30-40% of the supramaximal response amplitude; the calculation was made on the area of the steepest slope to the **stimulus-response curve**. On-line tracking was performed to detect changes in threshold current necessary to achieve the target amplitude; tracking steps were proportional to the error between target amplitude and the recorded one[54].

Subthreshold polarizing currents (100 msec in duration) were used to establish **threshold electrotonus**; they were set to +/-40% of the control threshold[55]. At different time intervals and after the application of polarizing currents, the threshold current required to obtain the target response amplitude was determined. The **current-threshold relationship** was obtained after application of 200 msec polarizing currents, stepped in 10% current intervals from 50% to 100% polarizing currents; excitability was assessed with 200 msec current step. Hyperpolazing current-threshold drift calculation was given as mean threshold reduction of the 2 most hyperpolarized intervals (i.e., 80%, 90%, 100% of threshold current).

Recovery cycle was performed using paired pulse stimuli: a supramaximal stimulus followed by a conditioning one at different interstimulus intervals (2-200 msec)[92]. Threshold changes at 2 and 2.5 msec interstimulus intervals were used to determine refractoriness. The minimum mean threshold change of 3 adjacent points defined superexcitability; instead, subexcitability was determined as the minimum mean threshold change obtained after a 10 msec interstimulus intervals.

4.5 BEHAVIORAL TESTS

Dynamic Aesthesiometer Test and Cold Plate Test were used to determine the alterations in pain perception and their changes due to OHP administration:

- **Dynamic Aesthesiometer Test** was used to detect symptoms of chronic OIPN. The mechanical nociceptive threshold was assessed using a Dynamic Aesthesiometer Test (model 37450, Ugo Basile Biological Instruments, Comerio, Italy), which generated a linearly increasing mechanical force. At each time point, after the acclimatization period, a pointed metallic filament (0.5-mm diameter) was applied to the plantar surface of the hind paw, which exerted a progressively increasing punctuate pressure, reaching up to 15 g within 15 seconds. The pressure evoking a clear voluntary hind-paw withdrawal response was recorded automatically and taken as representing the mechanical nociceptive threshold index. Results represented the maximal pressure (expressed in grams) tolerated by animals. There was an upper limit cut-off of 30 seconds, after which the mechanical stimulus was automatically terminated;

- **Cold Plate Test** was elected to detect acute OIPN. It was performed by using an apparatus (35100 - Hot/Cold Plate, Ugo Basile instruments, Comerio, Italy) composed by a Plexiglas cilinder and a thermostatic plate, able to reach variable temperatures. The animal was placed on the plate set at +4°C, free to move and walk. A blinded examiner determined the number of pain signs (ex: jumping, licking, increase anxiety etc.) in a trial of 5 minutes.

4.6 NEUROPATHOLOGY

Morphological analysis of caudal nerves.

Caudal nerves were harvested and processed for the morphological and morphometrical analysis. The tissues were fixed for 3 hours at room temperature in paraformaldehyde 4%/glutaraldehyde in glutaraldehyde 3%, post-fixed in OsO_4 and epoxy resin embedded. Morphological analysis was carried out on 1 µm-thick semi-thin sections stained with toluidine blue. At least two tissue blocks for each animal were sectioned and then examined with a light microscope.

Morphometrical analysis of caudal nerves

Harvested specimens were used for the morphometric examinations on toluidine blue stained 1-µm-thick semi-thin serial sections. For the morphometric analysis of myelinated fibers, sections were observed/pictures were taken with a photomicroscope (Nikon Eclipse E200; Leica Microsystems GmbH, Wetzlar, Germany) at a magnification of 60× and the morphometric analysis was performed using an automatic image analyzer (Image ProPlus 7.0, Meyer Instruments, Houston, US). In randomly selected sections collected from all specimens, all myelinated fibers evaluable in the analyzed space were counted and the external (total) and internal (axonal) diameters of myelinated fibers were measured, on at least 500

myelinated fibers/nerves. From both axonal and total fiber diameters, the histogram of fiber distribution was calculated and the ratio between the two diameters, the g-ratio (a well-established measure of degree of myelination), was automatically calculated for each set of individual axon and fiber diameter.

Intraepidermal nerve fibers density

Hind paws were collected after sacrifice and 5-mm round shaped were taken and immediately fixed in 2% paraphormaldehyde-lysine-periodate sodium. Section of 20 µm thickness were obtained and three sections from each footpad were randomly selected and immunostained with rabbit polyclonal antiprotein gene product 9.5 (PGP 9.5; GeneTex, Irvine, California, US) using a free-floating protocol. The total number of PGP-positive fibers IENFs were counted under a light microscope at 40X magnification with the assistance of a microscope-mounted video camera. Individual fibers were counted as they crossed the dermal–epidermal junction, and secondary branching within the epidermis will be excluded. The length of the epidermis was measured using a computerized system and the linear density of IENF/mm was thus obtained.

4.7 STATISTICAL ANALYSIS

Descriptive analysis was generated for all obtained variables. Parametric tests (*t-test*, *one-way Anova* followed by a 2-sided Dunnet test) where used for normally-distributed data and non-parametric tests (*Mann-Whitney U-test*, *Kruskal-Wallis test*, followed by pairwaise comparison, adjusted by the Bonferrroni correction for multiple tests) were used when they weren't normally distributed data; data where considered normally distributed if they passed the normality test (*Shapiro-Wilk Test of Normality*) and they fulfilled the central limit theorem (i.e., at least 30 values per group). Two-sided tests were employed. Significance was defined for all variables as p-value ≤ 0.05. All statistics were performed in SPSS (Statistical Package for Social Science: Version 20, SPSS Inc., Chicago, US), apart from NET data since Qtrac © has its own integrated package for statistical analysis (QtraS© Institute of Neurology, Queen Square, UK).

5 STUDY DESIGN

5.1 TASK 1 - PROOF OF CONCEPT: EMG AT REST AS AN *IN VIVO* INDIRECT EVIDENCE OF AXONAL HYPER-EXCITABILITY

5.1.1 Groups and treatment plan

Twenty-four Wistar female rats were divided into **3 groups** (n=8 each) as follows: **cisplatin** (CDDP) treated animals (group A, 2mg/kg, ip, 1qw); **paclitaxel** (PTX) treated ones (group B, 10mg/kg, iv, 1qw), **oxaliplatin** (OHP) treated one (group C, 5 mg/kg iv, 1qw).

5.1.2 Time points and variables collected

At base line standard nerve conduction studies (sensory recordings of distal caudal and digital nerves; motor recordings of caudal nerve) were performed to verify homogeneity among groups. EMG recordings at rest were performed to detect, indirectly, axonal hyperexcitability at these time points: at base line, at 24 hours after the single drug administration and at 7 days after administration.

See **Figure 16** for an overview of this Task.

Figure 16. Study design for TASK 1.

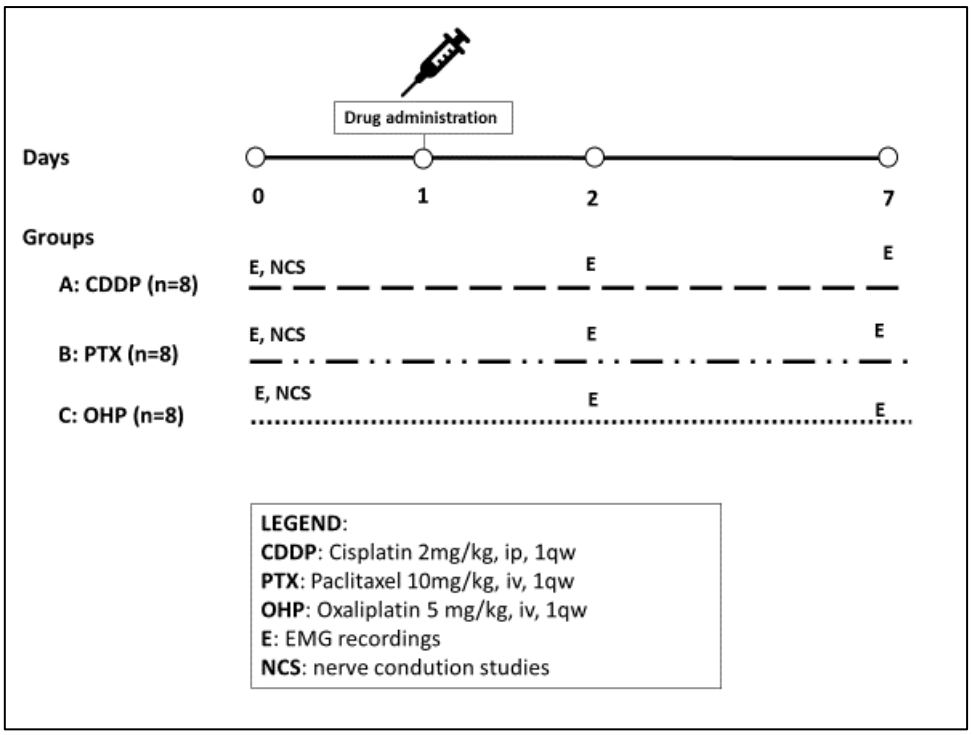

5.2 TASK 2 - ACUTE SETTING: NET RECORDINGS IN RATS AFTER A SINGLE OHP ADMINISTRATION

5.2.1 Groups and treatment plan

Twenty Wistar female rats were divided into **2 groups** (n=10 each) and treated as follows:

- **Group CTRL:** control animals (5% glucose solution, 1 qw);
- **Group OHP:** oxaliplatin treated ones (5 mg/kg iv, 1qw).

5.2.2 Time points and variables collected

The following variables were collected:

- **At base line**: nerve conduction studies (sensory recordings of distal caudal nerve and motor recordings of caudal nerve), Cold Plate Test;
- **After the administration**: Cold Plate Test (24 hours) and NET (caudal nerve, at 48 hours).

See **Figure 17** for an overview of this Task.

Figure 17. Study design for TASK 2.

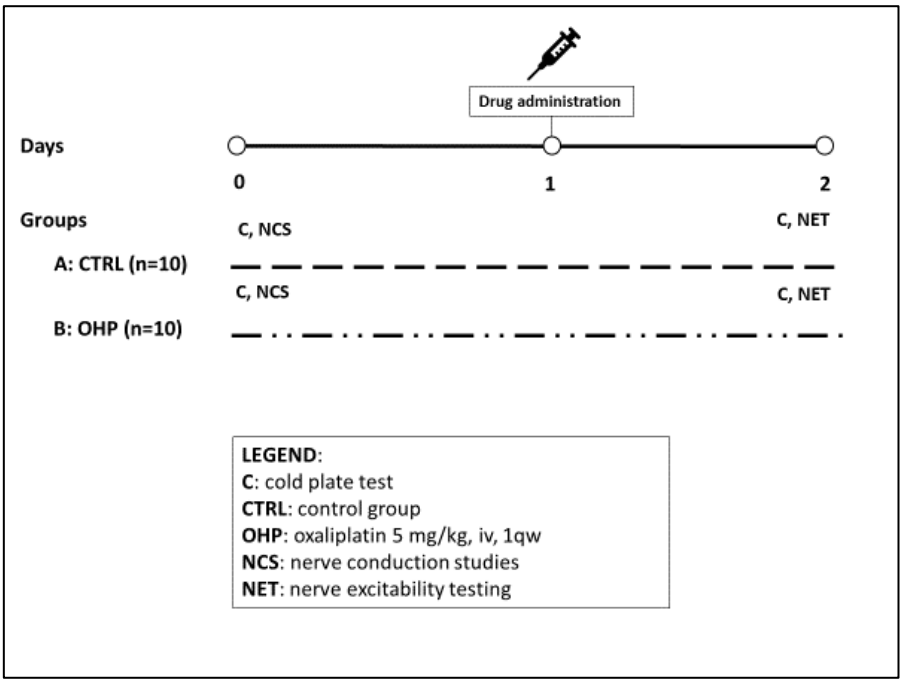

5.3 TASK 3 - CHRONIC SETTING: NET RECORDINGS IN RATS IN THE CONTEXT OF CHRONIC OHP ADMINISTRATION

5.3.1 Groups and treatment plan

Twenty Wistar female rats were divided into **2 groups** (n=10 each) and treated as follows:

- **Group CTRL:** control animals (5% glucose solution, 2 qwX4ws)
- **Group OHP:** oxaliplatin treated ones (3 mg/kg iv, 2qwX4ws).

5.3.2 Time points and variables collected

The following variables were collected:

- **At base line**: nerve conduction studies (sensory recordings of distal caudal, proximal caudal and digital nerves; motor recordings of caudal nerve), Dynamic and Cold Plate Test;
- **After the first administration**: Cold Plate Test (at 24 hours) and NET (caudal nerve, at 48 hours);
- **At the end of treatment:** nerve conduction studies, Dynamic and Cold Plate Test, NET (caudal nerve); harvesting of caudal nerve.
- **At 1 week after end of treatment**: NET (caudal nerve);
- **At 6 weeks after end of treatment**: nerve conduction studies, Dynamic and Cold Plate Test, NET (caudal nerve); harvesting of caudal nerves.

See **Figure 18** for an overview of the Schedule of this Task.

Figure 18. Schedule of TASK 3.

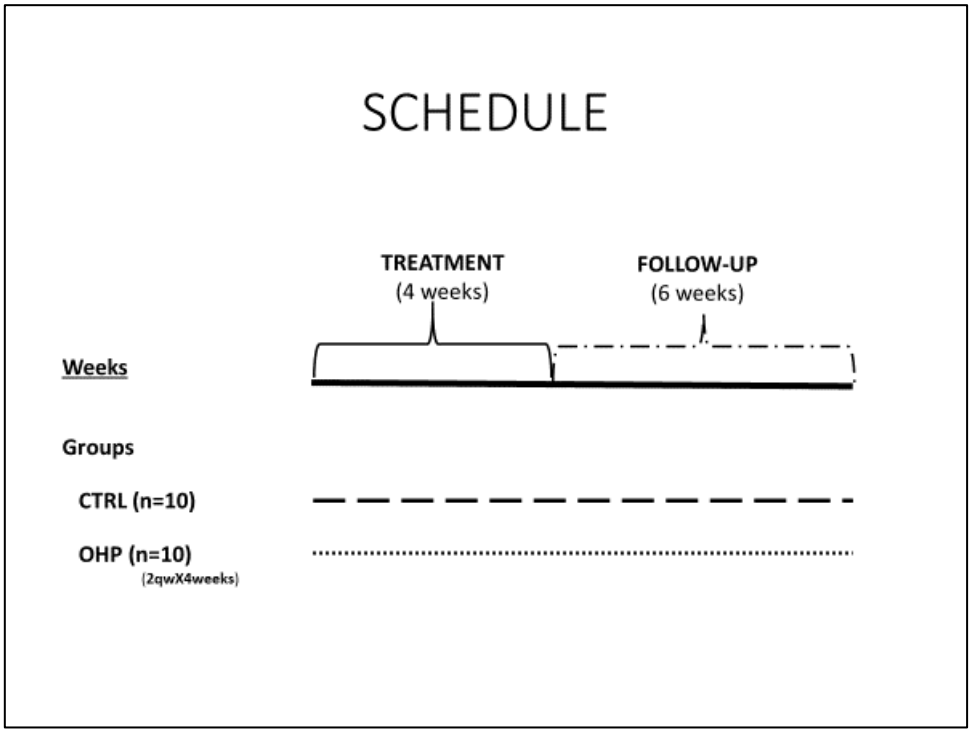

5.4 TASK 4 - REFINEMENT OF THE CHRONIC SETTING – A DOSE FINDING STUDY IN OHP TREATED RATS

5.4.1 Groups and treatment plan

Thirty-two Wistar female rats were divided into **4 groups** (n=8 each) and treated as follows:

- **Group CTRL:** control animals (5% glucose solution, 2 qwX4ws)
- **Group OHP3:** oxaliplatin 3 mg/Kg treated ones (3 mg/kg iv, 2qwX4ws)
- **Group OHP4:** oxaliplatin 4 mg/Kg treated ones (4 mg/kg iv, 2qwX4ws)
- **Group OHP5**: oxaliplatin 5 mg/Kg treated ones (5 mg/kg iv, 2qwX4ws)

5.4.2 Time points and variables collected

The following variables were collected:

- **At base line**: nerve conduction studies (sensory recordings of distal caudal, proximal caudal and digital nerves; motor recordings of caudal nerve), Cold Plate Test;
- **After the 1st administration**: Cold Plate Test (24 hours), NET (caudal nerve, at 24 hours);
- **At the end of treatment:** nerve conduction studies (sensory recordings of distal caudal, proximal caudal and digital nerves; motor recordings of caudal nerve), Cold Plate Test, NET (caudal nerve); harvesting of caudal nerves.

See **Figure 19** for an overview of the schedule of this Task.

Figure 19. Treatment arms for TASK 4.

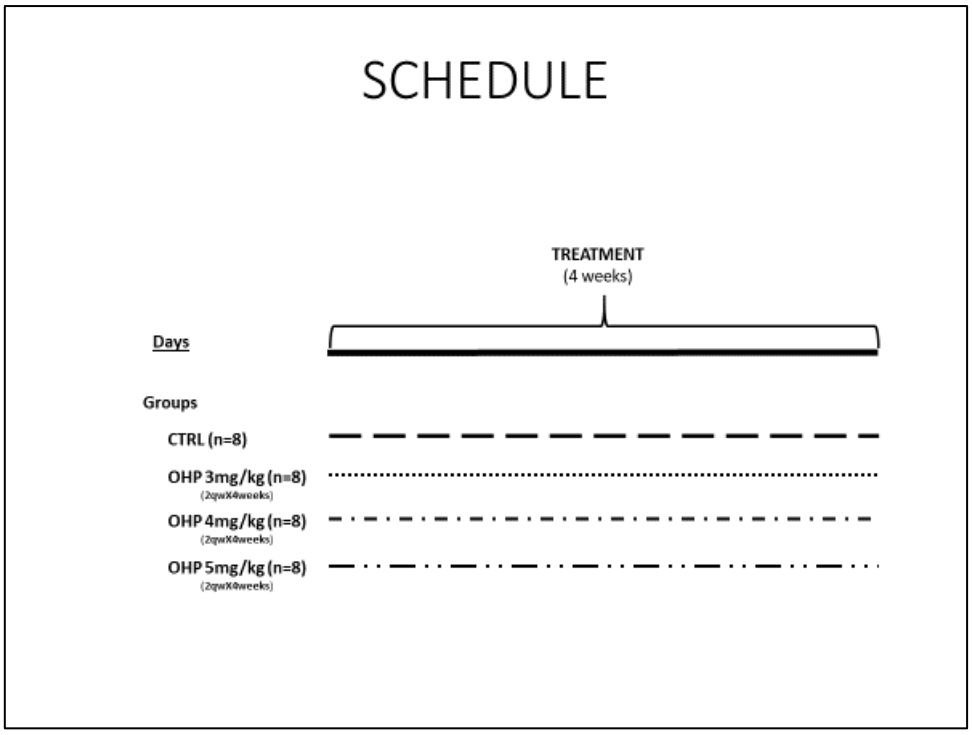

5.5 TASK 5 - TOPIRAMATE (TPM) AS A NEUROPROTECTANT AGENT AGAINST ACUTE OIPN IN RATS

5.5.1 Groups and treatment plan

Twenty-four Wistar female rats were divided into **3 groups** (n=8 each) and treated as follows:

- **Group CTRL:** control animals (5% glucose solution, 2 qwX4ws)
- **Group OHP:** oxaliplatin 5 mg/Kg treated ones (5 mg/kg iv, 1qw)
- **Group OHP+TPM:** oxaliplatin 5 mg/Kg + topiramate 100 mg/Kg treated ones (topiramate 100mg/Kg per os at 9am from day 0 to day 8; oxaliplatin 5 mg/kg iv, 1qw, at day 5 at 11 am)

5.5.2 Time points and variables collected

The following variables were collected:

- **At base line**: nerve conduction studies (sensory recordings of distal caudal, proximal caudal and digital nerves; motor recordings of caudal nerve);
- **Twenty-four hours after the administration**: NET (caudal nerve);
- **Forty-eight hours after the administration**: NET (caudal nerve);
- **Seventy-two-four hours after the administration**: nerve conduction studies (sensory recordings of distal caudal, proximal caudal and digital nerves; motor recordings of caudal nerve), NET (caudal nerve).

See **Table 1** for an overview of this Task.

Table 1. Study design for TASK 5.

GROUP	DAY 0	DAY 1	DAY 2	DAY 3	DAY 4	DAY5	DAY 6	DAY 7	DAY 8
CTRL	NCS	-	-	-	-	Vehicle iv	NET	-	NCS
OHP	NCS	-	-	-	-	OHP iv	NET	NET	NCS, NET
OHP+TPM	NCS	TPM per os	TPM per os	TPM per os	TPM per os	TPM per os + OHP iv	TPM per os, NET	TPM per os, NET	TPM per os, NCS, NET
NET: *nerve excitability testing;* ***NCS****: nerve conduction studies.*									

5.7 TASK 6 - TOPIRAMATE (TPM) AS A NEUROPROTECTANT AGENT AGAINST CHRONIC OIPN IN RATS

5.7.1 Groups and treatment plan

Forty Wistar female rats were divided into **4 groups** (n=10 each) and treated as follows:

- **Group CTRL:** control animals (5% glucose solution, 2 qwX4ws);
- **Group OHP:** oxaliplatin 5 mg/Kg treated ones (5 mg/kg iv, 1qw);
- **Group OHP+TPM:** oxaliplatin 5 mg/Kg + topiramate 100 mg/Kg treated ones (topiramate 100mg/Kg per os at 9am each day, starting 5 days before 1st Oxaliplatin injection and lasting until last Oxaliplatin administration; Oxaliplatin 5 mg/kg iv, 2qwX4ws, at 11am);
- **Group TPM:** topiramate 100 mg/Kg treated ones (topiramate 100mg/Kg per os at 9am each day with the same schedule as Group C).

5.7.2 Time points and variables collected

The following variables were collected (See **Figure 20** for an overview of the schedule of this Task):

- **At base line**: nerve conduction studies (sensory recordings of distal caudal, proximal caudal and digital nerves; motor recordings of caudal nerve), Dynamic Test;
- **At the end of treatment:** nerve conduction studies (sensory recordings of distal caudal, proximal caudal and digital nerves; motor recordings of caudal nerve), Dynamic Test, NET (caudal nerve); harvesting of caudal nerves and of right hind paw skin specimens.

Figure 20. Schedule for treatments of TASK 6.

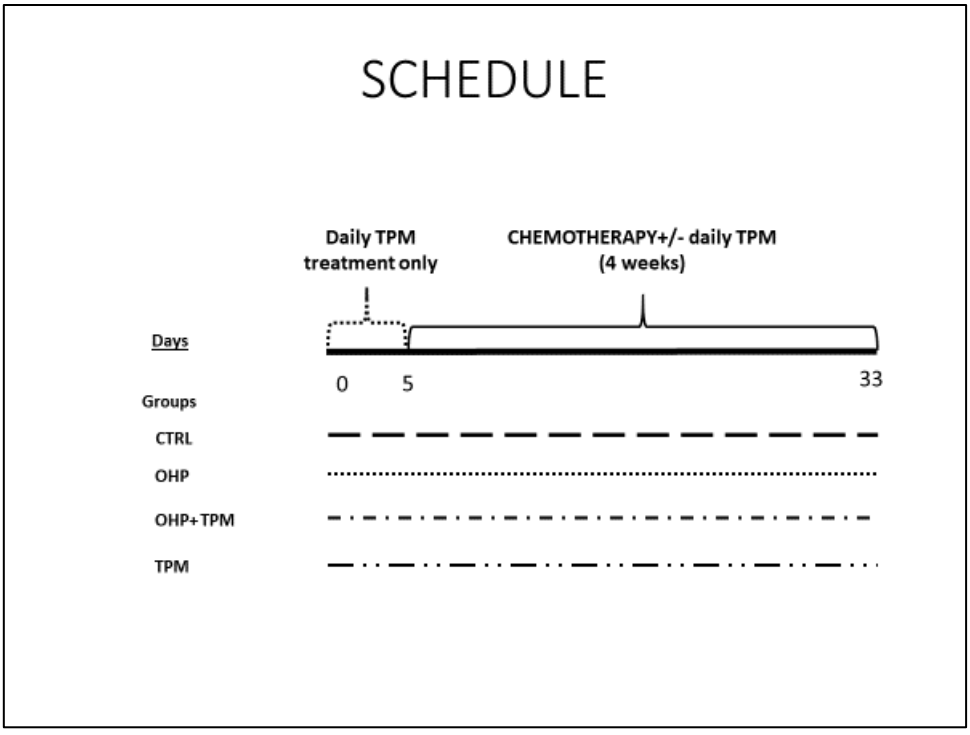

6 RESULTS

6.1 TASK 1 - PROOF OF CONCEPT: EMG AT REST AS AN *IN VIVO* INDIRECT EVIDENCE OF AXONAL HYPER-EXCITABILITY

In **TASK 1** EMG recordings were used to detect, indirectly, the presence of hyperexcitability after a single injection of three different chemotherapy drugs: Cisplatin (CDDP), Paclitaxel (PTX) and OHP. EMG recordings were performed at baseline, 24 hours after the administration and 7 days after it. To ensure homogeneity among groups, standard neurophysiology was performed at baseline. See **Study design** section for more details.

6.1.1 Baseline data

Descriptive statistic results for nerve conduction studies are reported in **Table 2**. **Table 3** summarizes statistical tests: no differences were present at base line for all neurophysiological parameters among all groups. EMG recordings were performed in all animals at base line; as can be seen in **Table 4** no spontaneous activity was present in any animal.

Table 2. Neurophysiological data at base line: descriptive statistics.

	Mean	Std. Deviation	Median	Percentile 25	Percentile 75
DC_AMP in CDDP group	95.05	25.05	86.10	81.00	102.50
DC_AMP in PTX group	95.61	41.58	92.15	64.75	128.50
DC_AMP in OHP group	89.39	27.92	79.50	71.95	107.45
DC_VEL in CDDP group	27.09	1.05	26.91	26.55	27.28
DC_VEL in PTX group	28.03	3.55	26.91	25.98	29.27
DC_ VEL in OHP group	26.71	1.82	26.32	25.65	27.54
D_AMP in CDDP group	98.89	21.46	94.00	83.55	115.45
D_AMP in PTX group	85.66	17.34	86.65	74.75	99.10
D_AMP in OHP group	81.45	17.49	81.55	75.30	93.30
D_VEL in CDDP group	37.33	1.38	37.67	36.21	38.31
D_VEL in PTX group	35.38	4.27	36.20	34.10	38.47
D_VEL in OHP group	36.31	4.23	36.59	31.97	39.48
M_AMP in CDDP group	6.36	2.27	7.05	4.90	7.75
M_AMP in PTX group	7.11	1.91	7.05	6.50	7.55
M_AMP in OHP group	7.77	4.93	6.85	4.00	10.75
M_VEL in CDDP group	42.41	2.67	42.55	40.99	43.96
M_VEL in PTX group	42.41	2.67	42.55	40.99	43.96
M_VEL in OHP group	42.60	3.58	43.02	41.67	43.48

***DC_AMP**: distal caudal nerve SNAP amplitude (µV); **DC_VEL**: distal caudal nerve sensory conduction velocity (m/sec); **D_AMP**: digital nerve SNAP amplitude (µV); **D_VEL**: digital nerve sensory conduction velocity (m/sec); **M_AMP**: caudal nerve CMAP amplitude (mV); **M_VEL**: caudal nerve motor conduction velocity.*

Table 3. Neurophysiological data at base line: Kruskall-Wallis test. ***DCAMP****: distal caudal nerve SNAP amplitude (µV);* ***DCVEL****: distal caudal nerve sensory conduction velocity (m/sec);* ***DAMP****: digital nerve SNAP amplitude (µV);* ***DVEL****: digital nerve sensory conduction velocity (m/sec);* ***MAMP****: caudal nerve CMAP amplitude (mV);* ***MVEL****: caudal nerve motor conduction velocity.*

Hypothesis Test Summary

	Null Hypothesis	Test	Sig.	Decision
1	The distribution of DCAMP is the same across categories of 1=CDDP; 2=PTX; 3=OHP.	Independent-Samples Kruskal-Wallis Test	,733	Retain the null hypothesis.
2	The distribution of DCVEL is the same across categories of 1=CDDP; 2=PTX; 3=OHP.	Independent-Samples Kruskal-Wallis Test	,651	Retain the null hypothesis.
3	The distribution of DAMP is the same across categories of 1=CDDP; 2=PTX; 3=OHP.	Independent-Samples Kruskal-Wallis Test	,368	Retain the null hypothesis.
4	The distribution of DVEL is the same across categories of 1=CDDP; 2=PTX; 3=OHP.	Independent-Samples Kruskal-Wallis Test	,704	Retain the null hypothesis.
5	The distribution of MAMP is the same across categories of 1=CDDP; 2=PTX; 3=OHP.	Independent-Samples Kruskal-Wallis Test	,945	Retain the null hypothesis.
6	The distribution of MVEL is the same across categories of 1=CDDP; 2=PTX; 3=OHP.	Independent-Samples Kruskal-Wallis Test	,998	Retain the null hypothesis.

Asymptotic significances are displayed. The significance level is ,05.

Table 4: EMG recordings at rest at base line.

GROUP	ANIMAL ID	QUADRICEPS FEMORIS	GASTROCNEMIOUS	FLEXOR DIGITORUM
GROUP A (CDDP treated)	*1*	Score 0	Score 0	Score 0
	2	Score 0	Score 0	Score 0
	3	Score 0	Score 0	Score 0
	4	Score 0	Score 0	Score 0
	5	Score 0	Score 0	Score 0
	6	Score 0	Score 0	Score 0
	7	Score 0	Score 0	Score 0
	8	Score 0	Score 0	Score 0
GROUP B (PTX TREATED)	*9*	Score 0	Score 0	Score 0
	10	Score 0	Score 0	Score 0
	11	Score 0	Score 0	Score 0
	12	Score 0	Score 0	Score 0
	13	Score 0	Score 0	Score 0
	14	Score 0	Score 0	Score 0
	15	Score 0	Score 0	Score 0
	16	Score 0	Score 0	Score 0
GROUP C (OHP treated)	*17*	Score 0	Score 0	Score 0
	18	Score 0	Score 0	Score 0
	19	Score 0	Score 0	Score 0
	20	Score 0	Score 0	Score 0
	21	Score 0	Score 0	Score 0
	22	Score 0	Score 0	Score 0
	23	Score 0	Score 0	Score 0
	24	Score 0	Score 0	Score 0
Score 0: no abnormal findings at rest; Score 1: increased insertional activity; Score 2: spontaneous high frequency firing lasting less than 2 seconds; Score 3: spontaneous high frequency firing lasting 2-5 seconds; Score 4: spontaneous high frequency firing lasting more than 5 seconds.				

6.1.2 Data after single drug administration

Twenty-four hours after drug administration all OHP treated animals showed abnormal findings of various degree; CDDP and PTX treated did not develop any abnormal spontaneous activity. **Table 5** summarizes scores for all alterations.

Table 5. EMG recordings at rest 24 hours after drug administration.

GROUP	ANIMAL ID	QUADRICEPS FEMORIS	GASTROCNEMIOUS	FLEXOR DIGITORUM
GROUP A (CDDP treated)	*1*	Score 0	Score 0	Score 0
	2	Score 0	Score 0	Score 0
	3	Score 0	Score 0	Score 0
	4	Score 0	Score 0	Score 0
	5	Score 0	Score 0	Score 0
	6	Score 0	Score 0	Score 0
	7	Score 0	Score 0	Score 0
	8	Score 0	Score 0	Score 0
GROUP B (PTX TREATED)	*9*	Score 0	Score 0	Score 0
	10	Score 0	Score 0	Score 0
	11	Score 0	Score 0	Score 0
	12	Score 0	Score 0	Score 0
	13	Score 0	Score 0	Score 0
	14	Score 0	Score 0	Score 0
	15	Score 0	Score 0	Score 0
	16	Score 0	Score 0	Score 0
GROUP C (OHP treated)	*17*	Score 3	Score 1	Score 4
	18	Score 4	Score 1	Score 3
	19	Score 4	Score 1	Score 4
	20	Score 2	Score 1	Score 1
	21	Score 4	Score 4	Score 3
	22	Score 2	Score 1	Score 2
	23	Score 3	Score 4	Score 4
	24	Score 4	Score 1	Score 4
Score 0: no abnormal findings at rest; Score 1: increased insertional activity; Score 2: spontaneous high frequency firing lasting less than 2 seconds; Score 3: spontaneous high frequency firing lasting 2-5 seconds; Score 4: spontaneous high frequency firing lasting more than 5 seconds.				

6.1.3 Data at 7 days after administration

EMG recordings at rest were back to the base line condition in all OHP animals; again, no alterations were seen in CDDP and PTX treated group. Data are shown in **Table 6**.

Table 6. EMG recordings at rest 7 days after drug administration.

GROUP	ANIMAL ID	QUADRICEPS FEMORIS	GASTROCNEMIOUS	FLEXOR DIGITORUM
GROUP A (CDDP treated)	*1*	Score 0	Score 0	Score 0
	2	Score 0	Score 0	Score 0
	3	Score 0	Score 0	Score 0
	4	Score 0	Score 0	Score 0
	5	Score 0	Score 0	Score 0
	6	Score 0	Score 0	Score 0
	7	Score 0	Score 0	Score 0
	8	Score 0	Score 0	Score 0
GROUP B (PTX TREATED)	*9*	Score 0	Score 0	Score 0
	10	Score 0	Score 0	Score 0
	11	Score 0	Score 0	Score 0
	12	Score 0	Score 0	Score 0
	13	Score 0	Score 0	Score 0
	14	Score 0	Score 0	Score 0
	15	Score 0	Score 0	Score 0
	16	Score 0	Score 0	Score 0
GROUP C (OHP treated)	*17*	Score 0	Score 1	Score 0
	18	Score 0	Score 0	Score 0
	19	Score 0	Score 0	Score 0
	20	Score 0	Score 0	Score 0
	21	Score 0	Score 0	Score 0
	22	Score 0	Score 0	Score 0
	23	Score 0	Score 0	Score 0
	24	Score 0	Score 0	Score 0
Score 0: no abnormal findings at rest; Score 1: increased insertional activity; Score 2: spontaneous high frequency firing lasting less than 2 seconds; Score 3: spontaneous high frequency firing lasting 2-5 seconds; Score 4: spontaneous high frequency firing lasting more than 5 seconds.				

6.1.4 Summary of inferences from TASK 1

Data from TASK 1 confirmed the presence of a transient state of hyperexcitability, only in the OHP treated group.

6.2 TASK 2 - ACUTE SETTING: NET RECORDINGS IN RATS AFTER A SINGLE OHP ADMINISTRATION

In **TASK 2** NET was used to detect, directly, the presence of hyperexcitability after a single injection of OHP. NET recordings were performed at baseline and after the administration. Cold Plate test was used to detect cold hyperalgesia at the same time points. To ensure homogeneity among groups, standard neurophysiology was performed at baseline. See **Study design** section for more details.

6.2.1 Baseline data

Descriptive statistic results for nerve conduction studies are reported in **Table 7**. **Table 8** summarizes statistical tests: no differences were present at base line for all neurophysiological parameters between the 2 groups. Cold plate test descriptive statistics are shown in **Table 9**; **Table 10** shows statistical testing: no significant differences were present between the 2 groups.

Table 7. Neurophysiological data at base-line: descriptive statistics.

	Mean	Std. Deviation	Median	Percentile 25	Percentile 75
DC_AMP in CTRL	48.00	9.29	47.90	39.90	54.20
DC_AMP in OHP	47.49	13.09	51.00	33.70	56.70
DC_VEL in CTRL	28.43	2.16	29.70	26.30	30.30
DC_VEL in OHP	28.91	2.02	28.80	28.00	30.30
M_AMP in CTRL	4.56	2.11	4.30	2.80	6.40
M_AMP in OHP	6.37	2.20	7.10	4.00	7.90
M_VEL in CTRL	40.07	1.75	40.80	38.50	41.70
M_VEL in OHP	38.76	4.30	40.00	38.50	41.70

***DC_AMP**: distal caudal nerve SNAP amplitude (µV); **DC_VEL**: distal caudal nerve sensory conduction velocity (m/sec); **M_AMP**: caudal nerve CMAP amplitude (mV); **M_VEL**: caudal nerve motor conduction velocity.*

Table 8. Neurophysiological data at base line: Mann-Whitney U-test. ***DCAMP**: distal caudal nerve SNAP amplitude (µV); **DCVEL**: distal caudal nerve sensory conduction velocity (m/sec); **MAMP**: caudal nerve CMAP amplitude (mV); **MVEL**: caudal nerve motor conduction velocity.*

Hypothesis Test Summary

	Null Hypothesis	Test	Sig.	Decision
1	The distribution of DCAMP is the same across categories of 1=CTRL; 2=OHP.	Independent-Samples Mann-Whitney U Test	,902[1]	Retain the null hypothesis.
2	The distribution of DCVEL is the same across categories of 1=CTRL; 2=OHP.	Independent-Samples Mann-Whitney U Test	,902[1]	Retain the null hypothesis.
3	The distribution of MAMP is the same across categories of 1=CTRL; 2=OHP.	Independent-Samples Mann-Whitney U Test	,209[1]	Retain the null hypothesis.
4	The distribution of MVEL is the same across categories of 1=CTRL; 2=OHP.	Independent-Samples Mann-Whitney U Test	,805[1]	Retain the null hypothesis.

Asymptotic significances are displayed. The significance level is ,05.

[1]Exact significance is displayed for this test.

Table 9. Cold Plate Test at base-line: descriptive statistics.

	Mean	Std. Deviation	Median	Percentile 25	Percentile 75
COLD150 in CTRL group	5.67	1.73	6.00	5.00	6.00
COLD150 in OHP group	5.22	2.59	6.00	4.00	6.00
COLD300 in CTRL group	10.44	3.36	12.00	8.00	13.00
COLD300 in OHP group	9.44	3.75	9.00	8.00	12.00
COLD150: number of signs from 0 to 150 seconds; **COLD300**: number of signs from 151 to 300 seconds.					

Table 10. Cold Plate Test at base-line: Mann-Whitney U-test. ***COLD150****: number of signs from 0 to 150 seconds;* ***COLD300****: number of signs from 151 to 300 seconds.*

Hypothesis Test Summary

	Null Hypothesis	Test	Sig.	Decision
1	The distribution of COLD150 is the same across categories of 1=CTRL; 2=OHP.	Independent-Samples Mann-Whitney U Test	,730[1]	Retain the null hypothesis.
2	The distribution of COLD300 is the same across categories of 1=CTRL; 2=OHP.	Independent-Samples Mann-Whitney U Test	,666[1]	Retain the null hypothesis.

Asymptotic significances are displayed. The significance level is ,05.

[1]Exact significance is displayed for this test.

6.2.2 Data after single OHP administration

Cold plate test descriptive statistics are shown in **Table 11**; **Table 12** shows statistical testing. Significant difference was present between the 2 groups: OHP treated group showed increased signs of cold hyperalgesia. For what regards NET, a difference was demonstrated between the 2 groups for recovery cycle parameters: **Table 13** and **Figure 21** shows values and levels of significance. OHP group showed superexcitability significantly set at less negative values (i.e. the curve was pulled upwards) compared to CTRL animals.

Table 11. Cold Plate Test after single OHP administration: descriptive statistics.

	Mean	Standard Deviation	Median	Percentile 25	Percentile 75
COLD150 in CTRL group	3.33	2.00	3.00	2.00	5.00
COLD150 in OHP group	3.22	1.09	3.00	3.00	4.00
COLD300 in CTRL group	6.22	3.93	5.00	3.00	9.00
COLD300 in OHP group	11.78	2.99	12.00	11.00	14.00
COLD150: number of signs from 0 to 150 seconds; **COLD300**: number of signs from 151 to 300 seconds.					

Table 12. Cold Plate Test after single OHP administration: Mann-Whitney U-test. ***COLD150POST****: number of signs from 0 to 150 seconds;* ***COLD300POST****: number of signs from 151 to 300 seconds.*

Hypothesis Test Summary

	Null Hypothesis	Test	Sig.	Decision
1	The distribution of COLD150POST is the same across categories of 1=CTRL;2=OHP.	Independent-Samples Mann-Whitney U Test	,863[1]	Retain the null hypothesis.
2	The distribution of COLD300POST is the same across categories of 1=CTRL;2=OHP.	Independent-Samples Mann-Whitney U Test	,006[1]	Reject the null hypothesis.

Asymptotic significances are displayed. The significance level is ,05.

[1]Exact significance is displayed for this test.

Table 13. NET statistics after single OHP administration: Mann Whitney U-Test

VARIABLE	*CTRL GROUP [median, (Q1,Q3)]*	*OHP GROUP [median, (Q1,Q3)]*	*Mann-Whitney U-test*
Stimulus-response and strength-duration properties			
Strength-duration time constant (msec)	0.164 (0.15, 0.194)	0.204 (0.187, 0.217)	p=0.28
Rheobase (mA)	-0.0879 (-0.129, -0.0635)	-0.0685 (-0.147, -0.0305)	p=0.64
Current Threshold properties			
Resting I/V slope	0.799 (0.778, 0.854)	0.844 (0.869, 0.92)	p=0.25
Minimum I/V slope	0.399 (0.294, 0.392)	0.265 (0.236, 0.326)	p=0.17
Hyperpolarazing I/V slope	0.507 (0.424, 0.58)	0.434 (0.401, 0.514)	p=0.59
Threshold electrotonus			
TEh(90-100 msec)	-87.5 (-91.7, -83.9)	-88.2 (-90.5, -77.2)	p=0.95
TEd(10-20 msec)	51.6 (50.3, 52.6)	52.8 (48.9, 53.2)	p=0.95
TEd(40-60 msec)	51 (50.3, 53)	49.4 (46.6, 50.5)	p=0.09
TEd(90-100 msec)	48.3 (47.7, 50.6)	47.6 (45.2, 48.1)	p=0.13
TEh(10-20 msec)	-58.3 (-62.5, -56.3 n=7)	-59.7 (-62.7, -55.3)	p=0.87
TEd(undershoot)	-3.33 (-4.95, -2.09)	-4.38 (-5.06, -3.18)	p=0.53
TEh(overshoot)	3.97 (3.46, 5.34)	7.24 (5.74, 9.69)	p=0.07
TEd(peak)	53.3 (52.4, 54.7)	52.9 (50.5, 54.1)	p=0.46
S2 accomodation	4.3 (1.89, 5.21)	5.95 (4.52, 6.63)	p=0.12
Accomodation half-time	48.8 (45.4, 66.2)	39.8 (36.1, 51.4)	p=0.19
TEh(20-40 msec)	-71.6 (-77.5, -67.9)	-72 (-76.2, -65.4)	p=0.87
TEh(slope 101-140 msec)	1.17 (1.07, 1.25)	1.01 (0.902, 1.28)	p=0.61
TEd20(peak)	26.7 (25.6, 28)	26.1 (25.1, 28.1)	p=0.69
TEd40(Accomodation)	5 (2.7, 5.45)	6.35 (5.4, 6.88)	p=0.07
TEd20(10-20 msec)	25.1 (23.9, 25.5)	24.4 (23.1, 25.1)	p=0.40
TEh20(10-20 msec)	-24.6 (-25.5, -23.7)	-24.5 (-25.6, -23.7)	p=0.95
Recovery Cycle			
Relative Refractory Period (msec)	0.273 (0.258, 0.336)	0.368 (0.355, 0.378)	p=0.30
Superexcitability (%)	-13.3 (-15, -11.6)	-6.8 (-8.08, -6.54)	**p<0.001*** **
Subexcitability (%)	2.18 (1.58, 3.12)	4.51 (1.52, 5.2)	p=0.14
Superexcitability at 7 msec	-9.67 (-11.5, -7.16)	-4.66 (-6.69, -3.63)	**p<0.01** **
Superexcitability at 5 msec	-12.8 (-14.2, -10.5)	-7.2 (-8.95, -6.09)	**p<0.00158*** **
Refractoriness at 2 msec	-3.66 (-6.44, -0.258)	7.12 (3.97, 9.6)	p=0.11
Refractoriness at 2.5msec	-11.4 (-13, -6.08)	-3.1 (-3.14, -2.27)	p=0.11

Figure 21. NET results after single OHP administration. ***A****: I/V relationship;* ***B****: Strength-duration time constant;* ***C****: Threshold electrotonus;* ***D****: Recovery Cycle.*

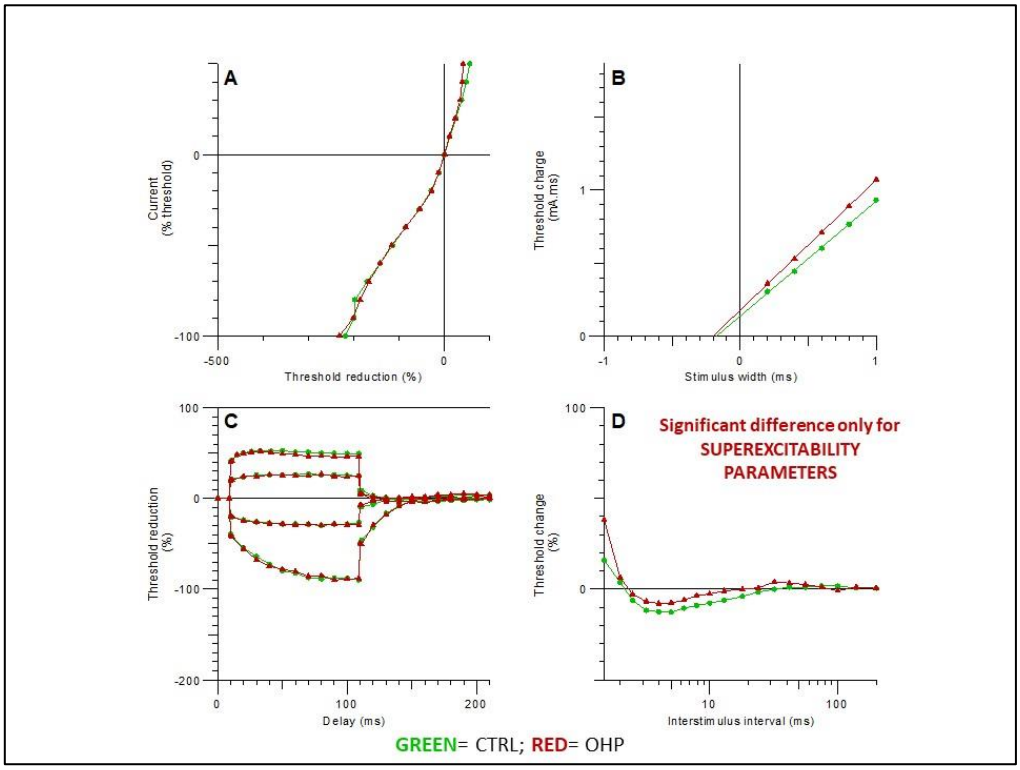

6.2.3 Summary of inferences from TASK 2

Both NET and Cold Plate test confirmed the induction of acute OIPN in the animal model.

6.3 TASK 3 - CHRONIC SETTING: NET RECORDINGS IN RATS IN THE CONTEXT OF CHRONIC OHP ADMINISTRATION

In **TASK 3**, the induction of both acute and chronic OIPN was sought for: a control group was compared to a OHP administered one (1 month of treatment). NET and Cold Plate Test were used to detect acute OIPN. Chronic OIPN was assessed thanks to standard neurophysiology and Dynamic Test. After the treatment, a follow-up period of 6 weeks was performed. Confirmatory neuropathological analyses were executed at the end of treatment and at the end of the observational period. To ensure homogeneity among groups, standard neurophysiology was performed at baseline. See **Study design** section for more details.

6.3.1 Baseline data

Descriptive statistic for nerve conduction studies data is reported in **Table 14**; in **Table 15** Mann-Whitney U-test results are reported: no differences were present between the 2 groups for all variables. Descriptive statistic for all behavioral tests is reported in **Table 16**; in **Table 17** Mann-Whitney U-test results are reported: no differences were present between the 2 groups for all variables.

Table 14. Neurophysiological data at baseline: descriptive statistics.

	Mean	Std. Deviation	Median	Percentile 25	Percentile 75
DC_AMP in CTRL group	53,70	7,34	53,95	47,10	58,30
DC_VEL in CTRL group	28,00	2,25	27,80	26,80	28,80
DC_AMP in OHP group	49,02	6,49	51,15	46,00	52,90
DC_VEL in OHP group	27,49	1,78	27,15	26,10	28,60
PC_AMP in CTRL group	131,91	22,68	128,35	116,50	140,30
PC_VEL in CTRL group	35,05	1,87	35,30	33,30	36,10
PC_AMP in OHP group	142,77	18,77	143,50	123,50	152,90
PC_VEL in OHP group	36,45	2,56	36,20	34,90	37,50
D_AMP in CTRL group	58,03	7,53	58,00	52,30	62,20
D_VEL in CTRL group	34,87	2,46	35,20	33,30	36,30
D_AMP in OHP group	54,54	6,08	55,40	52,00	58,30
D_VEL in OHP group	34,10	2,15	34,15	33,70	35,40
M_AMP in CTRL group	5,98	1,91	5,65	4,80	6,00
M_VEL in CTRL group	36,35	2,82	37,00	33,30	37,70
M_AMP in OHP group	7,05	1,93	7,45	6,10	8,00
M_VEL in OHP group	35,82	2,73	35,30	33,90	38,50

***DC_AMP**: distal caudal nerve SNAP amplitude (µV); **DC_VEL**: distal caudal nerve sensory conduction velocity (m/sec); **D_AMP**: digital nerve SNAP amplitude (µV); **D_VEL**: digital nerve sensory conduction velocity (m/sec); **M_AMP**: caudal nerve CMAP amplitude (mV); **M_VEL**: caudal nerve motor conduction velocity; **PC_AMP**: proximal caudal nerve SNAP amplitude (µV); **PC_VEL**: proximal caudal nerve sensory conduction velocity (m/sec).*

Table 15. Neurophysiological data at base-line: Mann-Whitney U-test results. ***DCAMP****: distal caudal nerve SNAP amplitude (µV);* ***DCVEL****: distal caudal nerve sensory conduction velocity (m/sec);* ***DAMP****: digital nerve SNAP amplitude (µV);* ***DVEL****: digital nerve sensory conduction velocity (m/sec);* ***MAMP****: caudal nerve CMAP amplitude (mV);* ***MVEL****: caudal nerve motor conduction velocity;* ***PCAMP****: proximal caudal nerve SNAP amplitude (µV);* ***PCVEL****: proximal caudal nerve sensory conduction velocity (m/sec).*

Hypothesis Test Summary

	Null Hypothesis	Test	Sig.	Decision
1	The distribution of CDAMP is the same across categories of 1=CTRL; 2=OHP.	Independent-Samples Mann-Whitney U Test	,165[1]	Retain the null hypothesis.
2	The distribution of CDVEL is the same across categories of 1=CTRL; 2=OHP.	Independent-Samples Mann-Whitney U Test	,579[1]	Retain the null hypothesis.
3	The distribution of CPAMP is the same across categories of 1=CTRL; 2=OHP.	Independent-Samples Mann-Whitney U Test	,190[1]	Retain the null hypothesis.
4	The distribution of CPVEL is the same across categories of 1=CTRL; 2=OHP.	Independent-Samples Mann-Whitney U Test	,315[1]	Retain the null hypothesis.
5	The distribution of DAMP is the same across categories of 1=CTRL; 2=OHP.	Independent-Samples Mann-Whitney U Test	,353[1]	Retain the null hypothesis.
6	The distribution of DVEL is the same across categories of 1=CTRL; 2=OHP.	Independent-Samples Mann-Whitney U Test	,529[1]	Retain the null hypothesis.
7	The distribution of MAMP is the same across categories of 1=CTRL; 2=OHP.	Independent-Samples Mann-Whitney U Test	,089[1]	Retain the null hypothesis.
8	The distribution of MVEL is the same across categories of 1=CTRL; 2=OHP.	Independent-Samples Mann-Whitney U Test	,796[1]	Retain the null hypothesis.

Asymptotic significances are displayed. The significance level is ,05.

[1]Exact significance is displayed for this test.

Table 16. Behavioral tests at base line: descriptive statistics.

	Mean	Std. Deviation	Median	Percentile 25	Percentile 75
COLD150 in CTRL group	3.70	2.41	3.50	2.00	5.00
COLD150 in OHP group	3.40	2.59	3.00	1.00	4.00
COLD300 in CTRL group	9.90	6.67	7.00	6.00	13.00
COLD300 in OHP group	10.30	9.01	7.00	4.00	11.00
DYN in CTRL group	30.36	2.02	30.43	28.77	30.70
DYN in OHP group	29.88	4.63	30.29	28.23	31.12

COLD150: number of signs from 0 to 150 seconds; **COLD300**: number of signs from 151 to 300 seconds; **DYN**: score for Dynamic test.

Table 17. Behavioral test at base-line: Mann-Whitney U-test. COLD150bas: number of signs from 0 to 150 seconds; **COLD300bas:** number of signs from 151 to 300 seconds; **DYNbas:** score for Dynamic test.

Hypothesis Test Summary

	Null Hypothesis	Test	Sig.	Decision
1	The distribution of COLD150bas is the same across categories of 1=CTRL; 2=OHP.	Independent-Samples Mann-Whitney U Test	,739[1]	Retain the null hypothesis.
2	The distribution of COLD300bas is the same across categories of 1=CTRL; 2=OHP.	Independent-Samples Mann-Whitney U Test	,796[1]	Retain the null hypothesis.
3	The distribution of DYNbas is the same across categories of 1=CTRL; 2=OHP.	Independent-Samples Mann-Whitney U Test	,579[1]	Retain the null hypothesis.

Asymptotic significances are displayed. The significance level is ,05.

[1]Exact significance is displayed for this test.

6.3.2 Data after 1st administration

Descriptive statistic for Cold Plate Test is reported in **Table 18**; in **Table 19** Mann-Whitney U-test results are reported: no differences were present between the 2 groups for all variables. For what regards NET, no difference was seen between the 2 groups; **Table 20** and **Figure 22** summarized the data.

Table 18. Cold plate test after 1st administration: descriptive statistics.

	Mean	Std. Deviation	Median	Percentile 25	Percentile 75
COLD150 in CTRL group	4.40	2.99	3.50	2.00	6.00
COLD150 in OHP group	4.40	3.24	4.00	2.00	6.00
COLD300 in CTRL group	8.50	3.47	7.50	5.00	12.00
COLD300 in OHP group	14.20	9.44	11.00	7.00	23.00

COLD150: number of signs from 0 to 150 seconds; **COLD300**: number of signs from 151 to 300 seconds; **DYN**: score for Dynamic test.

Table 19. Cold plate test after 1st administration: Mann-Whitney U-test. COLD150h24: number of signs from 0 to 150 seconds; **COLD300h24:** number of signs from 151 to 300 seconds.

Hypothesis Test Summary

	Null Hypothesis	Test	Sig.	Decision
1	The distribution of COLD150h24 is the same across categories of 1=CTRL; 2=OHP.	Independent-Samples Mann-Whitney U Test	,971[1]	Retain the null hypothesis.
2	The distribution of COLD300h24 is the same across categories of 1=CTRL; 2=OHP.	Independent-Samples Mann-Whitney U Test	,247[1]	Retain the null hypothesis.

Asymptotic significances are displayed. The significance level is ,05.

[1]Exact significance is displayed for this test.

Table 20. NET after 1st administration

VARIABLE	*CTRL GROUP [median, (Q1,Q3)]*	*OHP GROUP [median, (Q1,Q3)]*	*Mann-Whitney U-test*
Stimulus-response and strength-duration properties			
Strength-duration time constant (msec)	0.185 (0.168, 0.216)	0.209 (0.181, 0.22)	p=0.44
Rheobase (mA)	-0.129 (-0.177, -0.0803)	-0.0757 (-0.109, -0.0445)	p=0.20
Current Threshold properties			
Resting I/V slope	0.885 (0.861, 0.915)	0.908 (0.893, 0.976)	p=0.35
Minimum I/V slope	0.333 (0.282, 0.384)	0.361 (0.324, 0.363)	p=0.53
Hyperpolarazing I/V slope	0.638 (0.508, 0.706)	0.762 (0.646, 0.809)	p=0.05
Threshold electrotonus			
TEh(90-100 msec)	-72.5 (-79.6, -66.7)	-79.9 (-84.4, -74.2)	p=0.16
TEd(10-20 msec)	51.9 (51.4, 53.3)	52.3 (49.4, 53.1)	p=0.58
TEd(40-60 msec)	48.7 (48.3, 51)	47.7 (45.6, 49.6)	p=0.31
TEd(90-100 msec)	46.1 (44.5, 48)	44.6 (43.1, 46.6)	p=0.35
TEh(10-20 msec)	-57.3 (-60.5, -54.6)	-60.4 (-61.8, -59)	p=0.25
TEd(undershoot)	-5.56 (-6.88, -4.05)	-6.77 (-7.61, -3.76)	p=0.63
TEh(overshoot)	7.87 (6.11, 9.47)	7.02 (5.43, 8.24)	p=0.35
TEd(peak)	52.2 (51.5, 55.2)	52.6 (48.7, 53)	p=0.63
S2 accomodation	5.68 (5.01, 8.08)	5.97 (5.55, 7.1)	p=0.74
Accomodation half-time	43.3 (37, 52.9)	47.1 (38.1, 48.9)	p=0.80

VARIABLE	*CTRL GROUP [median, (Q1,Q3)]*	*OHP GROUP [median, (Q1,Q3)]*	*Mann-Whitney U-test*
TEh(20-40 msec)	-65.7 (-71.5, -61.6)	-70.1 (-72.4, -69.4)	p=0.11
TEh(slope 101-140 msec)	0.929 (0.68, 1.11)	1.02 (0.949, 1.13)	p=0.44
TEd20(peak)	26.3 (25.8, 27.4)	26 (24, 27.3)	p=0.58
TEd40(Accomodation)	5.3 (4.97, 7.4)	6.05 (5.05, 6.88)	p=0.97
TEd20(10-20 msec)	24.8 (24.2, 25.2)	25.1 (21.3, 25.9)	p=0.79
TEh20(10-20 msec)	-24.5 (-25.7, -23.1)	-24.7 (-25.1, -23.8)	p=0.85
Recovery Cycle			
Relative Refractory Period (msec)	0.457 (0.374, 0.514)	0.375 (0.366, 0.483)	p=0.66
Superexcitability (%)	-12.7 (-13.4, -11.6)	-12.6 (-13.4, -10)	p=0.74
Subexcitability (%)	4.91 (3.27, 6.13)	4.26 (2.21, 5.75)	p=0.63
Superexcitability at 7 msec	-10.9 (-13.4, -9.02)	-9.32 (-10.7, -8.51)	p=0.19
Superexcitability at 5 msec	-12.8 (-14, -11.7)	-13.2 (-14.1, -10.4)	p=0.97
Refractoriness at 2 msec	7.57 (-3.32, 17.2)	0.91 (-4.93, 9.23)	p=0.48
Refractoriness at 2.5msec	7.57 (-3.32, 17.2)	0.91 (-4.93, 9.23)	p=0.48

Figure 22. NET results after first OHP administration. ***A****: I/V relationship;* ***B****: Strength-duration time constant;* ***C****: Threshold electrotonus;* ***D****: Recovery Cycle.*

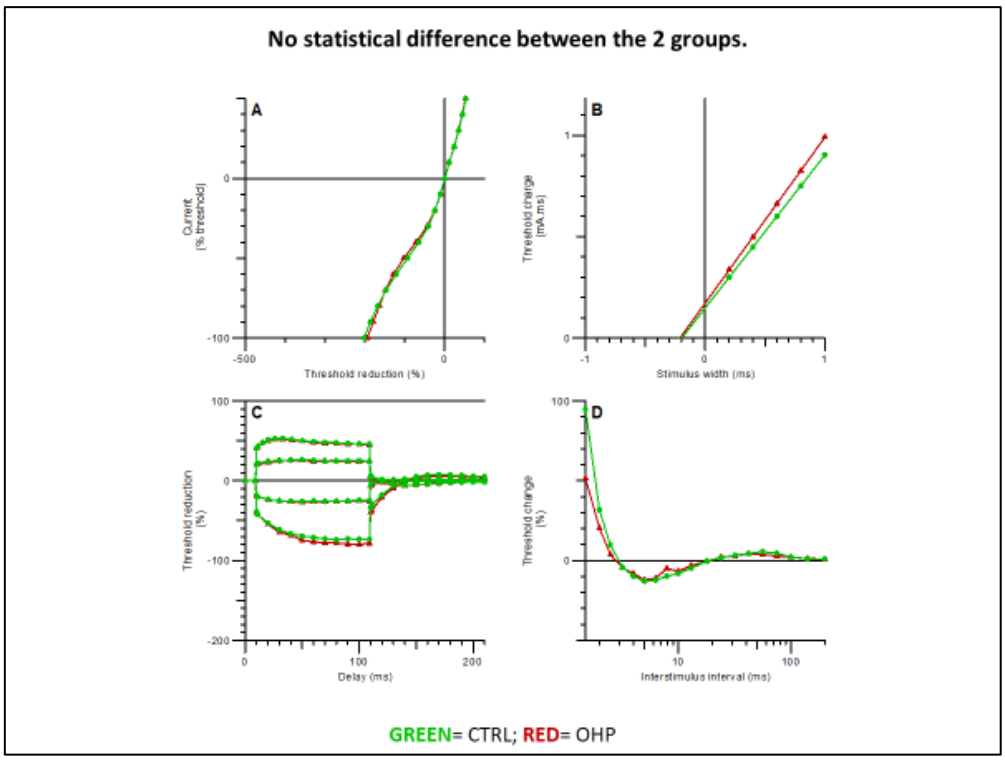

6.3.3 End of treatment data

Descriptive statistic for nerve conduction studies is reported in **Table 21**; **in Table 22** Mann-Whitney U-test results are reported: distal caudal and digital SNAP amplitude were significantly reduced in OHP group compared to controls (p-value 0.008 and 001 respectively). Descriptive statistic for all behavioral tests is reported in **Table 23**; in **Table 24** Mann-Whitney U-test results are reported: only Dynamic test score was reduced in OHP treated animals (p-value <0.001); cold plate test score was not different between the 2 groups. NET findings and statistical test results are shown in **Table 25** and **Figure 23**. There was a difference between the 2 groups only for recovery cycle parameters for what regards superexcitability (%), superexcitability at 7 and 5 msec (p-value respectively: <0.005, <0.001, 0.02).

Caudal nerve morphological analysis showed a rather mild axonopathy in treated animals (see **Figure 26** in which CTRL and OHP animal caudal nerves at end of treatment and at follow-up are shown).

Table 21. Neurophysiological data at end of treatment: descriptive statistics.

	Mean	Std. Deviation	Median	Percentile 25	Percentile 75
DC_AMP in CTRL group	64.11	22.64	58.30	51.40	63.40
DC_VEL in CTRL group	32.10	5.29	30.60	29.70	33.30
DC_AMP in OHP group	46.49	8.61	44.50	42.00	53.80
DC_VEL in OHP group	28.95	2.46	29.25	27.80	30.00
PC_AMP in CTRL group	129.42	16.85	132.70	129.00	136.40
PC_VEL in CTRL group	38.09	2.92	38.50	35.30	40.00
PC_AMP in OHP group	124.53	10.63	125.90	117.30	132.60
PC_VEL in OHP group	37.33	1.49	37.50	36.60	38.50
D_AMP in CTRL group	78.87	13.22	80.70	65.50	85.00
D_VEL in CTRL group	37.98	2.63	37.80	36.80	40.00
D_AMP in OHP group	55.44	9.32	55.95	48.10	62.10
D_VEL in OHP group	38.15	1.93	37.55	36.90	39.40
M_AMP in CTRL group	5.93	1.41	6.30	5.50	6.80
M_VEL in CTRL group	40.28	2.95	40.00	39.20	41.70
M_AMP in OHP group	5.96	2.31	5.70	4.30	7.50
M_VEL in OHP group	39.00	3.97	38.45	37.00	40.80

***DC_AMP**: distal caudal nerve SNAP amplitude (µV); **DC_VEL**: distal caudal nerve sensory conduction velocity (m/sec); **D_AMP**: digital nerve SNAP amplitude (µV); **D_VEL**: digital nerve sensory conduction velocity (m/sec); **M_AMP**: caudal nerve CMAP amplitude (mV); **M_VEL**: caudal nerve motor conduction velocity; **PC_AMP**: proximal caudal nerve SNAP amplitude (µV); **PC_VEL**: proximal caudal nerve sensory conduction velocity (m/sec).*

Table 22. Neurophysiological data at end of treatment: Mann-Whitney U-test. ***DCAMP****: distal caudal nerve SNAP amplitude (µV);* ***DCVEL****: distal caudal nerve sensory conduction velocity (m/sec);* ***DAMP****: digital nerve SNAP amplitude (µV);* ***DVEL****: digital nerve sensory conduction velocity (m/sec);* ***MAMP****: caudal nerve CMAP amplitude (mV);* ***MVEL****: caudal nerve motor conduction velocity;* ***PCAMP****: proximal caudal nerve SNAP amplitude (µV);* ***PCVEL****: proximal caudal nerve sensory conduction velocity (m/sec).*

Hypothesis Test Summary

	Null Hypothesis	Test	Sig.	Decision
1	The distribution of DCAMPend is the same across categories of 1=CTRL;2=OHP.	Independent-Samples Mann-Whitney U Test	,008[1]	Reject the null hypothesis.
2	The distribution of DCVELend is the same across categories of 1=CTRL;2=OHP.	Independent-Samples Mann-Whitney U Test	,113[1]	Retain the null hypothesis.
3	The distribution of CPAMPend is the same across categories of 1=CTRL;2=OHP.	Independent-Samples Mann-Whitney U Test	,211[1]	Retain the null hypothesis.
4	The distribution of CPVELend is the same across categories of 1=CTRL;2=OHP.	Independent-Samples Mann-Whitney U Test	,497[1]	Retain the null hypothesis.
5	The distribution of DAMPend is the same across categories of 1=CTRL;2=OHP.	Independent-Samples Mann-Whitney U Test	,001[1]	Reject the null hypothesis.
6	The distribution of DVELend is the same across categories of 1=CTRL;2=OHP.	Independent-Samples Mann-Whitney U Test	,720[1]	Retain the null hypothesis.
7	The distribution of MAMPend is the same across categories of 1=CTRL;2=OHP.	Independent-Samples Mann-Whitney U Test	,968[1]	Retain the null hypothesis.
8	The distribution of MVELend is the same across categories of 1=CTRL;2=OHP.	Independent-Samples Mann-Whitney U Test	,315[1]	Retain the null hypothesis.

Asymptotic significances are displayed. The significance level is ,05.

[1]Exact significance is displayed for this test.

Table 23. Behavioral test at end of treatment: descriptive statistics.

	Mean	Standard Deviation	Median	Percentile 25	Percentile 75
COLD150 in CTRL group	4.11	1.96	4.00	3.00	5.00
COLD150 in OHP group	3.50	1.72	3.50	2.00	4.00
COLD300 in CTRL group	8.44	3.32	7.00	6.00	10.00
COLD300 in OHP group	9.40	5.87	8.00	5.00	15.00
DYN in CTRL group	31.21	0.86	30.78	30.73	32.00
DYN in OHP group	23.27	4.10	25.23	21.37	25.70

COLD150: number of signs from 0 to 150 seconds; **COLD300**: number of signs from 151 to 300 seconds; **DYN**: score for Dynamic test.

Table 24. Behavioral test at end of treatment: Mann-Whitney U-test. COLD150end: number of signs from 0 to 150 seconds; **COLD300end:** number of signs from 151 to 300 seconds; **DYNend:** score for Dynamic test.

Hypothesis Test Summary

	Null Hypothesis	Test	Sig.	Decision
1	The distribution of COLD150end is the same across categories of 1=CTRL;2=OHP.	Independent-Samples Mann-Whitney U Test	,549[1]	Retain the null hypothesis.
2	The distribution of COLD300end is the same across categories of 1=CTRL;2=OHP.	Independent-Samples Mann-Whitney U Test	1,000[1]	Retain the null hypothesis.
3	The distribution of DYNend is the same across categories of 1=CTRL;2=OHP.	Independent-Samples Mann-Whitney U Test	,000[1]	Reject the null hypothesis.

Asymptotic significances are displayed. The significance level is ,05.

[1]Exact significance is displayed for this test.

Table 25. NET at end of treatment

VARIABLE	*CTRL GROUP*	*OHP GROUP*	*Mann-Whitney U-test*
Stimulus-response and strength-duration properties			
Strength-duration time constant (msec)	0.152 (0.144, 0.206)	0.214 (0.168, 0.228)	p=0.09
Rheobase (mA)	-0.181 (-0.223, -0.125)	-0.128 (-0.156, -0.0799)	p=0.12
Current Threshold properties			
Resting I/V slope	0.952 (0.861, 0.999)	0.917 (0.823, 0.926)	p=0.24
Minimum I/V slope	0.382 (0.277, 0.449)	0.307 (0.267, 0.359)	p=0.25
Hyperpolarazing I/V slope	0.575 (0.532, 0.624)	0.747 (0.589, 0.798)	p=0.05
Threshold electrotonus			
TEh(90-100 msec)	-69.5 (-77, -62.8)	-73 (-78, -68.8)	p=0.68
TEd(10-20 msec)	50.8 (49, 51.8)	51.1 (47.7, 52.6)	p=0.97
TEd(40-60 msec)	46.8 (44.6, 50)	50.1 (45.7, 51.9)	p=0.35
TEd(90-100 msec)	45.6 (44.2, 46.7)	44.7 (40.8, 47.8)	p=0.91
TEh(10-20 msec)	-53.9 (-55.1, -53.7)	-54.1 (-57.1, -53.6)	p=0.91
TEd(undershoot)	-6.06 (-6.59, -4.97)	-4.44 (-5.56, -3.81)	p=0.16
TEh(overshoot)	6.92 (5.66, 7.34)	7.12 (6.59, 7.91)	p=0.43
TEd(peak)	50.4 (49.5, 52.6)	52.4 (47.9, 53.1)	p=0.91
TEh(20-40 msec)	-62.7 (-64.9, -59.5)	-64.5 (-65.4, -61)	p=0.52
TEh(slope 101-140 msec)	0.726 (0.653, 0.866)	0.89 (0.832, 1.06)	p=0.25
TEd20(peak)	24.7 (24.1, 26.1)	26.4 (24.3, 27.2)	p=0.43
TEd40(Accomodation)	5.65 (5.45, 5.88)	5.8 (4.27, 6.95)	p=0.74
TEd20(10-20 msec)	23.3 (21.4, 24)	25.1 (23.6, 26.2)	**p=0.04***
TEh20(10-20 msec)	-23.2 (-24.6, -21.6)	-23 (-25.2, -22.3)	p=0.63
S2 accommodation	5.83 (4.92, 6)	5.9 (4.43, 7.75)	p=0.48
Accommodation half-time	38.4 (36.6, 50)	60.3 (50.1, 63.4)	**p<0.001****
TEh(slope 101-140 msec)	0.726 (0.653, 0.866)	0.89 (0.832, 1.06)	p=0.25
TEd20(peak)	24.7 (24.1, 26.1)	26.4 (24.3, 27.2)	p=0.43
TEd40(Accomodation)	5.65 (5.45, 5.88)	5.8 (4.27, 6.95)	p=0.74
TEh20(10-20 msec)	-23.2 (-24.6, -21.6)	-23 (-25.2, -22.3)	p=0.63
Recovery Cycle			
Relative Refractory Period (msec)	0.386 (0.365, 0.47)	0.486 (0.407, 0.569)	p=0.04*
Superexcitability (%)	-13.9 (-15.2, -13)	-6.18 (-9.16, -4.34)	**p<0.005****
Subexcitability (%)	5.07 (3.12, 5.37)	5.51 (4.12, 9.8)	p=0.25
Superexcitability at 5 msec	-13.9 (-16.4, -12.5)	-3.41 (-10.4, -1.04)	**p=0.02***
Superexcitability at 7 msec	-11.9 (-13.2, -8.34)	-4.32 (-5.84, -3.02)	**p<0.001****

VARIABLE	*CTRL GROUP*	*OHP GROUP*	*Mann-Whitney U-test*
Refractoriness at 2 msec	12.3 (9.01, 30.7)	34.9 (18.9, 48)	p=0.07
Refractoriness at 2.5msec	-2.17 (-4.57, 8.25)	8.96 (-0.516, 15)	p=0.07

Figure 23. NET results after end of treatment. ***A****: I/V relationship;* ***B****: Strength-duration time constant;* ***C****: Threshold electrotonus;* ***D****: Recovery Cycle.* Recovery cycle was significantly different between CTRL and OHP group, confirming the presence of acute OIPN.

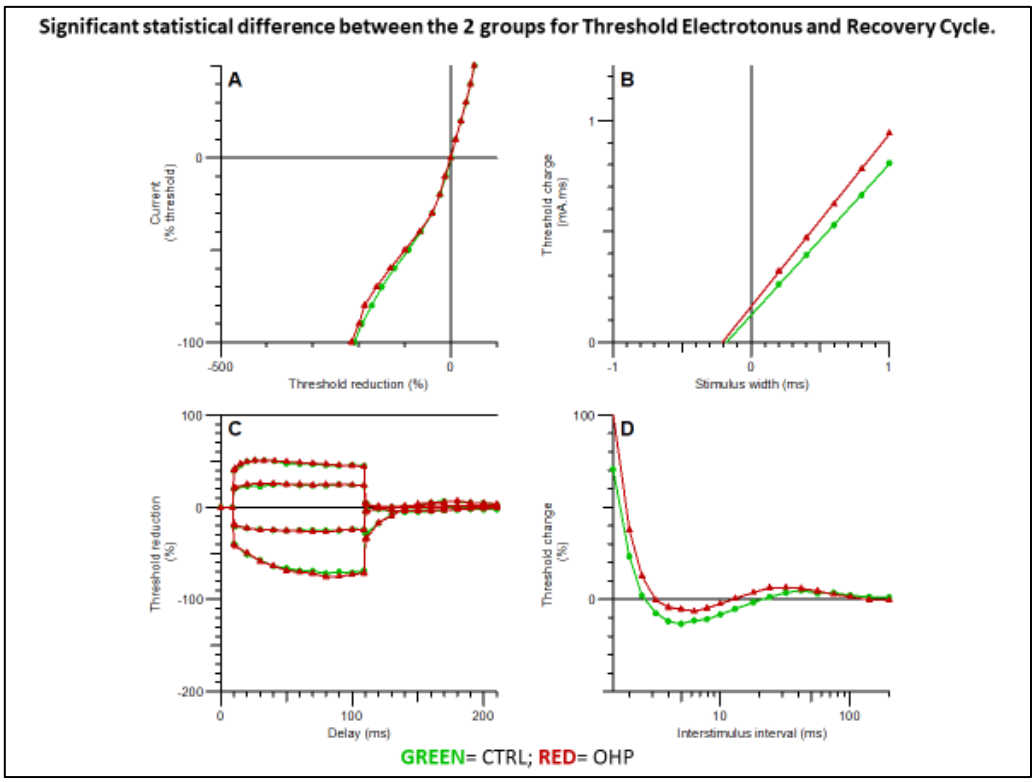

6.3.4 Data at 1 week after treatment.

NET findings and statistical test results are shown in **Table 26** and **Figure 24**; no difference was detected between the 2 groups.

Table 26. NET at 1 week of follow-up

VARIABLE	*CTRL GROUP [median, (Q1,Q3)]*	*OHP GROUP [median, (Q1,Q3)]*	*Mann-Whitney U-test*
Stimulus-response and strength-duration properties			
Strength-duration time constant (msec)	0.191 (0.12, 0.268)	0.19 (0.176, 0.224)	p=0.93
Rheobase (mA)	-0.0752 (-0.0794, -0.0448)	-0.203 (-0.207, -0.191)	p=0.12
Current Threshold properties			
Resting I/V slope	0.864 (0.818, 0.933)	0.88 (0.867, 1.03)	p=0.37
Minimum I/V slope	0.294 (0.257, 0.316)	0.264 (0.236, 0.307)	p=0.49
Hyperpolarazing I/V slope	0.663 (0.547, 0.826)	0.496 (0.473, 0.542)	p=0.06
Threshold electrotonus			
TEh(90-100 msec)	-75.6 (-86.5, -74.6)	-70.4 (-90.6, -61.9)	p=0.79
TEd(10-20 msec)	51.8 (48.6, 52.6)	48.5 (46.5, 50.3)	p=0.42
TEd(40-60 msec)	48.1 (41, 48.6)	46.3 (43.7, 49.5)	p=0.93
TEd(90-100 msec)	46 (39.4, 47.3)	44.7 (42.5, 47.4)	p=0.79
TEh(10-20 msec)	-57 (-60, -54)	-52.5 (-59, -51.3)	p=0.54
TEd(undershoot)	-4.04 (-6.31, -3.67)	-5.5 (-6.97, -3.24)	p=0.79
TEh(overshoot)	5.95 (4.31, 12)	2.36 (0.891, 4.81)	p=0.18
TEd(peak)	51.9 (48.5, 53.4)	49.5 (46.3, 51.5)	p=0.43
S2 accomodation	5.87 (3.98, 7.31)	3.3 (2.7, 5.76)	p=0.18
Accomodation half-time	44.1 (43.9, 46.2)	44.5 (32.1, 58.2)	p=0.79
TEh(20-40 msec)	-66 (-69.9, -65)	-59.3 (-65, -55.9)	p=0.54
TEh(slope 101-140 msec)	1.11 (0.687, 1.18)	0.753 (0.623, 1.06)	p=0.79
TEd20(peak)	25.7 (25.2, 27.1)	24.7 (23.2, 25.6)	p=0.43
TEd40(Accomodation)	5.9 (4.1, 10.8)	4.4 (3.52, 6.92)	p=0.43
TEd20(10-20 msec)	26.3 (24.4, 26.9)	22.5 (21.9, 23.4)	p=0.12
TEh20(10-20 msec)	-25.4 (-27.2, -23.2)	-24 (-25.8, -22.8)	p=0.66
Recovery Cycle			
Relative Refractory Period (msec)	0.295 (0.277, 0.387)	0.383 (0.303, 0.485)	p=0.79
Superexcitability (%)	-11.7 (-13.9, -11.6)	-9.62 (-10.4, -7.48)	p=0.33
Subexcitability (%)	2.08 (1.37, 2.65)	5.17 (3.83, 9.38)	p=0.18
Superexcitability at 7 msec	-8.32 (-9.86, -4.32)	-7.04 (-8.53, -4.75)	p=0.79
Superexcitability at 5 msec	-11.1 (-11.4, -4.96)	-8.81 (-11.1, -6.24)	p=0.93
Refractoriness at 2 msec	-2.15 (-3.4, 12.3)	12.9 (-2.5, 17.3)	p=0.79
Refractoriness at 2.5msec	-8.99 (-10.6, -2.26)	-2.32 (-7.78, 5.4)	p=0.43

Figure 24. NET results 1 week after end of treatment. ***A****: I/V relationship;* ***B****: Strength-duration time constant;* ***C****: Threshold electrotonus;* ***D****: Recovery Cycle.* No more significant differences were present between the 2 groups.

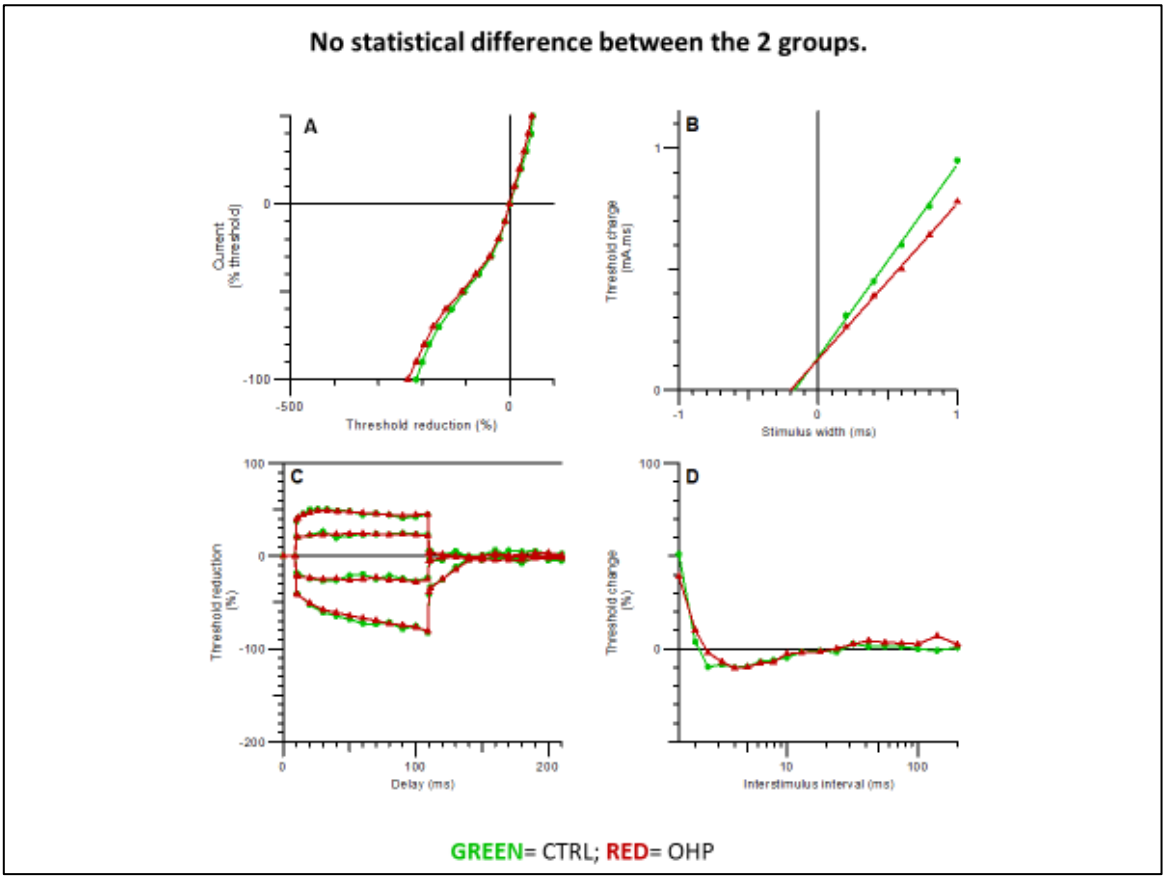

6.3.5 Data at 6 weeks after treatment

Descriptive statistic for nerve conduction studies is reported in **Table 27**; in **Table 28** Kruskal-Wallis test results are reported: no differences were seen between the groups. Descriptive statistic for all behavioral tests is reported in **Table 29**; in **Table 30** Mann-Whitney U-test results are reported: only Dynamic Test score was reduced in OHP treated animals (p-value 0.02); Cold Plate Test score was not different between the 2 groups. NET findings and statistical test results are shown **in Table 31** and **Figure 25**; data the same between the 2 groups.

Caudal nerve morphological analysis showed an almost complete recovery in treated animals (see **Figure 26** in which CTRL and OHP animal caudal nerves at end of treatment and at follow-up are shown).

Table 27. Neurophysiological data at 6 weeks of follow-up after treatment: descriptive statistics.

	Mean	Std. Deviation	Median	Percentile 25	Percentile 75
DC_AMP in CTRL group	92.58	30,76	95,80	65,90	98,40
DC_VEL in CTRL group	32.96	1,20	33,00	32,30	34,10
DC_AMP in OHP group	62.98	7,05	65,25	60,60	66,60
DC_VEL in OHP group	32.10	1,32	32,15	31,30	33,00
PC_AMP in CTRL group	155.24	15,27	154,20	148,00	161,70
PC_VEL in CTRL group	43.20	1,90	42,90	42,30	43,50
PC_AMP in OHP group	150.45	13,29	149,85	144,90	153,80
PC_VEL in OHP group	42.50	0,73	42,60	41,70	42,90
D_AMP in CTRL group	89.08	12,03	87,10	78,60	94,20
D_VEL in CTRL group	40.60	0,50	40,30	40,30	40,80
D_AMP in OHP group	90.38	11,99	87,75	80,50	95,80
D_VEL in OHP group	41.45	1,25	41,70	41,20	42,00
M_AMP in CTRL group	5.06	1,63	5,00	3,90	5,40
M_VEL in CTRL group	41.10	2,30	41,70	40,00	42,60
M_AMP in OHP group	6.27	2,00	5,75	4,80	7,80
M_VEL in OHP group	41.75	1,66	41,25	40,80	42,60

***DC_AMP**: distal caudal nerve SNAP amplitude (µV); **DC_VEL**: distal caudal nerve sensory conduction velocity (m/sec); **D_AMP**: digital nerve SNAP amplitude (µV); **D_VEL**: digital nerve sensory conduction velocity (m/sec); **M_AMP**: caudal nerve CMAP amplitude (mV); **M_VEL**: caudal nerve motor conduction velocity; **PC_AMP**: proximal caudal nerve SNAP amplitude (µV); **PC_VEL**: proximal caudal nerve sensory conduction velocity (m/sec).*

Table 28. Neurophysiological data at 6 weeks of follow-up after treatment: Mann-Whitney U-test. ***DCAMP****: distal caudal nerve SNAP amplitude (µV);* ***DCVEL****: distal caudal nerve sensory conduction velocity (m/sec);* ***DAMP****: digital nerve SNAP amplitude (µV);* ***DVEL****: digital nerve sensory conduction velocity (m/sec);* ***MAMP****: caudal nerve CMAP amplitude (mV);* ***MVEL****: caudal nerve motor conduction velocity;* ***PCAMP****: proximal caudal nerve SNAP amplitude (µV);* ***PCVEL****: proximal caudal nerve sensory conduction velocity (m/sec).*

Hypothesis Test Summary

	Null Hypothesis	Test	Sig.	Decision
1	The distribution of DCAMPfu is the same across categories of 1=CTRL; 2=OHP.	Independent-Samples Mann-Whitney U Test	,177[1]	Retain the null hypothesis.
2	The distribution of DCVELfu is the same across categories of 1=CTRL; 2=OHP.	Independent-Samples Mann-Whitney U Test	,329[1]	Retain the null hypothesis.
3	The distribution of CPAMPfu is the same across categories of 1=CTRL; 2=OHP.	Independent-Samples Mann-Whitney U Test	,429[1]	Retain the null hypothesis.
4	The distribution of CPVELfu is the same across categories of 1=CTRL; 2=OHP.	Independent-Samples Mann-Whitney U Test	,662[1]	Retain the null hypothesis.
5	The distribution of DAMPfu is the same across categories of 1=CTRL; 2=OHP.	Independent-Samples Mann-Whitney U Test	,662[1]	Retain the null hypothesis.
6	The distribution of DVELfu is the same across categories of 1=CTRL; 2=OHP.	Independent-Samples Mann-Whitney U Test	,126[1]	Retain the null hypothesis.
7	The distribution of MAMPfu is the same across categories of 1=CTRL; 2=OHP.	Independent-Samples Mann-Whitney U Test	,429[1]	Retain the null hypothesis.
8	The distribution of MVELfu is the same across categories of 1=CTRL; 2=OHP.	Independent-Samples Mann-Whitney U Test	,792[1]	Retain the null hypothesis.

Asymptotic significances are displayed. The significance level is ,05.

[1]Exact significance is displayed for this test.

Table 29. Behavioral test at 6 weeks of follow-up after treatment: descriptive statistics.

	Mean	Standard Deviation	Median	Percentile 25	Percentile 75
COLD150 in CTRL group	3.80	2.17	5.00	2.00	5.00
COLD150 in OHP group	2.83	2.32	2.00	1.00	4.00
COLD300 in CTRL group	6.40	3.21	6.00	6.00	7.00
COLD300 in OHP group	5.33	3.14	5.50	3.00	7.00
DYN in CTRL group	31.76	3.55	31.30	31.24	32.85
DYN in OHP group	26.33	1.51	26.30	24.87	27.50

COLD150: number of signs from 0 to 150 seconds; **COLD300**: number of signs from 151 to 300 seconds; **DYN**: score for Dynamic test.

Table 30. Behavioral tests at 6 weeks of follow-up after treatment: Mann Whitney U- test.

Hypothesis Test Summary

	Null Hypothesis	Test	Sig.	Decision
1	The distribution of COLD150fu is the same across categories of 1=CTRL; 2=OHP.	Independent-Samples Mann-Whitney U Test	,537[1]	Retain the null hypothesis.
2	The distribution of COLD300fu is the same across categories of 1=CTRL; 2=OHP.	Independent-Samples Mann-Whitney U Test	,537[1]	Retain the null hypothesis.
3	The distribution of DYNfu is the same across categories of 1=CTRL; 2=OHP.	Independent-Samples Mann-Whitney U Test	,017[1]	Reject the null hypothesis.

Asymptotic significances are displayed. The significance level is ,05.

[1]Exact significance is displayed for this test.

Table 31. NET at 6 weeks of follow-up after treatment

VARIABLE	*CTRL GROUP*	*OHP GROUP*	*Mann-Whitney U-test*
Stimulus-response and strength-duration properties			
Strength-duration time constant (msec)	0.244 (0.228, 0.249)	0.243 (0.218, 0.253)	p=1
Rheobase (mA)	-0.126 (-0.141, -0.112)	-0.0753 (-0.117, -0.0511)	p=0.48
Current Threshold properties			
Resting I/V slope	0.892 (0.874, 0.918)	0.853 (0.825, 0.892)	p=0.37
Minimum I/V slope	0.294 (0.257, 0.316)	0.264 (0.236, 0.307)	p=0.49
Hyperpolarazing I/V slope	0.663 (0.547, 0.826)	0.496 (0.473, 0.542)	p=0.06
Threshold electrotonus			
TEh(90-100 msec)	-75.6 (-86.5, -74.6)	-70.4 (-90.6, -61.9)	p=0.79
TEd(10-20 msec)	51.8 (48.6, 52.6)	48.5 (46.5, 50.3)	p=0.43
TEd(40-60 msec)	48.1 (41, 48.6)	46.3 (43.7, 49.5)	p=0.93
TEd(90-100 msec)	46 (39.4, 47.3)	44.7 (42.5, 47.4)	p=0.79
TEh(10-20 msec)	-56.9 (-58.4, -55.7)	-58.5 (-60.5, -56.8)	p=0.88
TEd(undershoot)	-5.05 (-5.22, -4.95)	-4.09 (-4.86, -3.52)	p=0.34
TEd(peak)	53.4 (52.3, 54.4)	52.5 (52, 53.6)	p=0.88
TEh(20-40 msec)	-68.2 (-70, -65.7)	-72.1 (-74, -69.4)	p=0.34
TEh(slope 101-140 msec)	1.06 (0.883, 1.14)	1.24 (1.15, 1.35)	p=0.11
TEd20(peak)	25.8 (25.5, 26.3)	26.3 (25.8, 27.1)	p=0.88
TEd40(Accomodation)	5.5 (5.28, 6.05)	5.5 (4.57, 6.55)	p=0.68
TEd20(10-20 msec)	23.8 (23.2, 24)	24.5 (23.8, 25.3)	p=0.34
TEh20(10-20 msec)	-23 (-25.2, -20.5)	-24.6 (-25.1, -24.2)	p=0.68
S2 accommodation	5.13 (4.82, 5.76)	5.68 (4.4, 6.96)	p=0.88
Accommodation half-time	41.2 (34.5, 48.5)	49.4 (43.8, 54.2)	p=0.34
Recovery Cycle			
Relative Refractory Period (msec)	0.277 (0.272, 0.318)	0.367 (0.332, 0.389)	p=0.34
Superexcitability (%)	13.1 (-14.9, -11.9)	-13.9 (-14.6, -11.8)	p=1
Subexcitability (%)	1.27 (1.17, 2.74)	1.79 (1.32, 2.23)	p=0.88
Superexcitability at 7 msec	-10.2 (-10.9, -9.5 n=4)	-12.3 (-12.8, -10.6)	p=0.34
Superexcitability at 5 msec	-11.6 (-12.5, -11.3)	-13.8 (-14.8, -12.1)	p=0.68
Refractoriness at 2 msec	-3.17 (-4.03, 0.661)	6.44 (2.95, 10.2)	p=0.48
Refractoriness at 2.5msec	-9.61 (-11.9, -5.91)	-3.35 (-7.42, -0.884)	p=0.68

Figure 25. NET results 6 weeks after end of treatment. ***A****: I/V relationship;* ***B****: Strength-duration time constant;* ***C****: Threshold electrotonus;* ***D****: Recovery Cycle.* There wasn't a significant difference between the 2 groups.

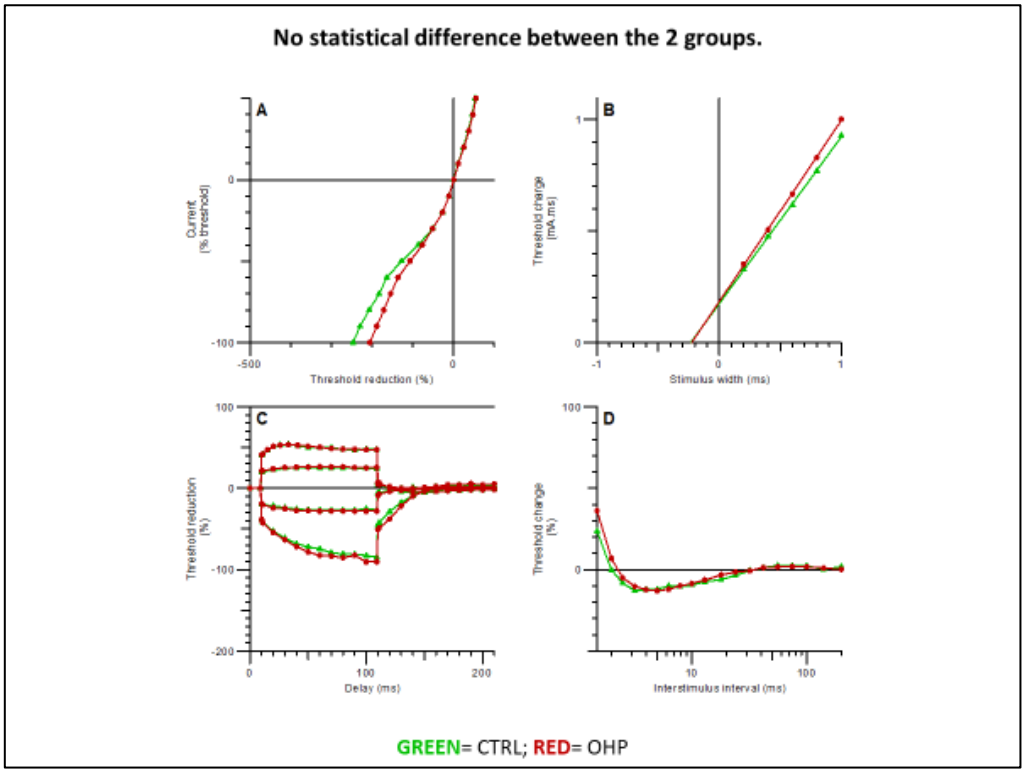

Figure 26. Caudal nerve morphology over the observational period (60x magnification). At the end of treatment (1 month) a rather mild axonopathy can be seen, which encountered an almost complete recovery at the end of follow-up (6 weeks after treatment).

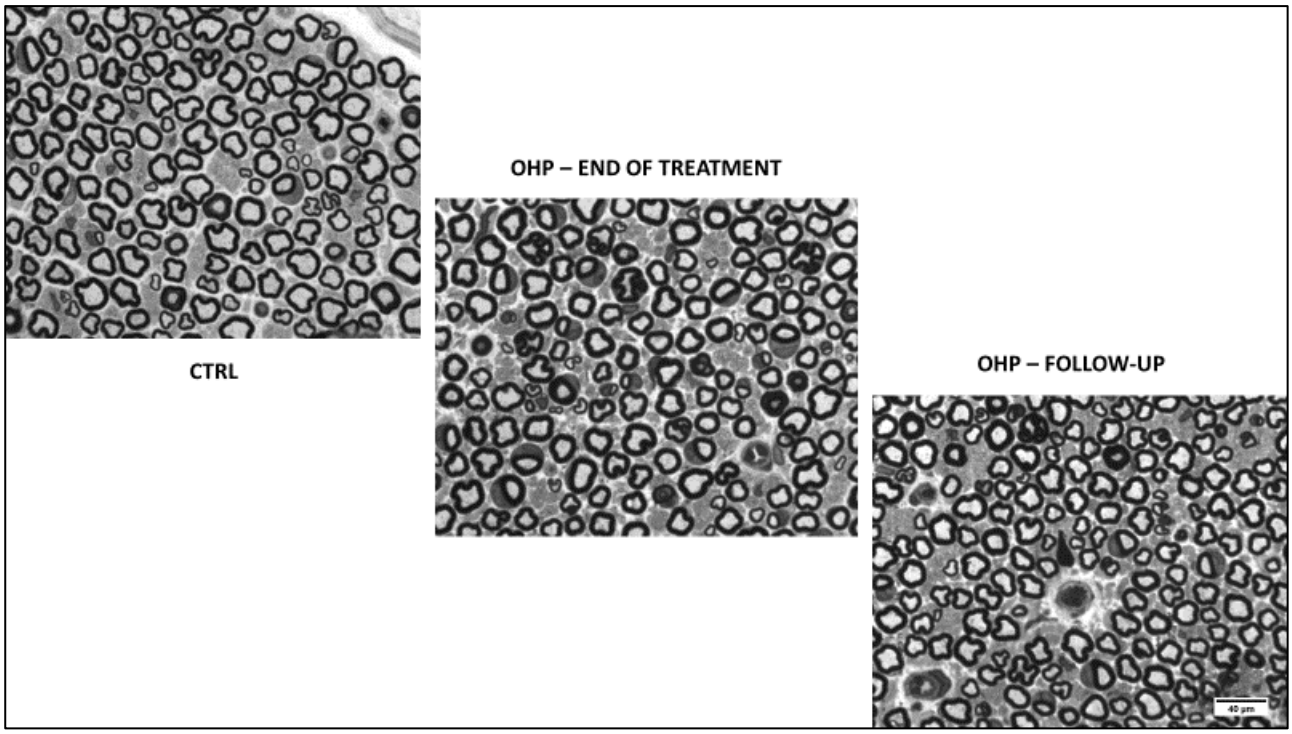

6.3.6 Summary of inferences from TASK 3

After the first administration, no signs of acute OIPN were present, but in TASK 3 the standard published chronic OHP schedule (3mg/Kg, iv, 2qw4ws)[46] was used. In TASK 1 and 2 a single injection of 5 mg/Kg was, in fact, performed. Moreover, at the end of treatment, despite the presence of acute OIPN, chronic OIPN induction was too mild and it underwent to an almost complete recovery. Thus, a refinement of the chronic model was necessary in order to better induce both conditions and better reproduce clinical evidence.

6.4 TASK 4 - REFINEMENT OF THE CHRONIC SETTING – A DOSE FINDING STUDY IN OHP TREATED RATS

In **TASK 4** a refinement of the schedule was performed. Three different OHP dosages (3, 4, and 5 mg/Kg, iv, 2qw4ws) were compared to choose the ideal one to reproduce at one both acute and chronic OIPN. NET and Cold Plate Test were used to detect acute OIPN. Chronic OIPN was assessed thanks to standard neurophysiology and Dynamic Test. Confirmatory neuropathological analyses were executed at the end of treatment. To ensure homogeneity among groups, standard neurophysiology was performed at baseline. See **Study design** section for more details.

6.4.1 Baseline data

Descriptive statistic for all nerve conduction studies data is reported in **Table 32**; in **Table 33** Kruskal-Wallis test results are reported: no differences were present among the 4 groups for all variables. Descriptive statistic for Cold Plate Test is reported in **Table 34**; in **Table 35** Kruskal-Wallis test results are reported: no differences were present among the 4 groups for all variables.

Table 32. Neurophysiological data at baseline: descriptive statistics.

	Mean	Std. Deviation	Median	Percentile 25	Percentile 75
CD_AMP in CTRL group	53	9	56	45	59
CD_AMP in OHP3 group	63.24	17.28	60.30	54.40	70.15
CD_AMP in OHP4 group	60.16	9.19	59.25	55.25	67.75
CD_AMP in OHP5 group	57.49	9.85	55.70	49.70	64.70
CD_VEL in CTRL group	24.44	1.84	24.51	22.83	25.87
CD_VEL in OHP3 group	25.21	1.26	25.42	23.91	26.32
CD_VEL in OHP4 group	24.40	1.49	25.00	22.82	25.54
CD_VEL in OHP5 group	24.75	2.28	24.20	23.26	26.58
CP_AMP in CTRL group	116.55	22.68	116.45	102.55	129.15
CP_AMP in OHP3 group	120.33	15.11	121.55	110.65	131.05
CP_AMP in OHP4 group	127.83	35.32	132.95	100.55	151.30
CP_AMP in OHP5 group	141.95	40.38	148.40	110.60	171.00
CP_VEL in CTRL group	31.26	2.49	31.42	29.56	33.00
CP_VEL in OHP3 group	33.15	5.24	32.44	28.44	36.86
CP_VEL in OHP4 group	33.33	2.93	33.37	31.10	36.15
CP_VEL in OHP5 group	33.22	2.58	34.20	31.80	34.89
D_AMP in CTRL group	64.09	17.01	61.85	49.25	74.95
D_AMP in OHP3 group	76.81	12.05	77.95	68.15	87.55
D_AMP in OHP4 group	73.93	20.94	77.35	63.60	86.50
D_AMP in OHP5 group	73.16	13.40	71.45	60.55	82.40
D_VEL in CTRL group	36.92	1.27	36.95	36.48	37.67
D_VEL in OHP3 group	36.68	2.43	36.71	35.19	37.91
D_VEL in OHP4 group	37.67	1.71	37.66	36.49	38.42
D_VEL in OHP5 group	37.83	3.15	37.35	34.73	40.86
M_AMP in CTRL group	9.54	3.70	10.25	6.95	12.40
M_AMP in OHP3 group	8.45	3.39	7.60	6.20	9.50
M_AMP in OHP4 group	6.31	2.63	7.40	3.55	8.55
M_AMP in OHP5 group	6.30	2.73	6.00	3.95	7.65
M_VEL in CTRL group	30.40	3.52	29.86	28.57	31.50
M_VEL in OHP3 group	31.54	3.30	30.89	28.78	33.90
M_VEL in OHP4 group	31.97	4.17	33.06	28.90	34.90
M_VEL in OHP5 group	32.30	4.82	32.53	27.59	35.76

CD_AMP: distal caudal nerve SNAP amplitude (μv); ***CD_VEL***: distal caudal nerve sensory conduction velocity (m/sec); ***D_AMP***: digital nerve SNAP amplitude (μv); ***D_VEL***: digital nerve sensory conduction velocity (m/sec); ***M_AMP***: caudal nerve CMAP amplitude (mV); ***M_VEL***: caudal nerve motor conduction velocity (m/sec); ***PC_AMP***: proximal caudal nerve SNAP amplitude (μv); ***PC_VEL***: proximal caudal nerve sensory conduction velocity (m/sec).

Table 33. Neurophysiological data at base- line: Kruskal-Wallis Test. ***CDAMP***: distal caudal nerve SNAP amplitude; ***CDVEL***: distal caudal nerve sensory conduction velocity; ***DAMP***: digital nerve SNAP amplitude; ***DVEL***: digital nerve sensory conduction velocity; ***MAMP***: caudal nerve CMAP amplitude; ***MVEL***: caudal nerve motor conduction velocity; ***PCAMP***: proximal caudal nerve SNAP amplitude; ***PCVEL***: proximal caudal nerve sensory conduction velocity.

Hypothesis Test Summary

	Null Hypothesis	Test	Sig.	Decision
1	The distribution of CDAMP is the same across categories of 1=CTRL; 2=OHP3; 3=OHP4; 4=OHP5.	Independent-Samples Kruskal-Wallis Test	,369	Retain the null hypothesis.
2	The distribution of CDVEL is the same across categories of 1=CTRL; 2=OHP3; 3=OHP4; 4=OHP5.	Independent-Samples Kruskal-Wallis Test	,647	Retain the null hypothesis.
3	The distribution of CPAMP is the same across categories of 1=CTRL; 2=OHP3; 3=OHP4; 4=OHP5.	Independent-Samples Kruskal-Wallis Test	,505	Retain the null hypothesis.
4	The distribution of CPVEL is the same across categories of 1=CTRL; 2=OHP3; 3=OHP4; 4=OHP5.	Independent-Samples Kruskal-Wallis Test	,428	Retain the null hypothesis.
5	The distribution of DAMP is the same across categories of 1=CTRL; 2=OHP3; 3=OHP4; 4=OHP5.	Independent-Samples Kruskal-Wallis Test	,384	Retain the null hypothesis.
6	The distribution of DVEL is the same across categories of 1=CTRL; 2=OHP3; 3=OHP4; 4=OHP5.	Independent-Samples Kruskal-Wallis Test	,682	Retain the null hypothesis.
7	The distribution of MAMP is the same across categories of 1=CTRL; 2=OHP3; 3=OHP4; 4=OHP5.	Independent-Samples Kruskal-Wallis Test	,132	Retain the null hypothesis.
8	The distribution of MVEL is the same across categories of 1=CTRL; 2=OHP3; 3=OHP4; 4=OHP5.	Independent-Samples Kruskal-Wallis Test	,834	Retain the null hypothesis.

Asymptotic significances are displayed. The significance level is ,05.

Table 34. Behavioral tests at base line: descriptive statistics.

	Mean	Std. Deviation	Median	Percentile 25	Percentile 75
COLD150 in CTRL group	4.88	2.90	4.00	3.00	7.00
COLD150 in OHP3 group	5.38	4.60	4.00	3.00	6.00
COLD150 in OHP4 group	5.00	3.34	3.50	2.50	8.00
COLD150 in OHP5 group	5.38	1.85	5.00	4.00	7.00
COLD300 in CTRL group	12.63	6.67	10.00	8.00	17.00
COLD300 in OHP3 group	11.75	6.88	10.50	8.00	11.50
COLD300 in OHP4 group	12.00	5.78	10.50	9.00	14.00
COLD300 in OHP5 group	11.13	3.40	11.00	8.00	14.00
COLD150: number of signs from 0 to 150 seconds; **COLD300**: number of signs from 151 to 300 seconds.					

Table 35. Cold plate at base-line: Mann-Whitney U-test. **COLD150**: number of signs from 0 to 150 seconds; **COLD300**: number of signs from 151 to 300 seconds.

Hypothesis Test Summary

	Null Hypothesis	Test	Sig.	Decision
1	The distribution of COLD150 is the same across categories of 1=CTRL; 2=OHP3; 3=OHP4; 4=OHP5.	Independent-Samples Kruskal-Wallis Test	,794	Retain the null hypothesis.
2	The distribution of COLD300 is the same across categories of 1=CTRL; 2=OHP3; 3=OHP4; 4=OHP5.	Independent-Samples Kruskal-Wallis Test	,988	Retain the null hypothesis.

Asymptotic significances are displayed. The significance level is ,05.

6.4.2 Data after the 1st administration

Descriptive statistic for Cold Plate Test is reported in **Table 36**; in **Table 37** Kruskal-Wallis test results are reported: Cold Plate test was not significant; however, OHP5 animals were not able to complete the whole observational period due to marked intolerance to the cold surface (3 animals out of 8), thus preventing a correct completion of data collection which might have revealed increased total number of signs compared to CTRL animals.

NET findings and statistical test results are shown in **Table 38** and **Figure 27**; some differences were present data the same among the 4 groups; OHP4 and OHP5 group showed a significant reduction in the minimum I/V slope (p-value 0.01 and 0.02 respectively). For Threshold electrotonus some alterations were seen in the OHP5 group for the components in response to hyperpolarization [TEh(slope101-140msec) p value 0.002].

Table 36. Cold plate test after 1st administration: descriptive statistics. Warning: OHP5 animals were not able to complete the whole observational period due to marked intolerance to the cold surface (3 animals out of 8).

	Mean	Standard Deviation	Median	Percentile 25	Percentile 75
COLD150 in CTRL group	5.00	2.51	5.50	2.50	7.00
COLD150 in OHP3 group	5.75	3.58	4.50	3.00	8.50
COLD150 in OHP4 group	5.75	4.20	4.50	2.50	9.00
COLD150 in OHP5 group	5.50	2.00	6.00	5.00	7.00
COLD300 in CTRL group	10.38	4.14	11.00	7.00	13.50
COLD300 in OHP3 group	14.63	7.76	15.50	7.00	20.50
COLD300 in OHP4 group	13.50	7.54	14.00	7.00	20.00
COLD300 in OHP5 group	12.88	9.01	10.00	8.50	15.00

COLD150ACUTE: number of signs from 0 to 150 seconds; **COLD300ACUTE**: number of signs from 151 to 300 seconds.

Table 37. Cold plate test after 1st administration: Mann-Whitney U-test. **COLD150ACUTE**: number of signs from 0 to 150 seconds; **COLD300ACUTE**: number of signs from 151 to 300 seconds. Warning: OHP5 animals were not able to complete the whole observational period due to marked intolerance to the cold surface (3 animals out of 8).

Hypothesis Test Summary

	Null Hypothesis	Test	Sig.	Decision
1	The distribution of COLD150ACUTE is the same across categories of 1=CTRL; 2=OHP3; 3=OHP4; 4=OHP5.	Independent-Samples Kruskal-Wallis Test	,987	Retain the null hypothesis.
2	The distribution of COLD300ACUTE is the same across categories of 1=CTRL; 2=OHP3; 3=OHP4; 4=OHP5.	Independent-Samples Kruskal-Wallis Test	,702	Retain the null hypothesis.

Asymptotic significances are displayed. The significance level is ,05.

Table 38. NET after 1st administration.

VARIABLE	*CTRL GROUP (median, Q1, Q3)*	*OHP3 GROUP (median, Q1, Q3, p-value VS CTRL)*	*OHP4 GROUP (median, Q1, Q3, p-value VS CTRL)*	*OHP5 GROUP (median, Q1, Q3, p-value VS CTRL)*
Stimulus-response and strength-duration properties				
Strength-duration time constant (msec)	0.176 (0.141, 0.226)	0.201 (0.181, 0.207) p=1	0.185 (0.156, 0.216) p=0.95	0.19 (0.165, 0.204) p=0.94
Rheobase (mA)	-0.0595 (-0.118, -0.0119)	-0.0458 (-0.142, -0.0018) p=0.90	-0.0664 (-0.139, 0.052) p=0.95	-0.0227 (-0.0526, 0.0198) p=0.63
Current Threshold properties				
Resting I/V slope	0.861 (0.843, 0.905)	0.885 (0.87, 0.928) p=0.39	0.921 (0.876, 1.03) p=0.18	0.829 (0.734, 0.85 n=6) p=0.24
Minimum I/V slope	0.425 (0.412, 0.455)	0.384 (0.366, 0.394) p=0.13	0.35 (0.3, 0.373) **p=0.01***	0.362 (0.343, 0.368) **p=0.02***
Hyperpolarazing I/V slope	0.667 (0.552, 0.669)	0.623 (0.561, 0.738) p=0.80	0.579 (0.507, 0.674) p=0.62	0.601 (0.513, 0.757) p=0.88
Threshold electrotonus				
TEh(90-100 msec)	-69.7 (-79.9, -67.6)	-67.8 (-76.3, -63.1) p=0.83	-75.6 (-80.4, -71.5) p=0.65	-87.4 (-103, -84.2) p=0.07
TEd(10-20 msec)	52.6 (49.8, 54.2)	49 (46.9, 50) p=0.12	50.4 (47.4, 53.8) p=0.65	52.7 (51.8, 52.7) p=1
TEd(40-60 msec)	50 (46.7, 50.6)	47.1 (45.4, 47.8) p=0.267	47.6 (46.5, 48.5) p=0.31	51.5 (50.3, 51.8) p=0.38
TEd(90-100 msec)	46.8 (45.1, 47.3 n=7)	44.6 (42.5, 44.9) p=0.12	46.6 (45.8, 46.7) p=0.53	48.3 (47.8, 48.8) p=0.18
TEh(10-20 msec)	-58.7 (-59.4, -57.1)	-52.7 (-56.7, -52.2) p=0.38	-56.3 (-58.4, -54.6) p=0.41	-58.1 (-58.5, -57.8) p=0.67
TEd(undershoot)	-3.85 (-4.45, -3.27)	-3.92 (-4.27, -3.69) p=0.83	-4.52 (-6.84, -2.37) p=1	-4.59 (-6.12, -4.24) p=0.27
TEd(overshoot)	5.34 (5.27, 5.88)	5.99 (4.96, 7.02) p=0.83	6.01 (3.07, 9.24) p=1	8.64 (8.25, 8.93) p=0.12
TEd(peak)	52.4 (50.1, 54.9)	50 (47.3, 50.4) p=0.18	50.5 (48, 53.6) p=0.65	53.4 (52.5, 53.8) p=1
TEh(20-40 msec)	-68.4 (-69, -65.7)	-60.9 (-66.3, -58) p=0.52	-65.5 (-72.3, -60.2) p=0.93	-70.2 (-76.8, -69.6) p=0.12
TEh(slope 101-140 msec)	0.804 (0.761, 0.859)	0.727 (0.628, 0.922) p=0.83	0.764 (0.547, 1.03) p=1	1.07 (1.05, 1.24) **p=0.02***
TEd20(peak)	25.5 (25, 27.2)	24.7 (24.7, 24.9) p=0.38	25.1 (23.3, 26.8) p=0.53	26.6 (25.9, 26.9) p=0.83
TEd40(Accomodation)	5.3 (4.4, 6)	4.4 (3.95, 5.25) p=0.52	6.6 (5.2, 7.3)	3.8 (3.5, 5.3)

VARIABLE	*CTRL GROUP (median, Q1, Q3)*	*OHP3 GROUP (median, Q1, Q3, p-value VS CTRL)*	*OHP4 GROUP (median, Q1, Q3, p-value VS CTRL)*	*OHP5 GROUP (median, Q1, Q3, p-value VS CTRL)*
			p=0.41212	p=0.38
TEd20(10-20 msec)	24.2 (23.6, 24.6)	21.8 (21.7, 22.8) p=0.27	23.2 (22, 24.2) p=0.41	25.4 (24.1, 25.5) p=0.67
TEh20(10-20 msec)	-25 (-26.8, -24)	-23.2 (-24.1, -22.5) p=0.38	-23.5 (-23.9, -23.3 n=4) p=0.23	-24.4 (-25.4, -24.1) p=0.83
S2 accommodation	5.61 (4.34, 6.68)	4.73 (4.47, 5.43) p=1	5.1 (3.27, 6.98) p=0.79	4.15 (3.7, 5.55) p=0.52
Accommodation half-time	42 (33.6, 44.6)	58.3 (49, 58.3) p=0.38	39 (36.1, 40.6) p=0.65	51.7 (45.6, 53.9) p=0.38
Recovery Cycle				
Relative Refractory Period (msec)	0.37 (0.357, 0.402)	0.392 (0.349, 0.466) p=1	0.434 (0.4, 0.75) p=0.13	0.436 (0.387, 0.493) p=0.27
Refractoriness at 2 msec	8.69 (5.9, 21 n=7)	16.2 (4.71, 42.6) p=0.80	25.4 (15.3, 53.8) p=0.23	25 (22.8, 72.2) p=0.34
Refractoriness at 2.5msec	-2.37 (-6.34, 1.11)	-1.68 (-4.65, 11.1) p=0.53	1.98 (-0.737, 8.76) p=0.14	4.47 (-2.88, 13.1) p=0.43
Superexcitability (%)	-11.5 (-12.7, -7.95)	-12.3 (-13, -11.1) p=0.38	-7.55 (-12.6, -5.26) p=0.54	-13.2 (-13.6, -8.48) p=0.53
Subexcitability (%)	3.03 (2.14, 4.77 n=7)	5.15 (3.26, 6.29 n=7) p=0.097	6.52 (3.93, 116) p=0.16	4.18 (2.41, 5.66) p=0.75
Superexcitability at 5 msec	-11 (-12.8, -8.86 n=7)	-13.7 (-14.7, -11.6 n=7) p=0.26	-5.03 (-12.9, -0.889) p=0.38	-8.95 (-12, -7.27) p=0.87
Superexcitability at 7 msec	-8.82 (-11.5, -5.48 n=7)	-9.61 (-12.1, -8.36 n=7) p=0.45	-2.65 (-10.4, -0.45) p=0.38	-10.3 (-13.8, -9.09) p=0.27

Figure 27. NET after 1st administration. ***A****: I/V relationship;* ***B****: Strength-duration time constant;* ***C****: Threshold electrotonus;* ***D****: Recovery Cycle.* There wasn't a significant difference between OHP3 and CTRL groups; whereas, current threshold properties were different for OHP4 and OHP5 groups. Threshold electrotonus was significant only for the OHP5 groups. See **Table 38** for more details.

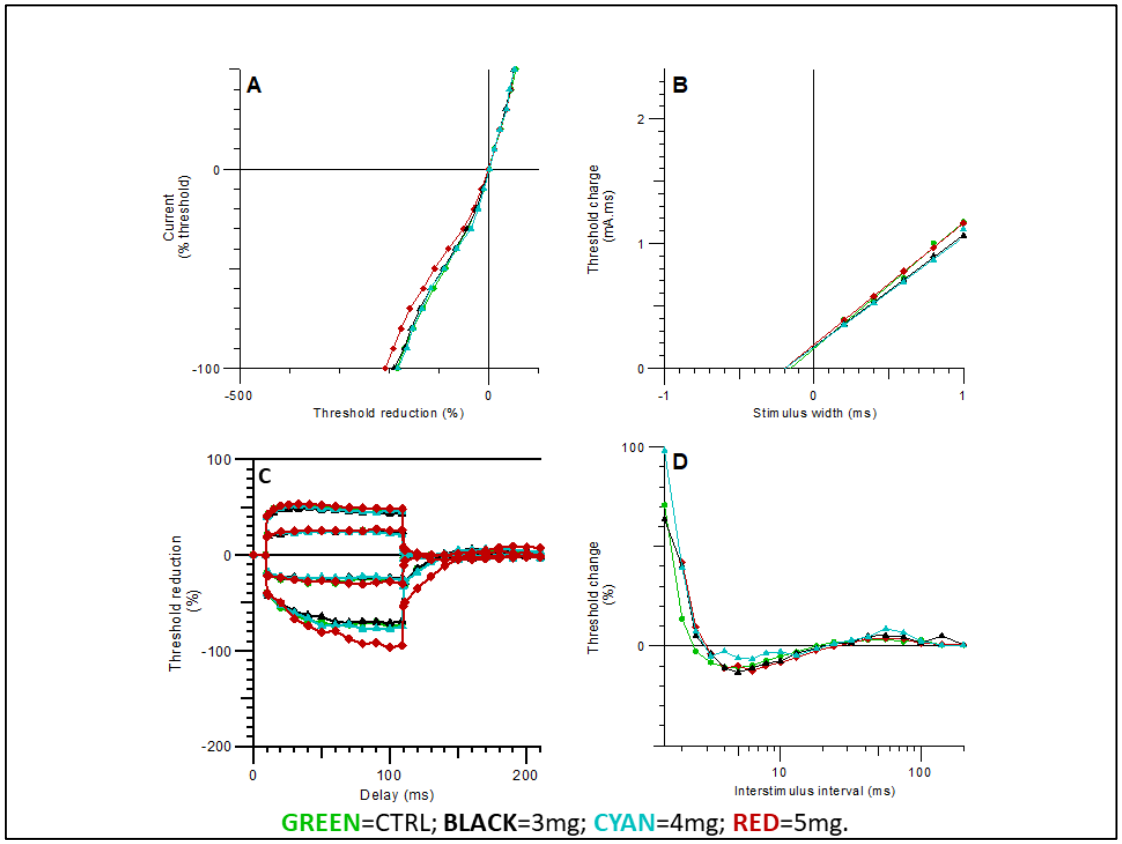

6.4.3 End of treatment data

Descriptive statistic for all neurophysiological data is reported in **Table 39**; in **Table 40** Kruskal-Wallis test results are reported: distal caudal and digital SNAP amplitude showed a significant difference (p-value 0.001 and <0.001 respectively) as well as distal caudal nerve sensory conduction velocity (p-value 0.009); moreover, pairwise comparison, adjusted by the Bonferroni correction for multiple tests, demonstrated that:

- distal caudal SNAP amplitude was different between OHP5 and CTRL groups (p-value 0.001) and no difference was present between CTRL and OHP3, CTRL and OHP4;
- digital SNAP amplitude was different only between OHP5 and CTRL and between OHP4 and CTRL groups (p-value 0.002 and 0.003 respectively) and no difference was present between CTRL and OHP3;
- distal caudal nerve sensory conduction velocity was different between OHP5 and CTRL groups (p-value 0.005) and no difference was present between CTRL and OHP3, CTRL and OHP4.

Descriptive statistic for Cold Plate test is reported in **Table 41**; OHP4 and OHP5 animals displayed a too much painful behavior: the test was precociously suspended and the data, being biased, were not collected and available for multiple comparisons. The test was considered as “overall positive” in both groups. in **Table 42** Kruskal-Wallis test results for CRTL versus OHP3 groups are reported: a difference in number of signs was detected at 300 msec (p-value 0.005).

NET findings and statistical test results are shown in **Table 43** and **Figure 28**, **29**, **30** and **31**. Briefly, OHP3 was different to CTRL only for one parameter in Threshold electrotonus in response to hyperpolarizing currents (p-value 0.01). Instead, OHP4 and OHP5 showed a statistical difference for many more parameters in stimulus-response curve (rheobase), threshold electrotonus (in response to hyperpolarizing currents) and recovery cycle (superexcitability). Notably, the number of statistically different parameters and their significance versus CTRL group was far higher in OHP5 group than OHP4 one.

Caudal nerve morphological findings are shown in **Figure 32** with a dose-dependent effect on axonopathy development: OHP3 showed some only minor alterations, whereas OHP4 and OHP5 showed a clear axonopathy, more evident at the highest dosage.

In **Figure 33** weight trend for all groups is shown; no group developed a perilous decrease in weight (i.e., more than 20% of the base-line value).

Table 39. Neurophysiological data at end of treatment: descriptive statistics.

	Mean	Std. Deviation	Median	Percentile 25	Percentile 75
CD_AMP in CTRL group	63.90	9,66	62,45	57,20	71,30
CD_AMP in OHP3 group	62.75	16,13	59,20	48,25	76,70
CD_AMP in OHP4 group	46.43	10,68	49,50	39,95	53,10
CD_AMP in OHP5 group	36.04	9,19	36,35	29,60	38,25
CD_VEL in CTRL group	30.50	1,78	29,70	29,10	32,30
CD_VEL in OHP3 group	28.49	2,00	29,40	26,90	29,70
CD_VEL in OHP4 group	24.26	1,36	24,60	23,65	24,90
CD_VEL in OHP5 group	24.31	3,41	23,05	21,60	27,65
CP_AMP in CTRL group	160.49	28,72	172,70	129,30	183,65
CP_AMP in OHP3 group	136.80	15,14	133,15	124,00	151,15
CP_AMP in OHP4 group	142.95	20,20	139,15	128,55	156,55
CP_AMP in OHP5 group	133.46	23,61	123,25	117,55	153,05
CP_VEL in CTRL group	35.01	2,25	35,30	33,00	35,70
CP_VEL in OHP3 group	33.34	3,70	33,35	31,10	35,50
CP_VEL in OHP4 group	33.99	2,66	34,70	31,65	35,70
CP_VEL in OHP5 group	32.09	1,29	31,70	31,30	33,15
D_AMP in CTRL group	87.18	20,95	84,65	78,60	93,65
D_AMP in OHP3 group	77.54	14,61	78,10	70,65	81,30
D_AMP in OHP4 group	73.11	10,56	77,45	65,05	79,00
D_AMP in OHP5 group	62.28	7,74	62,55	55,95	66,85
D_VEL in CTRL group	34.95	2,89	35,00	32,20	37,10
D_VEL in OHP3 group	34.94	2,18	34,80	33,70	36,80
D_VEL in OHP4 group	33.85	3,04	33,70	31,84	36,40
D_VEL in OHP5 group	31.86	1,69	32,20	30,65	32,55
M_AMP in CTRL group	7.26	1,53	7,00	6,00	8,80
M_AMP in OHP3 group	8.52	3,55	9,70	5,05	10,70
M_AMP in OHP4 group	7.23	3,21	6,15	5,15	8,25
M_AMP in OHP5 group	5.77	1,25	5,55	5,30	6,80
M_VEL in CTRL group	35.79	3,39	35,25	32,80	37,90
M_VEL in OHP3 group	34.10	1,75	34,20	32,80	35,55
M_VEL in OHP4 group	34.98	2,29	35,40	33,50	36,00
M_VEL in OHP5 group	33.26	2,05	32,65	32,00	33,90

CD_AMP: distal caudal nerve SNAP amplitude (μv); ***CD_VEL***: distal caudal nerve sensory conduction velocity (m/sec); ***D_AMP***: digital nerve SNAP amplitude (μv); ***D_VEL***: digital nerve sensory conduction velocity (m/sec); ***M_AMP***: caudal nerve CMAP amplitude (mV); ***M_VEL***: caudal nerve motor conduction velocity (m/sec); ***PC_AMP***: proximal caudal nerve SNAP amplitude (μv); ***PC_VEL***: proximal caudal nerve sensory conduction velocity (m/sec).

Table 40. Neurophysiological data at end of treatment: Kruskal-Wallis test. Pairwise comparison, adjusted by the Bonferroni correction for multiple tests, demonstrated that CDAMPEND was different between OHP5 and CTRL groups (p-value 0.001); DAMPEND was different between OHP5 and CTRL and between OHP4 and CTRL groups (p-value 0.002 and 0.003 respectively); CDVELEND was different between OHP5 and CTRL groups (p-value 0.005). ***CDAMPEND***: distal caudal nerve SNAP amplitude; ***CDVELEND***: distal caudal nerve sensory conduction velocity; ***DAMPEND***: digital nerve SNAP amplitude; ***DVELEND***: digital nerve sensory conduction velocity; ***MAMPEND***: caudal nerve CMAP amplitude; ***MVELEND***: caudal nerve motor conduction velocity; ***PCAMPEND***: proximal caudal nerve SNAP amplitude; ***PCVELEND***: proximal caudal nerve sensory conduction velocity.

Hypothesis Test Summary

	Null Hypothesis	Test	Sig.	Decision
1	The distribution of CDAMPEND is the same across categories of 1=CTRL; 2=OHP3; 3=OHP4; 4=OHP5.	Independent-Samples Kruskal-Wallis Test	,001	Reject the null hypothesis.
2	The distribution of CDVELEND is the same across categories of 1=CTRL; 2=OHP3; 3=OHP4; 4=OHP5.	Independent-Samples Kruskal-Wallis Test	,000	Reject the null hypothesis.
3	The distribution of CPAMPEND is the same across categories of 1=CTRL; 2=OHP3; 3=OHP4; 4=OHP5.	Independent-Samples Kruskal-Wallis Test	,110	Retain the null hypothesis.
4	The distribution of CPVELEND is the same across categories of 1=CTRL; 2=OHP3; 3=OHP4; 4=OHP5.	Independent-Samples Kruskal-Wallis Test	,127	Retain the null hypothesis.
5	The distribution of DAMPEND is the same across categories of 1=CTRL; 2=OHP3; 3=OHP4; 4=OHP5.	Independent-Samples Kruskal-Wallis Test	,009	Reject the null hypothesis.
6	The distribution of DVELEND is the same across categories of 1=CTRL; 2=OHP3; 3=OHP4; 4=OHP5.	Independent-Samples Kruskal-Wallis Test	,074	Retain the null hypothesis.
7	The distribution of MAMPEND is the same across categories of 1=CTRL; 2=OHP3; 3=OHP4; 4=OHP5.	Independent-Samples Kruskal-Wallis Test	,303	Retain the null hypothesis.
8	The distribution of MVELEND is the same across categories of 1=CTRL; 2=OHP3; 3=OHP4; 4=OHP5.	Independent-Samples Kruskal-Wallis Test	,244	Retain the null hypothesis.

Asymptotic significances are displayed. The significance level is ,05.

Table 41. Cold Plate Test at end of treatment: descriptive statistics.

	Mean	Std. Deviation	Median	Percentile 25	Percentile 75
COLD150 in CTRL group	5.87	2.36	5.50	4.00	8.00
COLD150 in OHP3 group	7.75	5.18	6.50	3.50	11.50
COLD150 in OHP4 group	**	**	**	**	**
COLD150 in OHP5 group	**	**	**	**	**
COLD300 in CTRL group	8.75	2.49	8.00	7.00	10.50
COLD300 in OHP3 group	20.12	9.96	17.00	13.50	28.50
COLD300 in OHP4 group	**	**	**	**	**
COLD300 in OHP5 group	**	**	**	**	**

COLD150ACUTE: number of signs from 0 to 150 seconds; **COLD300ACUTE**: number of signs from 151 to 300 seconds.
****: the test was suspended precociously for a too much painful behavior in more than 50% of animals.*

Table 42. Cold Plate Test at end of treatment: Mann-Whitney U-test. Warning*: in OHP4 and OHP5 the test was suspended precociously for a too much painful behavior in more than 50% of animals, so no values were available to a comparison to CTRL group.*

Hypothesis Test Summary

	Null Hypothesis	Test	Sig.	Decision
1	The distribution of COLD150END is the same across categories of 1=CTRL; 2=OHP3.	Independent-Samples Mann-Whitney U Test	,798[1]	Retain the null hypothesis.
2	The distribution of COLD300END is the same across categories of 1=CTRL; 2=OHP3.	Independent-Samples Mann-Whitney U Test	,005[1]	Reject the null hypothesis.

Asymptotic significances are displayed. The significance level is ,05.

[1]Exact significance is displayed for this test.

Table 43. NET at end of treatment

VARIABLE	*CTRL GROUP (median, Q1, Q3)*	*OHP3 GROUP (median, Q1, Q3, p-value VS CTRL)*	*OHP4 GROUP (median, Q1, Q3, p-value VS CTRL)*	*OHP5 GROUP (median, Q1, Q3, p-value VS CTRL)*
Stimulus-response and strength-duration properties				
Strength-duration time constant (msec)	0.194 (0.166, 0.2)	0.196 (0.166, 0.26) p=0.57	0.145 (0.12, 0.154) p=0.08298	0.152 (0.143, 0.18) p=0.28
Rheobase (mA)	-0.0463 (-0.103, -0.0343)	-0.0195 (-0.0476, 0.0374) p=0.19	0.0294 (-0.011, 0.0881) **p=0.03***	0.158 (0.15, 0.176) **p=0.001****
Current Threshold properties				
Resting I/V slope	0.877 (0.787, 0.924)	0.896 (0.82, 0.986) p=0.54	0.862 (0.812, 0.894 n=6) p=0.53	0.798 (0.778, 0.807 n=7) p=0.45
Minimum I/V slope	0.398 (0.244, 0.431)	0.336 (0.263, 0.434) p=1	0.391 (0.375, 0.473 n=8) p=0.39689	0.419 (0.387, 0.438 n=8) =0.33566
Hyperpolarazing I/V slope	0.605 (0.598, 0.666)	0.609 (0.578, 0.72) p=0.63	0.637 (0.548, 0.713 n=8) p=0.95	0.589 (0.534, 0.671) p=0.64
Threshold electrotonus				
TEh(90-100 msec)	-78 (-79.6, -75)	-81.6 (-82.8, -78.9) p=0.15	-87.5 (-111, -78.3) p=0.16	-97.9 (-104, -95.5) **p=0.001****
TEd(10-20 msec)	52.2 (50.6, 56.2)	52.6 (51.1, 53.3) p=0.95	52.8 (51.2, 54.9) p=1	54.2 (52, 54.3) p=0.95
TEd(40-60 msec)	48.7 (45.9, 53)	50.3 (47.8, 53.5) p=0.46	51.3 (50.6, 51.9) p=0.28	50.2 (47.9, 52.1) p=0.95
TEd(90-100 msec)	47.5 (45.1, 47.6)	47.1 (46.6, 49.9) p=0.54	48 (47.8, 48.5 n=8) **p=0.04***	46.7 (45.8, 48.8 n=7) p=0.79
TEh(10-20 msec)	-55 (-60, -45.6)	-58.2 (-59.7, -57.2) p=0.28	-64.2 (-67, -60.7 n=8) **p=0.01***	-68.2 (-74.9, -67.8) **p<0.001*****
TEd(undershoot)	-4.88 (-5.89, -4.21)	-5.06 (-6.17, -3.56) p=0.95	-4.11 (-4.82, -3.14) p=0.16	-3.49 (-4.4, -3.19) **p=0.04***
TEd(overshoot)	6.69 (5.61, 9.4 n=8)	3.92 (2.49, 8.22 n=7) p=0.28	7.83 (6.2, 9.45) p=0.78	8.69 (8.01, 9.95) p=0.66

VARIABLE	*CTRL GROUP (median, Q1, Q3)*	*OHP3 GROUP (median, Q1, Q3, p-value VS CTRL)*	*OHP4 GROUP (median, Q1, Q3, p-value VS CTRL)*	*OHP5 GROUP (median, Q1, Q3, p-value VS CTRL)*
TEd(peak)	53.4 (50.9, 57)	52.6 (51.2, 55) p=0.86	53.9 (52.3, 56.2) p=0.80	54.5 (52.5, 54.6) p=0.95
TEh(20-40 msec)	-67.8 (-68.9, -61.1)	-70 (-71.7, -66) p=0.19	-79 (-85.9, -70.3 n=8) **p=0.03***	-82.3 (-97.2, -81.2) **p<0.001*****
TEh(slope 101-140 msec)	1.04 (0.969, 1.14)	1.16 (0.918, 1.22) p=0.69433	1.2 (1.07, 1.59) p=0.16	1.39 (1.37, 1.7) p=0.008**
TEd20(peak)	26 (24.7, 29.1)	26.7 (25.3, 27.6) p=0.78	27.8 (25.5, 30) p=0.44	28.7 (28.5, 30.2) p=0.09
TEd40(Accomodation)	6.1 (4.55, 8.23)	5 (3.95, 6.65) p=0.69	6 (4.05, 7.95) p=0.44	5 (4.65, 8.1) p=0.86
TEd20(10-20 msec)	23.6 (22.7, 25)	25.3 (24.2, 25.6) p=0.33	24 (22.8, 26) p=0.64	27.7 (26.4, 27.8) **p=0.006****
TEh20(10-20 msec)	-23.1 (-24.3, -20.2)	-25.1 (-26.3, -25) **p=0.01****	-25.7 (-28.6, -24 n=8) p=0.10	-27.4 (-28.2, -27.4) **p=0.006****
S2 accommodation	5.91 (4.49, 8.1)	4.67 (3.44, 6.77) p=0.28	5.72 (3.98, 8.02) p=0.57	5.53 (3.94, 8.33) p=0.69
Accommodation half-time	42.7 (39.4, 53.6)	47.1 (43.7, 58.4) p=0.28	50.6 (46.2, 54.3) p=0.28	33.1 (24.8, 47.6) p=0.28
Recovery Cycle				
Relative Refractory Period (msec)	0.435 (0.312, 0.472)	0.364 (0.343, 0.75) p=0.40	0.346 (0.325, 0.45) p=0.95	0.388 (0.337, 0.447) p=0.61
Refractoriness at 2 msec	24.5 (0.902, 29)	8.2 (2.91, 16.2) p=1	8.17 (2.78, 48.6) p=0.69	7.51 (2.98, 16.7) p=0.19
Refractoriness at 2.5msec	5.26 (-7.35, 10.5)	-8.34 (-8.86, -4.81) p=0.43	-4.34 (-5.17, 15.1) p=0.80	-0.948 (-7.83, 1.07) p=0.33
Superexcitability (%)	-11.4 (-15.7, -9.36)	-9.93 (-11.3, -3.6) p=0.19	-7.19 (-8.89, -6.57) **p=0.01***	-9.89 (-10.5, -7.65) p=0.15
Subexcitability (%)	4.12 (2.87, 7.06)	6.42 (2.7, 11.2) p=0.50	4.14 (3.03, 4.71) p=0.96	5.34 (1.4, 8.11) p=0.86
Superexcitability at 5 msec	-12.2 (-14.9, -10.8)	-10.9 (-12.2, 2.98) p=0.23	-6.05 (-7.86, -2.67) **p=0.02***	-7.43 (-9.15, -5.68) **p<0.005****
Superexcitability at 7 msec	-10.1 (-14.9, -8.87)	-7.78 (-9.88, 7.09) p=0.06	-4.45 (-6.89, -3) **p=0.01***	-5.41 (-7.77, -4.18) **p=0.01***

Figure 28. I/V curve after the end of treatment. A comparison between CTRL group with all treatment arms is shown.

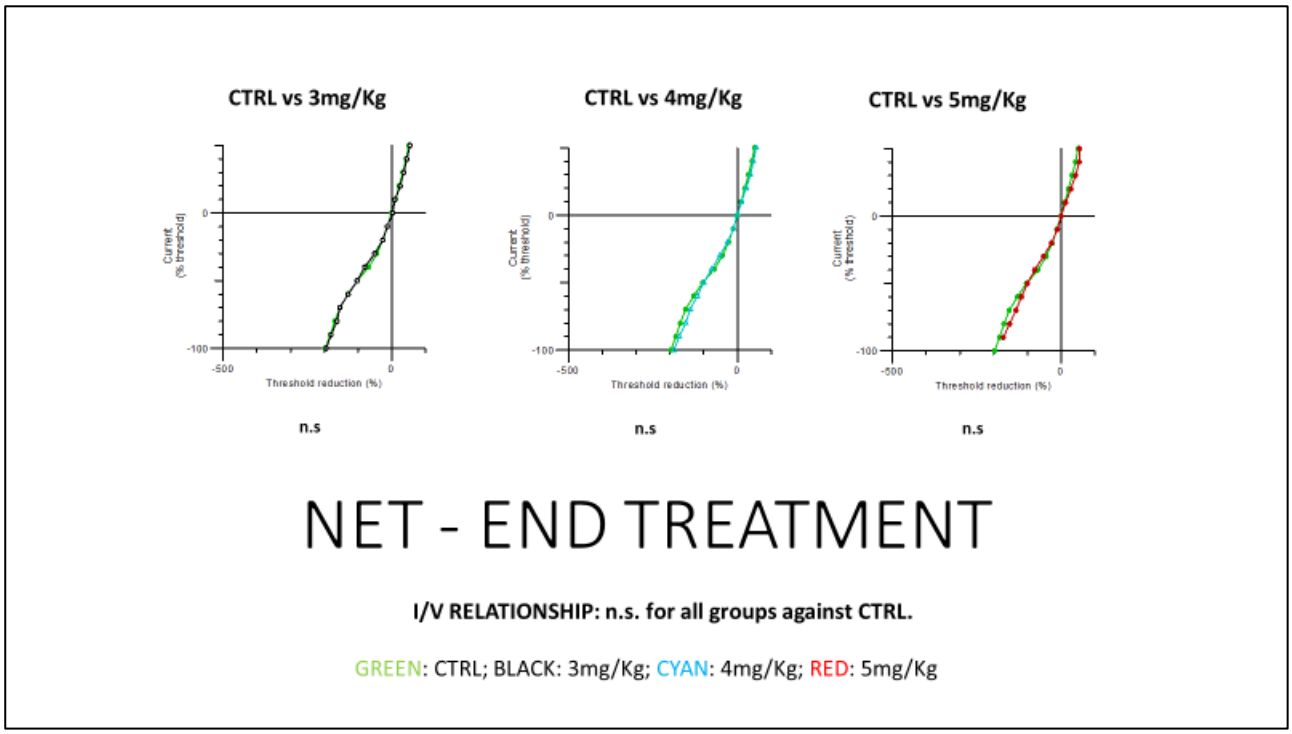

Figure 29. Strength duration time constant after the end of treatment. A comparison between CTRL group with all treatment arms is shown.

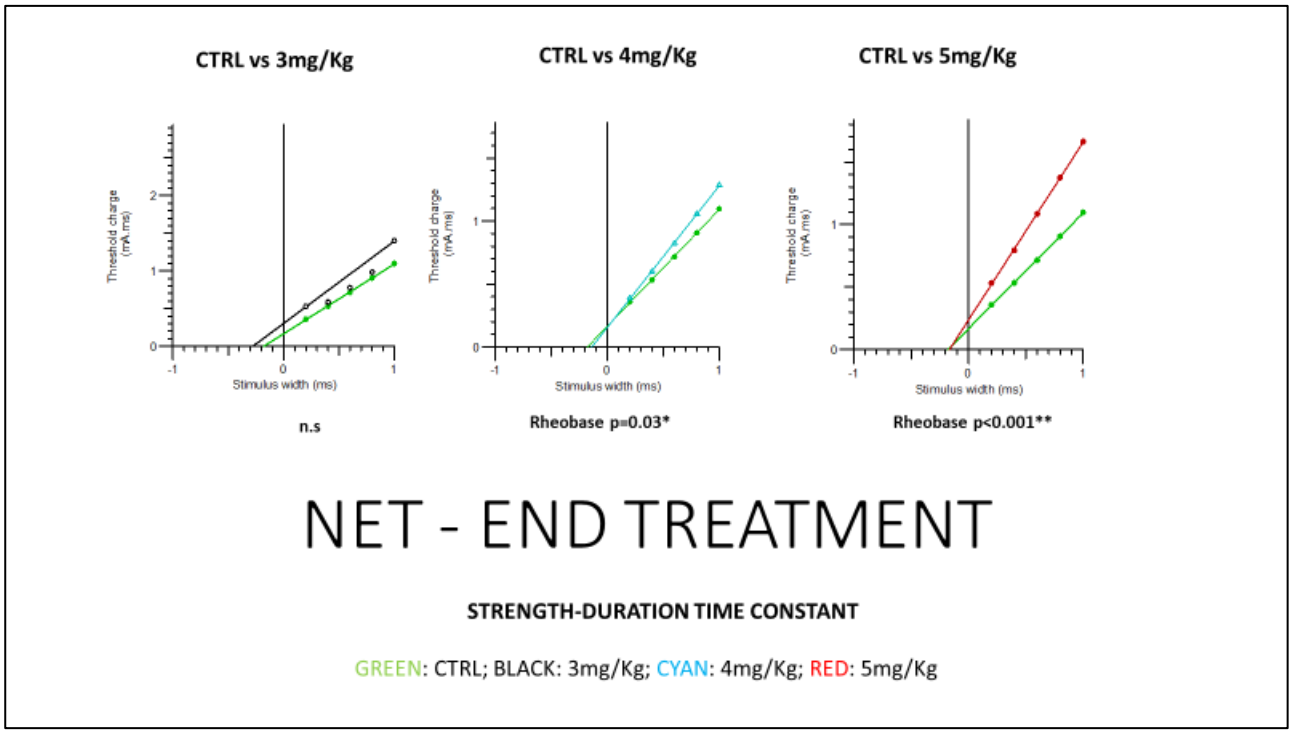

Figure 30. Threshold Electrotonus after the end of treatment. A comparison between CTRL group with all treatment arms is shown.

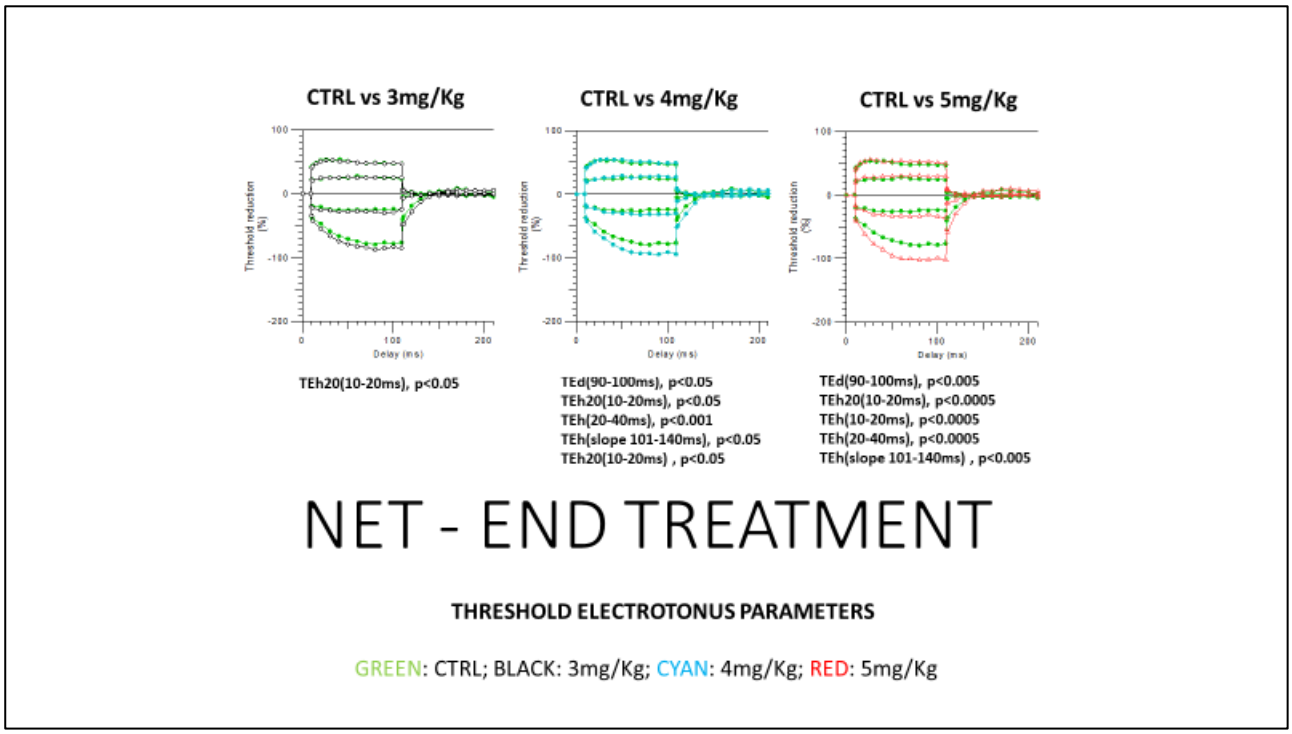

Figure 31. Recovery Cycle after the end of treatment. A comparison between CTRL group with all treatment arms is shown.

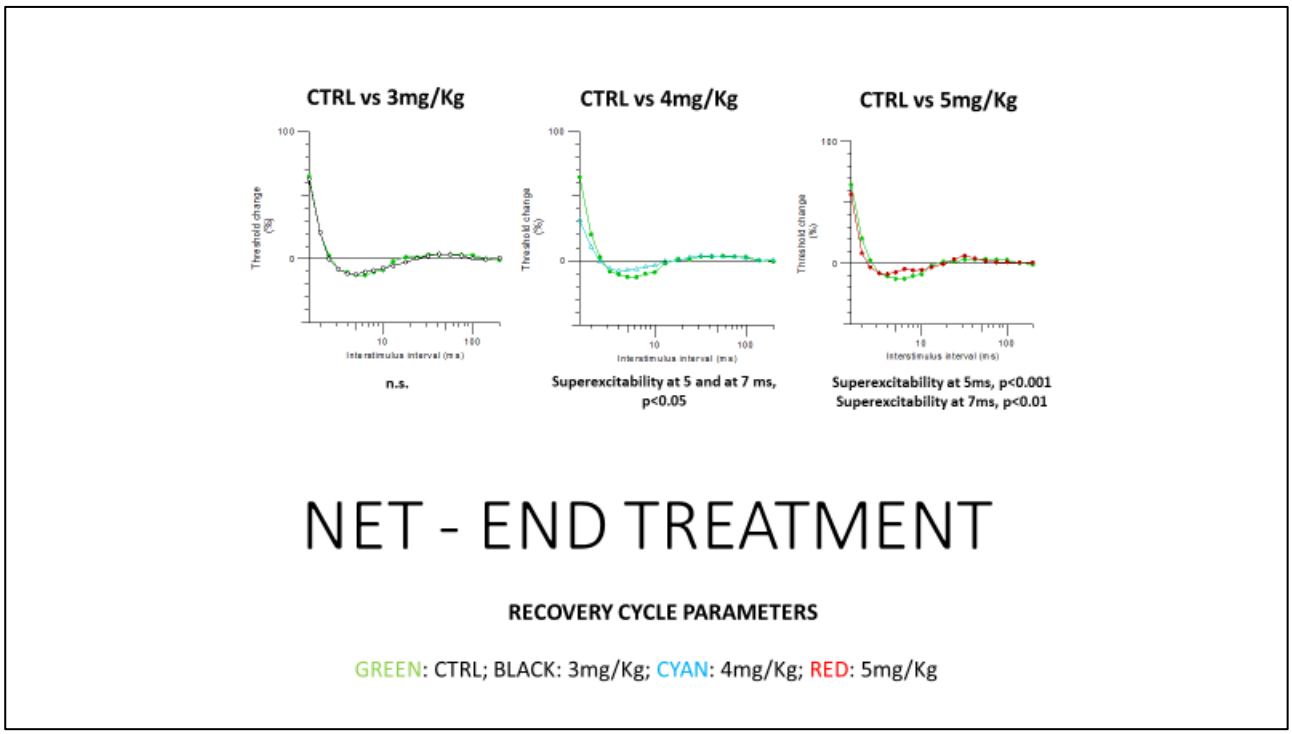

Figure 32. Caudal nerve morphology at the end of treatment (60x magnification). The images show a dose-dependent axonal loss. The 5mg/Kg group shows the higher degree of axonal loss and the clear presence of degenerating fibers.

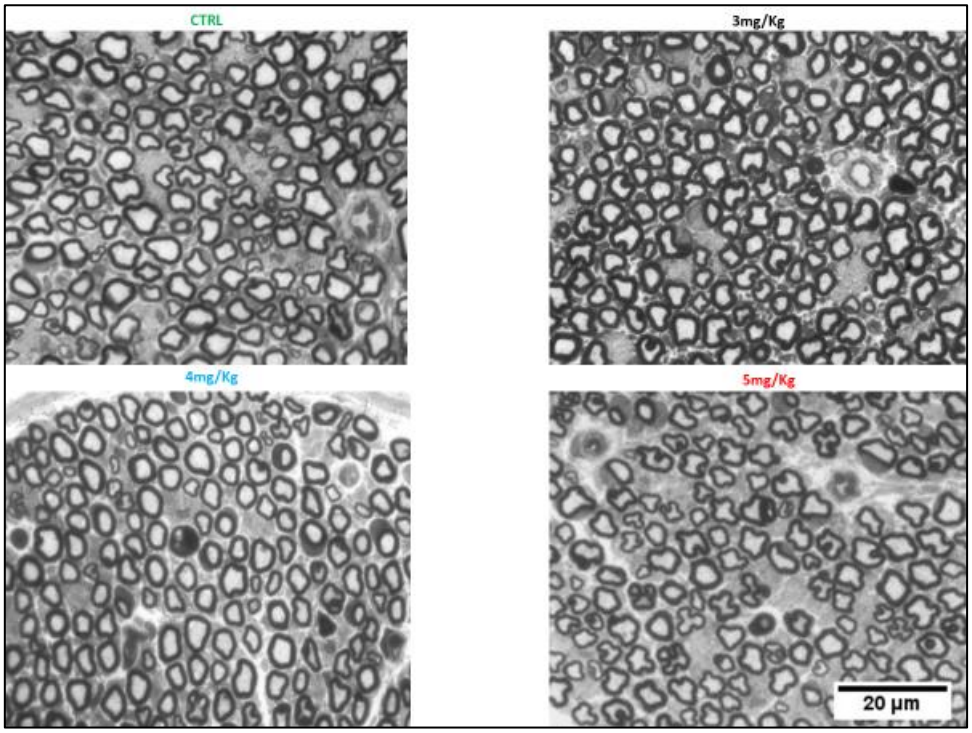

Figure 33. Body weight for all groups during the observational period. No group showed a severe weight loss during the observational period.

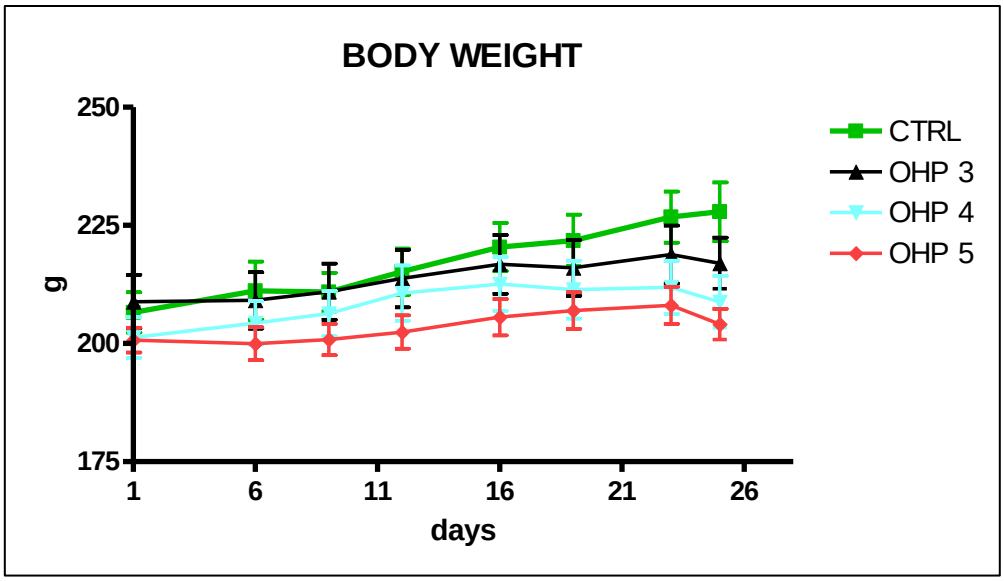

6.4.4 Summary of inferences from TASK 4

Data from **TASK 4** showed that OHP5 group had the ideal schedule to reproduce both acute and chronic OIPN; moreover, animal welfare was preserved too. Thus, the OHP5 group schedule was elected as the one to be used in subsequent experiments.

6.5 TASK 5 - TOPIRAMATE (TPM) AS A NEUROPROTECTANT AGENT AGAINST ACUTE OIPN IN RATS

In **TASK 5** it was verified if TPM was able to decrease acute OIPN. A single OHP injection was performed. Three groups were compared: CTRL, OHP and OHP+TPM group (TPM was administered daily starting 5 days before OHP injections). NET monitoring was performed at 24, 48 and 72 hours after OHP administration. To ensure homogeneity standard neurophysiology was performed at baseline. For more details, see **Study design** section.

6.5.1 Baseline data

Descriptive statistic for nerve conduction studies data is reported in **Table 44**; in **Table 45** Kruskal-Wallis test results are reported: no differences were present among the 3 groups for all variables.

Table 44. Neurophysiological data at base-line: descriptive statistics

	Mean	Std. Deviation	Median	Percentile 25	Percentile 75
DC_AMP in CTRL group	72.69	20.98	73.20	61.35	81.85
DC_AMP in OHP group	69.32	29.37	73.00	43.90	94.90
DC_AMP in OHP+TPM group	84.75	17.58	87.45	69.15	100.80
DC_VEL in CTRL group	29.53	2.27	29.70	27.94	30.79
DC_VEL in OHP group	30.74	4.97	30.15	26.43	34.65
CD_VEL in OHP+TPM group	31.71	2.95	32.26	30.00	33.90
DC_AMP in CTRL group	178.06	31.31	178.55	150.50	201.20
CP_AMP in OHP group	181.50	29.00	183.85	157.40	192.80
CP_AMP in OHP+TPM group	172.54	33.44	183.25	149.25	191.45
CP_VEL in CTRL group	38.60	1.88	38.49	37.04	40.27
CP_VEL in OHP group	37.32	4.55	35.29	34.09	41.39
CP_VEL in OHP+TPM group	39.47	2.88	40.00	37.75	41.68
D_AMP in CTRL group	87.89	19.30	83.30	74.05	103.10
D_AMP in OHP group	90.04	24.06	93.50	78.70	105.10
D_AMP in OHP+TPM group	81.93	23.42	87.50	77.70	94.75
D_VEL in CTRL group	35.49	3.32	35.16	33.74	38.68
D_VEL in OHP group	37.12	1.70	36.65	35.58	38.71
D_VEL in OHP+TPM group	37.69	3.35	37.33	36.14	39.47
M_AMP in CTRL group	5.76	1.95	5.60	4.75	6.15
M_AMP in OHP group	6.31	2.57	5.80	4.55	8.05
M_AMP in OHP+TPM group	6.80	3.71	5.45	4.25	8.75
M_VEL in CTRL group	40.92	3.10	40.41	39.21	43.48
M_VEL in OHP group	38.49	4.70	38.46	36.47	39.61

	Mean	Std. Deviation	Median	Percentile 25	Percentile 75
M_VEL in OHP+TPM group	41.53	2.95	41.25	40.41	43.56

DC_AMP: distal caudal nerve SNAP amplitude (µv); ***DC_VEL***: distal caudal nerve sensory conduction velocity (m/sec); ***D_AMP***: digital nerve SNAP amplitude (µv); ***D_VEL***: digital nerve sensory conduction velocity (m/sec); ***M_AMP***: caudal nerve CMAP amplitude (mV); ***M_VEL***: caudal nerve motor conduction velocity (m/sec); ***PC_AMP***: proximal caudal nerve SNAP amplitude (µv); ***PC_VEL***: proximal caudal nerve sensory conduction velocity (m/sec).

Table 45. Neurophysiological data at base-line: Kruskal-Wallis test.

Hypothesis Test Summary

	Null Hypothesis	Test	Sig.	Decision
1	The distribution of DCAMP is the same across categories of 1=CTRL; 2=OHP; 3=OHPTPM.	Independent-Samples Kruskal-Wallis Test	,733	Retain the null hypothesis.
2	The distribution of DCVEL is the same across categories of 1=CTRL; 2=OHP; 3=OHPTPM.	Independent-Samples Kruskal-Wallis Test	,651	Retain the null hypothesis.
3	The distribution of PCAMP is the same across categories of 1=CTRL; 2=OHP; 3=OHPTPM.	Independent-Samples Kruskal-Wallis Test	,573	Retain the null hypothesis.
4	The distribution of PCVEL is the same across categories of 1=CTRL; 2=OHP; 3=OHPTPM.	Independent-Samples Kruskal-Wallis Test	,482	Retain the null hypothesis.
5	The distribution of DAMP is the same across categories of 1=CTRL; 2=OHP; 3=OHPTPM.	Independent-Samples Kruskal-Wallis Test	,368	Retain the null hypothesis.
6	The distribution of DVEL is the same across categories of 1=CTRL; 2=OHP; 3=OHPTPM.	Independent-Samples Kruskal-Wallis Test	,704	Retain the null hypothesis.
7	The distribution of MAMP is the same across categories of 1=CTRL; 2=OHP; 3=OHPTPM.	Independent-Samples Kruskal-Wallis Test	,945	Retain the null hypothesis.
8	The distribution of MVEL is the same across categories of 1=CTRL; 2=OHP; 3=OHPTPM.	Independent-Samples Kruskal-Wallis Test	,988	Retain the null hypothesis.

Asymptotic significances are displayed. The significance level is ,05.

6.5.2 Data at 24 hours

NET findings and statistical test results are shown in **Table 46** and **Figure 34**. Compared to CTRL group, **OHP** group showed a few significantly different values in threshold electrotonus; no other differences were demonstrated. Instead, compared to CTRL group, **OHP+TPM** group showed mainly a decreased resting I/V slope (p-vale <0.001) and a difference in parameters for threshold electrotonus and recovery cycle; notably refractoriness and superexcitability significant values were set at more negative values.

Table 46. NET findings at 24 hours.

VARIABLE	*CTRL GROUP*	*OHP GROUP [median (Q1, Q3), p value VS CTRL]*	*OHP+TPM GROUP [median (Q1, Q3), p value VS CTRL]*
Stimulus-response and strength-duration properties			
Strength-duration time constant (msec)	0.183 (0.156, 0.207)	0.152 (0.142, 0.209) p=0.64	0.142 (0.133, 0.144) p=0.10
Rheobase (mA)	2.88 (2.82, 2.93)	2.96 (2.89, 2.97) p=0.16	1.54 (0.0879, 3.01) p=1
Current Threshold properties			
Resting I/V slope	0.921 (0.896, 0.944)	0.924 (0.807, 0.966) p=0.88	0.77 (0.688, 0.814) **p<0.001*** **
Minimum I/V slope	0.321 (0.277, 0.424)	0.363 (0.335, 0.381) p=0.50536	0.368 (0.337, 0.4) p=0.94972
Hyperpolarazing I/V slope	0.674 (0.543, 0.832)	0.715 (0.621, 0.754) p=1	0.569 (0.413, 0.602) p=0.11
Threshold electrotonus			
TEh(90-100 msec)	-77.1 (-90.7, -74.1)	-84.5 (-94, -75.2) p=0.57	-96.5 (-124, -93.3) **p=0.002****
TEd(10-20 msec)	53.1 (50.8, 55.2)	51.6 (48.3, 53.2) p=0.33	56.2 (55.6, 57.1) **p=0.04***
TEd(40-60 msec)	50.1 (48.4, 52.3)	49.6 (46.5, 51.4) p=0.64	53.8 (52.3, 55.4 n=8) **p=0.02***
TEd(90-100 msec)	48.2 (45.6, 48.7)	46.5 (46, 49.4) p=1	51.3 (50, 52.4) **p=0.001****
TEh(10-20 msec)	-56.8 (-60.4, -55.7)	-61 (-65.6, -58.2) p =0.28	-66.4 (-69, -65.7) **p=0.0001*****
TEd(undershoot)	-5.45 (-7.47, -4.06)	-7.57 (-8.02, -6.37) p=0.33	-4.45 (-6.17, -3.34) p=0.44
TEh(overshoot)	6.24 (4.95, 7.09)	9.02 (8.23, 9.53) **p=0.006****	11.2 (9.39, 13.1) **p<0.001*****
TEd(peak)	54 (51.1, 55.8)	53.6 (50.4, 54.9) p=0.64538	56.4 (56.4, 58 n=8) p=0.03792*
TEh(20-40 msec)	-66.1 (-72.5, -64.1)	-71.1 (-78.9, -68.5) p=0.20	-83.6 (-87.7, -80.5) **p=0.0001*****
TEh(slope 101-140 msec)	0.969 (0.906, 1.12)	1.15 (0.952, 1.26) p=0.44	1.45 (1.37, 1.61) **p=0.001****
TEd20(peak)	26.7 (26, 27.7)	27.6 (25.2, 29) p=0.88	30.1 (29.7, 30.7) **p<0.001*****
TEd40(Accomodation)	7.15 (6.45, 8.23)	6.55 (5.17, 9.82) p=0.96	6.4 (4.6, 7.47) p=0.50
TEd20(10-20 msec)	25 (24.6, 25.8)	25 (22.4, 25.2) p=0.50	28.2 (25.2, 28.7) p=0.06
TEh20(10-20 msec)	-23.8 (-24.8, -23.7)	-24.3 (-27.1, -23.4) p=0.80	-28.5 (-28.9, -27.1) **p<0.001*****
S2 accommodation	6.78 (6.31, 7.33)	5.53 (3.32, 8.21) p=0.57	6.39 (5.08, 7.65) p=0.72
Accommodation half-time	49.2 (45, 53.2)	50.5 (47, 55.7) p=0.65	50 (40.2, 58.1) p=0.95913
Recovery Cycle			
Relative Refractory Period (msec)	0.365 (0.298, 0.4)	0.345 (0.294, 0.387) p=0.42	0.239 (0.223, 0.268) **p<0.005****
Refractoriness at 2msec	6.62 (-0.719, 10.8)	5.94 (-2.19, 10.6) p=0.75	-10.7 (-12.8, -3) **p=0.01***
Refractoriness at 2.5msec	-4.53 (-7.81, 0.162)	-5.59 (-9.14, -1.85) p=0.50	-17.2 (-19.3, -10.2) **p<0.01****
Superexcitability (%)	-13.2 (-14.7, -8.85)	-10.5 (-12.8, -3.96) p=0.23	-18.8 (-20.5, -15.4) **p<0.005****
Subexcitability (%)	5.43 (2.41, 8.5)	3.19 (1.86, 5.79) p=0.50	2.64 (2.31, 3.02) p=0.16

VARIABLE	*CTRL GROUP*	*OHP GROUP [median (Q1, Q3), p value VS CTRL]*	*OHP+TPM GROUP [median (Q1, Q3), p value VS CTRL]*
Superexcitability at 5 msec	-12.7 (-15.2, -8.77)	-8.34 (-12.1, -5.93) p=0.23	-17.5 (-19.2, -15.2) **p=0.02***
Superexcitability at 7 msec	-11.2 (-13.3, -7.14)	-7.66 (-9.67, -4.58) p=0.19	-13.6 (-15, -12.9) p=0.10

Figure 34. Threshold Electrotonus and Recovery cycle variations at 24 hours. ***A****: threshold electrotonus of OHP group;* ***B****: recovery cycle of OHP group;* ***C****: threshold electrotonus of OHP+TPM group;* ***D****: recovery cycle of OHP+TPM group.* Compared to CTRL group, OHP group showed a few significantly different values in threshold electrotonus. Instead, OHP+TPM group showed a decreased resting I/V slope and a difference in parameters for threshold electrotonus and recovery cycle; notably refractoriness and superexcitability significant values were set at more negative values. See **Table 46** for more details.

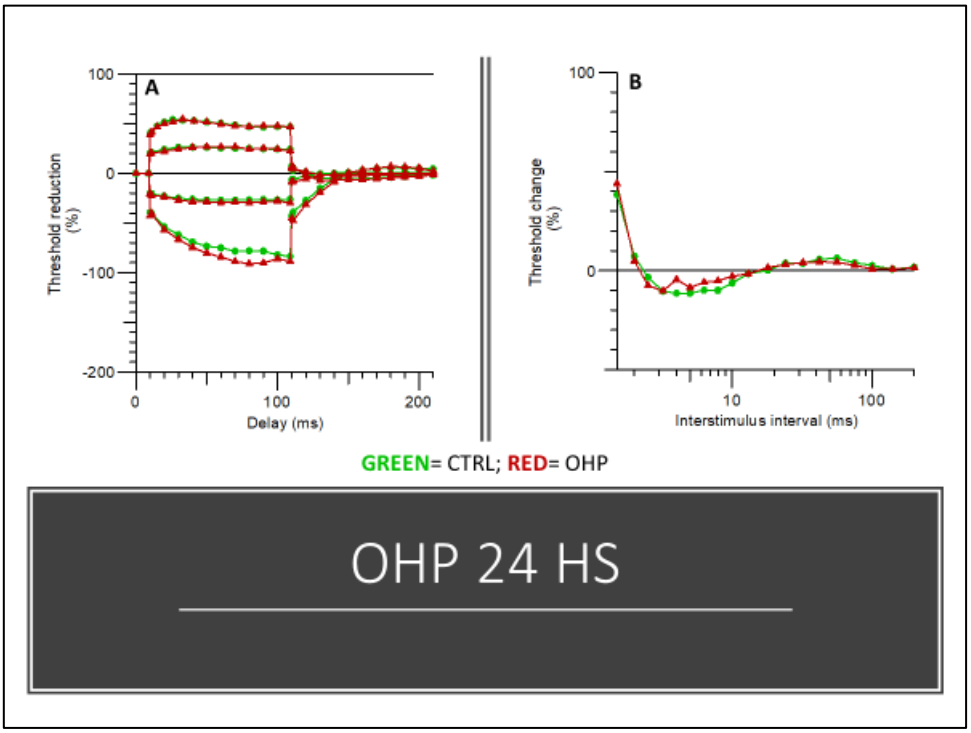

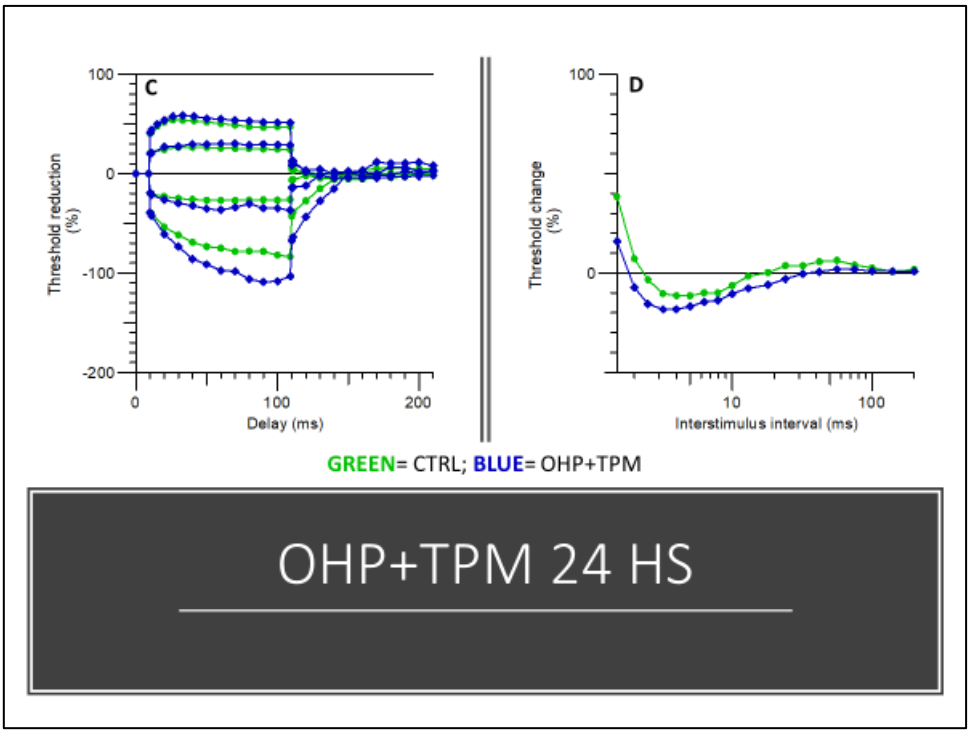

6.5.3 Data at 48 hours

NET findings and statistical test results are shown in **Table 47** and **Figure 35**. Compared to CTRLs, **OHP** group showed a few significantly different values in threshold electrotonus; notably, refractoriness parameters were also different. Compared to CTRLs, **OHP+TPM** group showed mainly a decreased resting I/V slope (p-vale <0.001) and a difference in most parameters for threshold electrotonus; for recovery cycle, only some refractoriness values were set significantly at more negative values, but these values were less negative than the one at 24 hours.

Table 47. NET findings at 48 hours.

VARIABLE	*CTRL GROUP*	*OHP GROUP [median (Q1, Q3), p value VS CTRL]*	*OHP+TPM GROUP [median (Q1, Q3), p value VS CTRL]*
Stimulus-response and strength-duration properties			
Strength-duration time constant (msec)	0.183 (0.156, 0.207)	0.12 (0.0852, 0.218) p=0.44	0.173 (0.141, 0.18) p=0.58
Rheobase (mA)	2.88 (2.82, 2.93)	2.98 (2.92, 3.01) **p=0.03***	1.53 (0.0795, 2.99) p=1
Current Threshold properties			
Resting I/V slope	0.921 (0.896, 0.944)	0.967 (0.85, 1.02) p=0.57	0.733 (0.729, 0.807) **p<0.0005*****
Minimum I/V slope	0.321 (0.277, 0.424)	0.327 (0.32, 0.339) p=0.96	0.365 (0.346, 0.433) p=0.33
Hyperpolarazing I/V slope	0.674 (0.543, 0.832)	0.607 (0.581, 0.652) p=0.53	0.572 (0.473, 0.61) p=0.19
Threshold electrotonus			
TEh(90-100 msec)	-77.1 (-90.7, -74.1)	-91.7 (-101, -84.8) p=0.10	-106 (-115, -96.1) **p=0.005****
TEd(10-20 msec)	53.1 (50.8, 55.2)	52.5 (52.3, 53.4) p=0.7209	56 (53.2, 57) p=0.38
TEd(40-60 msec)	50.1 (48.4, 52.3)	52 (50.9, 52.4) p=0.23	52.3 (50.6, 55) p=0.33
TEd(90-100 msec)	48.2 (45.6, 48.7)	47.2 (45.6, 49) p=0.88	50.7 (48.8, 52.4) **p=0.03***
TEh(10-20 msec)	-56.8 (-60.4, -55.7)	-60.6 (-60.8, -57.2) p=0.50	-67.1 (-67.7, -65.2) **p<0.001*****
TEd(undershoot)	-5.45 (-7.47, -4.06)	-5.57 (-11.6, -3.63) p=0.72	-3.21 (-6.24, -1.79) =0.16
TEh(overshoot)	6.24 (4.95, 7.09)	5.43 (2.51, 9.82) p=0.88	8.06 (7.26, 10.3) **p=0.02***
TEd(peak)	54 (51.1, 55.8)	54 (53.6, 55) p=0.88	56.3 (54.7, 57.6) p=0.33
TEh(20-40 msec)	-66.1 (-72.5, -64.1)	-72.3 (-74.6, -71.1) p=0.10	-86.1 (-86.7, -81) **p=0.001****
TEh(slope 101-140 msec)	0.969 (0.906, 1.12)	1.22 (1.12, 1.28) p=0.06	1.4 (1.36, 1.71) **p=0.001****
TEd20(peak)	26.7 (26, 27.7)	28.3 (26.4, 29.8) p=0.23	29.8 (28.4, 30.2) **p=0.05***
TEd40(Accomodation)	7.15 (6.45, 8.23)	6.55 (5.07, 7.57) p=0.28	5.9 (5.2, 7.18 n=8) p=0.32821
TEd20(10-20 msec)	25 (24.6, 25.8)	24.1 (23.6, 26.2) p=0.50	27.3 (26.2, 28.2 n=8) **p=0.03***
TEh20(10-20 msec)	-23.8 (-24.8, -23.7)	-25.6 (-26.3, -24.8) **p=0.05***	-27.9 (-28.8, -26.9) **p=0.001****
S2 accommodation	6.78 (6.31, 7.33)	6.99 (5, 7.82) p=0.8	5.6 (4.5, 7.2) p=0.38
Accommodation half-time	49.2 (45, 53.2)	58.8 (49.5, 64.2) p=0.13	41.7 (37.7, 48.3) p=0.23
Recovery Cycle			
Relative Refractory Period (msec)	0.365 (0.298, 0.4)	0.276 (0.242, 0.305) **p=0.02***	0.3 (0.239, 0.304) p=0.07
Refractoriness at 2msec	6.62 (-0.719, 10.8)	-4 (-5.95, 1.08)	-1.69 (-6.92, -0.0445)

VARIABLE	*CTRL GROUP*	*OHP GROUP [median (Q1, Q3), p value VS CTRL]*	*OHP+TPM GROUP [median (Q1, Q3), p value VS CTRL]*
		p=0.05*	**p=0.05***
Refractoriness at 2.5msec	-4.53 (-7.81, 0.162)	-11.4 (-13.2, -8.61) **p=0.05***	-10 (-12.9, -6.43) **p=0.05***
Superexcitability (%)	-13.2 (-14.7, -8.85)	-14.3 (-17, -10.7) p=0.33	-14 (-16, -12.7) p=0.28
Subexcitability (%)	5.43 (2.41, 8.5)	1.66 (1.63, 2.66) p=0.08	2.16 (1.86, 2.62) p=0.08
Superexcitability at 5 msec	-12.7 (-15.2, -8.77)	-14.3 (-17.9, -7.89) p=0.38	-13.3 (-14.6, -12.8) p=0.57
Superexcitability at 7 msec	-11.2 (-13.3, -7.14)	-7.08 (-14.4, -6.75) p=1	-12.3 (-12.9, -11.4) p=0.72

Figure 35. Threshold Electrotonus and Recovery cycle variations at 48 hours. ***A****: threshold electrotonus of OHP group;* ***B****: recovery cycle of OHP group;* ***C****: threshold electrotonus of OHP+TPM group;* ***D****: recovery cycle of OHP+TPM group.* OHP group showed different values in threshold electrotonus; refractoriness parameters were also different. OHP+TPM group showed a decreased resting I/V slope and a difference for threshold electrotonus; for recovery cycle, only some refractoriness values were set significantly at more negative values, but these values were less negative than the one at 24 hours. See **Table 47** for more details.

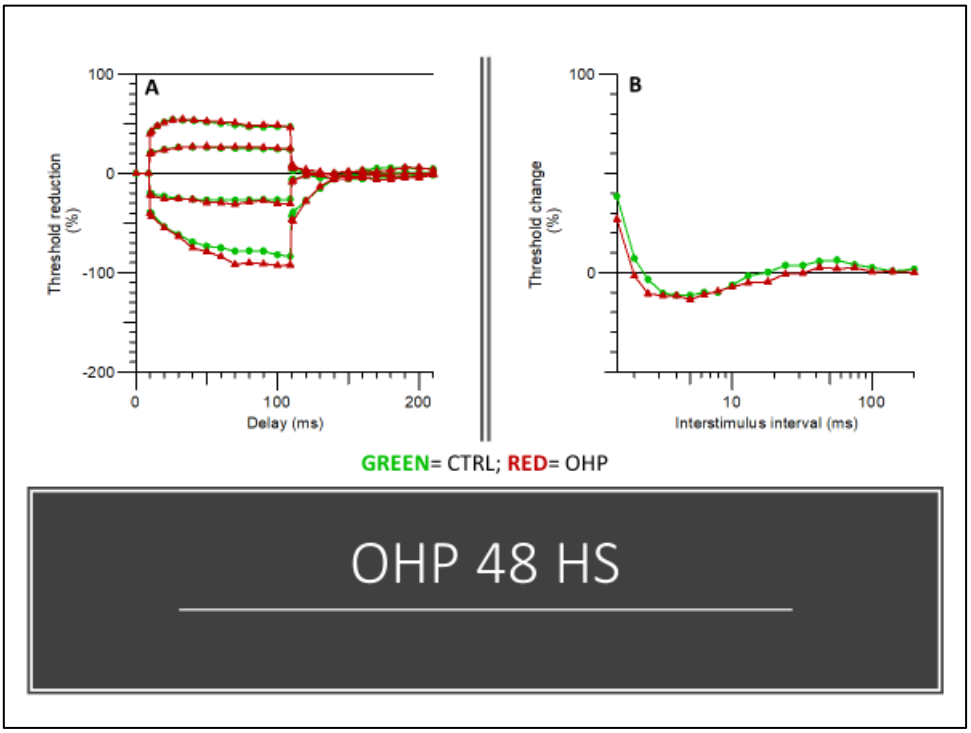

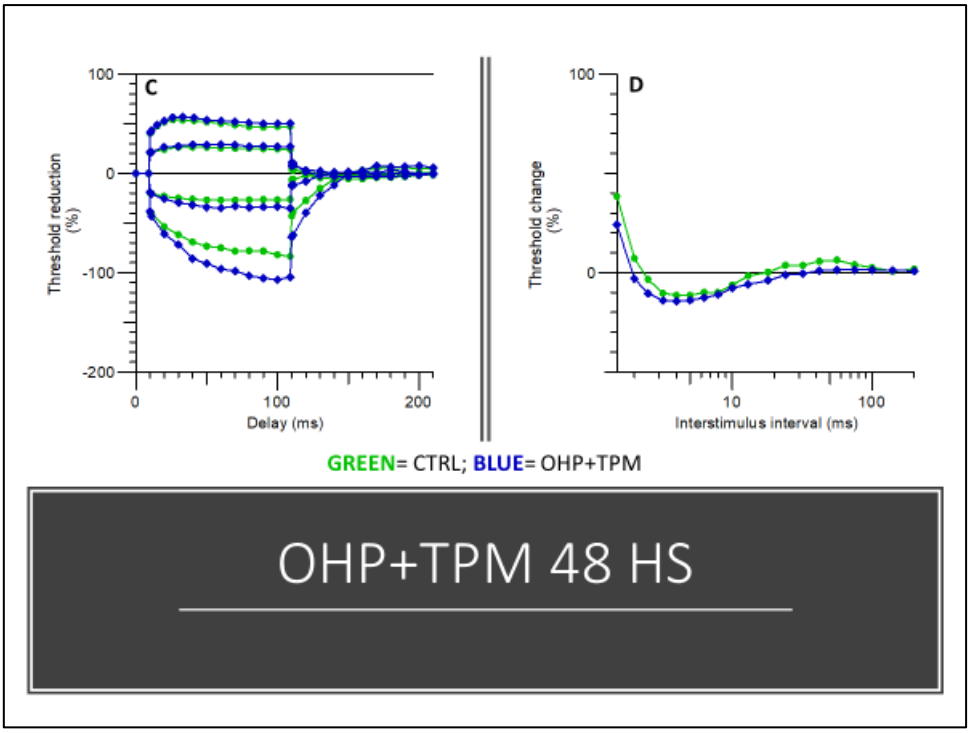

6.5.4 Data at 72 hours

Descriptive statistic for all nerve conduction studies data is reported in **Table 48**; in **Table 49** Kruskal-Wallis test results are reported: no differences were present among the 3 groups for all variables.

NET findings and statistical test results are shown in **Table 50** and **Figure 36**. Compared to CTRLs, **OHP** group showed mainly an increased superexcitability (at 2 msec, p-value 0.03) at recovery cycle. Compared to CTRLs, **OHP+TPM** group showed mainly a difference in a few parameters for all curves apart from recovery cycle: superxcitability was the same compared to CTRL group.

Table 48. Neurophysiological data at 72 hours: descriptive statistics.

	Mean	Standard Deviation	Median	Percentile 25	Percentile 75
CD_AMP in CTRL group	95.05	25.05	86.10	81.00	102.50
CD_AMP in OHP group	95.61	41.58	92.15	64.75	128.50
CD_AMP in OHP+TPM group	89.39	27.92	79.50	71.95	107.45
CD_VEL in CTRL group	27.09	1.05	26.91	26.55	27.28
CD_VEL in OHP group	28.03	3.55	26.91	25.98	29.27
CD_VEL in OHP+TPM group	26.71	1.82	26.32	25.65	27.54
CP_AMP in CTRL group	188.39	21.82	192.60	171.20	196.95
CP_AMP in OHP group	170.95	33.99	172.70	157.75	194.95
CP_AMP in OHP+TPM group	171.24	44.44	163.60	127.95	217.30
CP_VEL in CTRL group	34.63	2.55	34.49	32.81	35.30
CP_VEL in OHP group	35.80	2.86	34.89	33.71	38.30
CP_VEL in OHP+TPM group	35.26	1.22	35.22	34.49	36.15
D_AMP in CTRL group	98.89	21.46	94.00	83.55	115.45
D_AMP in OHP group	85.66	17.34	86.65	74.75	99.10
D_AMP in OHP+TPM group	81.45	17.49	81.55	75.30	93.30
D_VEL in CTRL group	37.33	1.38	37.67	36.21	38.31
D_VEL in OHP group	35.38	4.27	36.20	34.10	38.47
D_VEL in OHP+TPM group	36.31	4.23	36.59	31.97	39.48
M_AMP in CTRL group	6.36	2.27	7.05	4.90	7.75
M_AMP in OHP group	7.11	1.91	7.05	6.50	7.55
M_AMP in OHP+TPM group	7.77	4.93	6.85	4.00	10.75
M_VEL in CTRL group	42.41	2.67	42.55	40.99	43.96
M_VEL in OHP group	43.09	3.17	42.55	41.67	44.53
M_VEL in OHP+TPM group	42.60	3.58	43.02	41.67	43.48

DC_AMP: distal caudal nerve SNAP amplitude (μv); ***DC_VEL***: distal caudal nerve sensory conduction velocity (m/sec); ***D_AMP***: digital nerve SNAP amplitude (μv); ***D_VEL***: digital nerve sensory conduction velocity (m/sec); ***M_AMP***: caudal nerve CMAP amplitude (mV); ***M_VEL***: caudal nerve motor conduction velocity (m/sec); ***PC_AMP***: proximal caudal nerve SNAP amplitude (μv); ***PC_VEL***: proximal caudal nerve sensory conduction velocity (m/sec).

Table 49. Neurophysiological data at 72 hours: Kruskall-Wallis test.

Hypothesis Test Summary

	Null Hypothesis	Test	Sig.	Decision
1	The distribution of DCAMPend is the same across categories of 1=CTRL; 2=OHP; 3=OHPTPM.	Independent-Samples Kruskal-Wallis Test	,453	Retain the null hypothesis.
2	The distribution of DCVELend is the same across categories of 1=CTRL; 2=OHP; 3=OHPTPM.	Independent-Samples Kruskal-Wallis Test	,311	Retain the null hypothesis.
3	The distribution of PCAMPend is the same across categories of 1=CTRL; 2=OHP; 3=OHPTPM.	Independent-Samples Kruskal-Wallis Test	,949	Retain the null hypothesis.
4	The distribution of PCVELend is the same across categories of 1=CTRL; 2=OHP; 3=OHPTPM.	Independent-Samples Kruskal-Wallis Test	,422	Retain the null hypothesis.
5	The distribution of DAMPend is the same across categories of 1=CTRL; 2=OHP; 3=OHPTPM.	Independent-Samples Kruskal-Wallis Test	,751	Retain the null hypothesis.
6	The distribution of DVELend is the same across categories of 1=CTRL; 2=OHP; 3=OHPTPM.	Independent-Samples Kruskal-Wallis Test	,343	Retain the null hypothesis.
7	The distribution of MAMPend is the same across categories of 1=CTRL; 2=OHP; 3=OHPTPM.	Independent-Samples Kruskal-Wallis Test	,884	Retain the null hypothesis.
8	The distribution of MVELend is the same across categories of 1=CTRL; 2=OHP; 3=OHPTPM.	Independent-Samples Kruskal-Wallis Test	,101	Retain the null hypothesis.

Asymptotic significances are displayed. The significance level is ,05.

Table 50. NET at 72 hours

VARIABLE	*CTRL GROUP*	*OHP GROUP [median (Q1, Q3), p value VS CTRL]*	*OHP+TPM GROUP [median (Q1, Q3), p value VS CTRL]*
Stimulus-response and strength-duration properties			
Strength-duration time constant (msec)	0.183 (0.156, 0.207)	0.174 (0.129, 0.188) p=0.7209	0.145 (0.138, 0.1828) p=0.2345
Rheobase (mA)	2.88 (2.82, 2.93)	2.94 (2.91, 2.97) p=0.06	-0.111 (-0.175, -0.0675) **p=0.0001*** **
Current Threshold properties			
Resting I/V slope	0.921 (0.896, 0.944)	0.899 (0.727, 0.979) p=1	0.812 (0.691, 0.852) **p=0.001** **
Minimum I/V slope	0.321 (0.277, 0.424)	0.421 (0.415, 0.427) p=0.15	0.338 (0.294, 0.405) p=0.88
Hyperpolarazing I/V slope	0.674 (0.543, 0.832)	0.507 (0.486, 0.517) **p<0.005** **	0.518 (0.478, 0.597) **p=0.04***
Threshold electrotonus			
TEh(90-100 msec)	-77.1 (-90.7, -74.1)	-74.4 (-86.2, -72.5) p=0.57	-76 (-89.7, -72) p=0.88
TEd(10-20 msec)	53.1 (50.8, 55.2)	51.5 (50.6, 51.6) p=0.33	50.2 (48.6, 50.8) **p=0.02***
TEd(40-60 msec)	50.1 (48.4, 52.3)	49.5 (47.6, 51) p=0.50	46.4 (45.8, 47.2) **p=0.02***
TEd(90-100 msec)	48.2 (45.6, 48.7)	48.6 (46.4, 51) p=0.38	45.5 (44.8, 46.4) p=0.28
TEh(10-20 msec)	-56.8 (-60.4, -55.7)	-55.2 (-61.6, -53.4) p=0.57	-60.2 (-61.5, -56.4) p=0.33
TEd(undershoot)	-5.45 (-7.47, -4.06)	-4.32 (-5.43, -2.68) p=0.23	-4.39 (-8.15, -3.12) p=0.88
TEh(overshoot)	6.24 (4.95, 7.09)	9.34 (7.29, 9.52) **p=0.04***	5.18 (4.49, 7.51) p=0.78
TEd(peak)	54 (51.1, 55.8)	52 (51.6, 53.3) p=0.80	49.8 (48.6, 50.9) **p=0.04***
TEh(20-40 msec)	-66.1 (-72.5, -64.1)	-69.8 (-73.8, -67.9) p=0.44	-70.4 (-73.1, -65.3) p=0.79845
TEh(slope 101-140 msec)	0.969 (0.906, 1.12)	0.993 (0.911, 1.14) p=0.80	1.07 (0.912, 1.31) p=0.64
TEd20(peak)	26.7 (26, 27.7)	27.4 (26.4, 29) p=0.33	24.6 (23.9, 25.1) **p=0.02***
TEd40(Accomodation)	7.15 (6.45, 8.23)	6.1 (5.62, 7.93) p=0.38	6.55 (3.1, 9.25) p=0.96
TEd20(10-20 msec)	25 (24.6, 25.8)	23.5 (22, 24.1) p=0.08	22.3 (21.8, 23.3) **p=0.002** **
TEh20(10-20 msec)	-23.8 (-24.8, -23.7)	-26.4 (-27.8, -24) p=0.23	-25.1 (-25.9, -24) p=0.38
S2 accommodation	6.78 (6.31, 7.33)	4.69 (1.35, 5.82) p=0.08	4.11 (3.03, 6.89) p=0.28
Accommodation half-time	49.2 (45, 53.2)	53.4 (47, 70.9) p=0.28	47.1 (42.2, 53.6) p=0.88
Recovery Cycle			
Relative Refractory Period (msec)	0.365 (0.298, 0.4)	0.392 (0.37, 0.64) p=0.19	0.343 (0.312, 0.409) p=0.72
Refractoriness at 2msec	6.62 (-0.719, 10.8)	8.74 (5.33, 18.3) p=0.44	6.49 (1.05, 9.68) p=0.72
Refractoriness at 2.5msec	-4.53 (-7.81, 0.162)	-2.81 (-5.82, 6.42) p=0.33	-7.98 (-8.89, -3.62) p=0.44
Superexcitability (%)	-13.2 (-14.7, -8.85)	-11.5 (-12.8, -5.84) p=0.44	-12.8 (-15.2, -10.4 n=8) p=0.79845
Subexcitability (%)	5.43 (2.41, 8.5)	3.92 (2.07, 7.95) p=0.72	2.74 (2.33, 3.41) p=0.16
Superexcitability at 5 msec	-12.7 (-15.2, -8.77)	-7.35 (-9.79, -3.47) p=0.13	-11 (-15.2, -10.5) p=1
Superexcitability at 7 msec	-11.2 (-13.3, -7.14)	-0.984 (-4.32, -0.225) **p=0.03***	-11.6 (-13.4, -8.02) p=0.80

Figure 36. Threshold Electrotonus and Recovery cycle variations at 48 hours. ***A****: threshold electrotonus of OHP group;* ***B****: recovery cycle of OHP group;* ***C****: threshold electrotonus of OHP+TPM group;* ***D****: recovery cycle of OHP+TPM group.* OHP group showed an increased superexcitability at recovery cycle. OHP+TPM group showed the same superxcitability as CTRL group. See **Table 50** for more details.

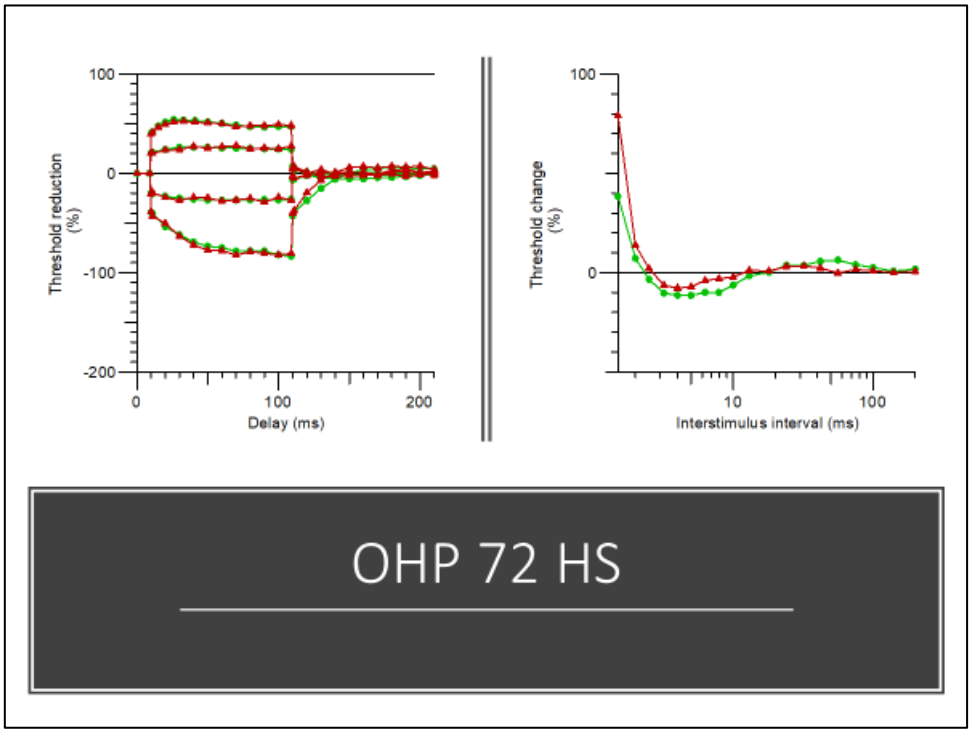

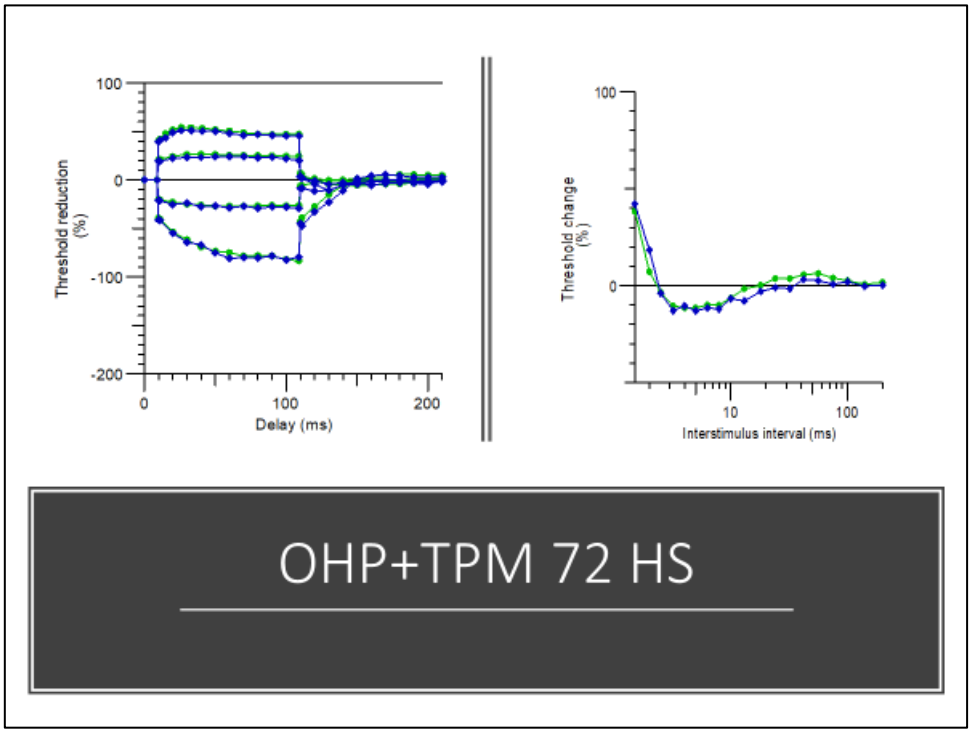

6.5.5 Summary of inferences from TASK 5

NET monitoring over the observational period allowed to confirm that the co-treatment with TPM was able to decrease acute OIPN due to a single OHP injections, abolishing the hallmark of axonal hyperexcitability: alterations in recovery cycle. Therefore, there were the basis to proceed with a last experiment in order to verify the effect of TPM co-treatment on both acute and chronic OIPN.

6.6 TASK 6 - TOPIRAMATE (TPM) AS A NEUROPROTECTANT AGENT AGAINST CHRONIC OIPN IN RATS

6.6.1 Baseline data

Descriptive statistic for all nerve conduction studies data is reported in **Table 51**; in **Table 52** Kruskal-Wallis test results are reported: no differences were present among the 4 groups for all variables. Descriptive statistic for Dynamic Test is reported in **Table 53**; in **Table 54** Kruskal-Wallis test results are reported: no differences were present among the 4 groups for all variables.

Table 51. Neurophysiological data at baseline: descriptive statistics.

	Mean	Std. Deviation	Median	Percentile 25	Percentile 75
CD_AMP in CTRL group	54.39	7.67	54.60	49.70	58.00
CD_AMP in OHP group	60.40	12.94	60.10	52.50	67.10
CD_AMP in OHP+TPM group	60.92	14.30	66.10	51.90	68.70
CD_AMP in TPM group	59.46	12.22	59.50	53.10	71.00
CD_VEL in CTRL group	26.68	1.44	26.30	25.40	28.30
CD_VEL in OHP group	26.31	2.14	26.10	24.20	28.00
CD_VEL in OHP+TPM group	25.72	1.84	25.40	24.60	26.30
CD_VEL in TPM group	25.62	1.78	24.80	24.40	27.30
CP_AMP in CTRL group	135.67	30.13	135.80	109.80	151.30
CP_AMP in OHP group	152.26	23.38	149.45	134.00	168.90
CP_AMP in OHP+TPM group	143.57	18.55	144.45	127.80	158.90
CP_AMP in TPM group	145.56	21.86	147.60	133.00	158.50
CP_VEL in CTRL group	37.17	1.80	37.75	36.10	38.50
CP_VEL in OHP group	37.15	1.24	37.00	36.60	37.00
CP_VEL in OHP+TPM group	36.94	1.33	36.80	36.10	38.50
CP_VEL in TPM group	36.77	1.47	37.00	36.10	38.00
D_AMP in CTRL group	69.09	7.09	67.60	65.90	75.40
D_AMP in OHP group	62.50	6.64	63.60	59.20	67.90
D_AMP in OHP+TPM group	72.35	9.23	74.40	66.60	75.50
D_AMP in TPM group	61.63	12.79	60.85	51.10	67.00
D_VEL in CTRL group	36.63	1.69	36.80	36.43	37.30
D_VEL in OHP group	36.25	1.31	36.15	35.00	37.00
D_VEL in OHP+TPM group	37.02	1.00	36.80	35.90	37.80
D_VEL in TPM group	36.14	.82	36.15	35.70	36.80
M_AMP in CTRL group	6.23	2.01	6.05	5.20	7.10
M_AMP in OHP group	9.39	3.21	9.20	7.10	12.30

M_AMP in OHP+TPM group	7.97	4.08	6.60	4.30	11.30
M_AMP in TPM group	8.73	3.89	7.90	7.10	11.40
M_VEL in CTRL group	41.25	1.76	41.35	40.80	42.60
M_VEL in OHP group	40.98	1.82	40.80	40.00	41.70
M_VEL in OHP+TPM group	41.17	2.02	41.25	39.20	42.60
M_VEL in TPM group	40.81	1.75	40.80	40.00	41.70

DC_AMP: distal caudal nerve SNAP amplitude (µv); ***DC_VEL***: distal caudal nerve sensory conduction velocity (m/sec); ***D_AMP***: digital nerve SNAP amplitude (µv); ***D_VEL***: digital nerve sensory conduction velocity (m/sec); ***M_AMP***: caudal nerve CMAP amplitude (mV); ***M_VEL***: caudal nerve motor conduction velocity (m/sec); ***PC_AMP***: proximal caudal nerve SNAP amplitude (µv); ***PC_VEL***: proximal caudal nerve sensory conduction velocity (m/sec).

Table 52. Neurophysiological data at base-line: Kruskal-Wallis Test.

Hypothesis Test Summary

	Null Hypothesis	Test	Sig.	Decision
1	The distribution of DCAMP is the same across categories of 1=CTRL; 2=OHP; 3=OHPTPM; 4=TPM.	Independent-Samples Kruskal-Wallis Test	,303	Retain the null hypothesis.
2	The distribution of DCVEL is the same across categories of 1=CTRL; 2=OHP; 3=OHPTPM; 4=TPM.	Independent-Samples Kruskal-Wallis Test	,456	Retain the null hypothesis.
3	The distribution of CPAMP is the same across categories of 1=CTRL; 2=OHP; 3=OHPTPM; 4=TPM.	Independent-Samples Kruskal-Wallis Test	,420	Retain the null hypothesis.
4	The distribution of CPVEL is the same across categories of 1=CTRL; 2=OHP; 3=OHPTPM; 4=TPM.	Independent-Samples Kruskal-Wallis Test	,963	Retain the null hypothesis.
5	The distribution of DAMP is the same across categories of 1=CTRL; 2=OHP; 3=OHPTPM; 4=TPM.	Independent-Samples Kruskal-Wallis Test	,051	Retain the null hypothesis.
6	The distribution of DVEL is the same across categories of 1=CTRL; 2=OHP; 3=OHPTPM; 4=TPM.	Independent-Samples Kruskal-Wallis Test	,162	Retain the null hypothesis.
7	The distribution of MAMP is the same across categories of 1=CTRL; 2=OHP; 3=OHPTPM; 4=TPM.	Independent-Samples Kruskal-Wallis Test	,183	Retain the null hypothesis.
8	The distribution of MVEL is the same across categories of 1=CTRL; 2=OHP; 3=OHPTPM; 4=TPM.	Independent-Samples Kruskal-Wallis Test	,721	Retain the null hypothesis.

Asymptotic significances are displayed. The significance level is ,05.

Table 53. Dynamic Test at base line: descriptive statistics.

	Mean	Std. Deviation	Median	Percentile 25	Percentile 75
DYN in CTRL group	31.34	3.49	30.93	28.80	31.92
DYN in OHP group	28.79	3.95	29.75	28.28	30.45
DYN in OHP+TPM group	31.35	3.38	30.83	29.37	31.67
DYN in TPM group	31.37	3.85	30.35	29.13	31.78

DYN: score for Dynamic test.

Table 54. Dynamic Test at base line: descriptive statistics: Kruskal-Wallis Test.

Hypothesis Test Summary

	Null Hypothesis	Test	Sig.	Decision
1	The distribution of DYN is the same across categories of 1=CTRL; 2=OHP; 3=OHPTPM; 4=TPM.	Independent-Samples Kruskal-Wallis Test	,551	Retain the null hypothesis.

Asymptotic significances are displayed. The significance level is ,05.

6.6.2 End of treatment data

Descriptive statistic for all nerve conduction studies data is reported in **Table 55**; in **Table 56** Kruskal-Wallis test results are reported: proximal and distal caudal nerve SNAP amplitude and distal caudal nerve sensory conduction velocity were different among the groups (p-value 0.001, <0.001, 0.04 respectively); moreover, pairwise comparison versus CTRL, adjusted by the Bonferroni correction for multiple tests, demonstrated that:

- Proximal caudal nerve SNAP amplitude: in OHP group it was significantly decreased compared to CTRL (p-value 0.01); OHP+TPM and TPM groups weren't different to CTRL group;
- Distal caudal nerve SNAP amplitude: in OHP group it was significantly decreased compared to CTRL (p-value 0.03); OHP+TPM and TPM groups weren't different to CTRL one;
- Distal caudal nerve conduction velocity: in OHP group it was slightly decreased compared to CTRL nearly reaching the value of significance (p-value 0.046); OHP+TPM and TPM groups weren't different to CTRL one.

Descriptive statistic for Dynamic Test is reported in **Table 57**; in **Table 58** Kruskal-Wallis test results are reported: a difference among the groups was demonstrated (p-value 0.002); moreover, pairwise comparison versus CTRL, adjusted by the Bonferroni correction for multiple tests, demonstrated that in OHP group it was significantly decreased compared to CTRL (p-value 0.03); OHP+TPM and TPM groups weren't different to CTRL.

NET findings and statistical test results are shown in **Table 59** and **Figure 37**. Compared to CTRL group, OHP one showed mainly an increased superexcitability (at 5msec p-values 0.01) in recovery cycle, a finding that was not present in OHP+TPM and TPM groups. Compared to CTRL one, all others showed also some statistical differences for current threshold properties and threshold electrotonus.

Morphometric analysis of caudal nerve descriptive statistics and one-way Anova test is reported in **Table 60**: a significant decrease in fiber density was present only in OHP group compared to CTRL one. **Figure 38** shows main morphological features compatible with an evident axonopathy only in OHP group. **Figure 39** shows fiber density distribution for each fiber diameter class (ranging from 1 to 10 μm).

IENF descriptive statistics and one-way Anova test is reported in **Table 61**: a significant decrease was present only in OHP group compared to CTRL one. **Figure 40** shows main morphological features matching these observations.

In **Figure 41** weight monitoring for all groups is shown; no group developed a perilous decrease in weight (i.e., more than 20% of the base-line value).

Table 55. Neurophysiological data at end of treatment: descriptive statistics.

	Mean	Std. Deviation	Median	Percentile 25	Percentile 75
CD_AMP in CTRL group	54.39	7.67	54.60	49.70	58.00
CD_AMP in OHP group	60.40	12.94	60.10	52.50	67.10
CD_AMP in OHP+TPM group	60.92	14.30	66.10	51.90	68.70
CD_AMP in TPM group	59.46	12.22	59.50	53.10	71.00
CD_VEL in CTRL group	26.68	1.44	26.30	25.40	28.30
CD_VEL in OHP group	26.31	2.14	26.10	24.20	28.00
CD_VEL in OHP+TPM group	25.72	1.84	25.40	24.60	26.30
CD_VEL in TPM group	25.62	1.78	24.80	24.40	27.30
CP_AMP in CTRL group	135.67	30.13	135.80	109.80	151.30
CP_AMP in OHP group	152.26	23.38	149.45	134.00	168.90
CP_AMP in OHP+TPM group	143.57	18.55	144.45	127.80	158.90
CP_AMP in TPM group	145.56	21.86	147.60	133.00	158.50
CP_VEL in CTRL group	37.17	1.80	37.75	36.10	38.50
CP_VEL in OHP group	37.15	1.24	37.00	36.60	37.00
CP_VEL in OHP+TPM group	36.94	1.33	36.80	36.10	38.50
CP_VEL in TPM group	36.77	1.47	37.00	36.10	38.00
D_AMP in CTRL group	69.09	7.09	67.60	65.90	75.40
D_AMP in OHP group	62.50	6.64	63.60	59.20	67.90
D_AMP in OHP+TPM group	72.35	9.23	74.40	66.60	75.50
D_AMP in TPM group	61.63	12.79	60.85	51.10	67.00
D_VEL in CTRL group	36.63	1.69	36.80	36.43	37.30
D_VEL in OHP group	36.25	1.31	36.15	35.00	37.00
D_VEL in OHP+TPM group	37.02	1.00	36.80	35.90	37.80
D_VEL in TPM group	36.14	.82	36.15	35.70	36.80
M_AMP in CTRL group	6.23	2.01	6.05	5.20	7.10
M_AMP in OHP group	9.39	3.21	9.20	7.10	12.30
M_AMP in OHP+TPM group	7.97	4.08	6.60	4.30	11.30
M_AMP in TPM group	8.73	3.89	7.90	7.10	11.40
M_VEL in CTRL group	41.25	1.76	41.35	40.80	42.60
M_VEL in OHP group	40.98	1.82	40.80	40.00	41.70
M_VEL in OHP+TPM group	41.17	2.02	41.25	39.20	42.60
M_VEL in TPM group	40.81	1.75	40.80	40.00	41.70

DC_AMP: distal caudal nerve SNAP amplitude (µv); ***DC_VEL***: distal caudal nerve sensory conduction velocity (m/sec); ***D_AMP***: digital nerve SNAP amplitude (µv); ***D_VEL***: digital nerve sensory conduction velocity (m/sec); ***M_AMP***: caudal nerve CMAP amplitude (mV); ***M_VEL***: caudal nerve motor conduction velocity (m/sec); ***PC_AMP***: proximal caudal nerve SNAP amplitude (µv); ***PC_VEL***: proximal caudal nerve sensory conduction velocity (m/sec).

Table 56. Neurophysiological data at end of treatment: Kruskal-Wallis Test. Pairwise comparison, adjusted by the Bonferroni correction for multiple tests, demonstrated that CDAMPend was different only between OHP and CTRL groups (p-value 0.001); PCAMPend was different between OHP and CTRL groups (p-value 0.003); DCVELEND was different only between OHP and CTRL groups (p-value 0.046). ***DCAMPend***: distal caudal nerve SNAP amplitude; ***DCVELend***: distal caudal nerve sensory conduction velocity; ***DAMPend***: digital nerve SNAP amplitude; ***DVELend***: digital nerve sensory conduction velocity; ***MAMPend***: caudal nerve CMAP amplitude; ***MVELend***: caudal nerve motor conduction velocity; ***PCAMPend***: proximal caudal nerve SNAP amplitude; ***PCVELend***: proximal caudal nerve sensory conduction velocity.

Hypothesis Test Summary

	Null Hypothesis	Test	Sig.	Decision
1	The distribution of DCAMPend is the same across categories of 1=CTRL; 2=OHP; 3=OHPTPM; 4=TPM.	Independent-Samples Kruskal-Wallis Test	,000	Reject the null hypothesis.
2	The distribution of DCVELend is the same across categories of 1=CTRL; 2=OHP; 3=OHPTPM; 4=TPM.	Independent-Samples Kruskal-Wallis Test	,038	Reject the null hypothesis.
3	The distribution of CPAMPend is the same across categories of 1=CTRL; 2=OHP; 3=OHPTPM; 4=TPM.	Independent-Samples Kruskal-Wallis Test	,001	Reject the null hypothesis.
4	The distribution of CPVELend is the same across categories of 1=CTRL; 2=OHP; 3=OHPTPM; 4=TPM.	Independent-Samples Kruskal-Wallis Test	,927	Retain the null hypothesis.
5	The distribution of DAMPend is the same across categories of 1=CTRL; 2=OHP; 3=OHPTPM; 4=TPM.	Independent-Samples Kruskal-Wallis Test	,843	Retain the null hypothesis.
6	The distribution of DVELend is the same across categories of 1=CTRL; 2=OHP; 3=OHPTPM; 4=TPM.	Independent-Samples Kruskal-Wallis Test	,625	Retain the null hypothesis.
7	The distribution of MAMPend is the same across categories of 1=CTRL; 2=OHP; 3=OHPTPM; 4=TPM.	Independent-Samples Kruskal-Wallis Test	,681	Retain the null hypothesis.
8	The distribution of MVELend is the same across categories of 1=CTRL; 2=OHP; 3=OHPTPM; 4=TPM.	Independent-Samples Kruskal-Wallis Test	,988	Retain the null hypothesis.

Asymptotic significances are displayed. The significance level is ,05.

Table 57. Dynamic Test at end of treatment: descriptive statistics.

	Mean	Standard Deviation	Median	Percentile 25	Percentile 75
DYN in CTRL group	31.58	3.26	30.55	29.52	32.86
DYN in OHP group	26.82	3.76	26.13	24.77	26.77
DYN in OHP+TPM group	28.38	6.40	28.12	26.63	29.45
DYN in TPM group	30.22	1.06	30.29	29.03	30.57

DYN: score for Dynamic test.

Table 58. Dynamic Test at end of treatment: Kruskal-Wallis Test. Pairwise comparison, adjusted by the Bonferroni correction for multiple tests, demonstrated that DYNend was different only between OHP and CTRL groups (p-value 0.003). ***DYNend****: score for Dynamic test.*

Hypothesis Test Summary

	Null Hypothesis	Test	Sig.	Decision
1	The distribution of DYNend is the same across categories of 1=CTRL; 2=OHP; 3=OHPTPM; 4=TPM.	Independent-Samples Kruskal-Wallis Test	,002	Reject the null hypothesis.

Asymptotic significances are displayed. The significance level is ,05.

Table 59. NET at the end of treatment.

VARIABLE	*CTRL GROUP (median, Q1, Q3)*	*OHP GROUP (median, Q1, Q3, p-value VS CTRL)*	*OHP+TPM GROUP (median, Q1, Q3, p-value VS CTRL)*	*TPM GROUP (median, Q1, Q3, p-value VS CTRL)*
Stimulus-response and strength-duration properties				
Strength-duration time constant (msec)	0.167 (0.15, 0.184)	0.21 (0.192, 0.23) p=0.14	0.16 (0.147, 0.199) p=0.96	0.164 (0.15, 0.2) p=0.82
Rheobase (mA)	-0.085 (-0.126, 0.0534)	0.044 (0.0182, 0.106) p=0.14	0.125 (0.0894, 0.16) **p=0.03***	0.011 (-0.0717, 0.0436) p=0.46
Current Threshold properties				
Resting I/V slope	0.853 (0.821, 0.912)	0.72 (0.644, 0.772) **p=0.02***	0.771 (0.708, 0.788) **p<0.005****	0.88 (0.826, 0.9) p=0.96
Minimum I/V slope	0.34 (0.302, 0.397)	0.334 (0.299, 0.387) p=0.94	0.406 (0.365, 0.442) p=0.10	0.352 (0.347, 0.384) p=0.57
Hyperpolarazing I/V slope	0.555 (0.524, 0.643)	0.461 (0.447, 0.583) p=0.28	0.526 (0.513, 0.559) p=0.52	0.615 (0.553, 0.817) p=0.54
Threshold electrotonus				
TEh(90-100 msec)	-84.4 (-97.4, -73.1)	-119 (-122, -112) **p=0.01***	-104 (-110, -98.6) **p=0.01***	-94.1 (-99.7, -83.1) p=0.46
TEd(10-20 msec)	50.3 (48.7, 54.2)	55.6 (49, 57.5) p=0.54	55.6 (50.9, 56.1) p=0.27	52.5 (51.7, 55.5) p=0.14
TEd(40-60 msec)	48.3 (47, 50.3)	56.7 (49.3, 61.7) p=0.24	51.6 (48.8, 52.2) p=0.46	48.5 (48.4, 49.3) p=0.70
TEd(90-100 msec)	45.5 (44.6, 47.7)	51.1 (46, 52.3) p=0.30	50.2 (47.4, 51.1) p=0.20	46.6 (46, 47.2) p=0.69647
TEh(10-20 msec)	-60.4 (-61.5, -56.4 n=10)	-74.6 (-77.7, -70.6) **p=0.02***	-70.8 (-73.8, -65.6) **p=0.01***	-63.6 (-66.2, -61.6) p=0.05
TEd(undershoot)	-4.45 (-6.11, -3.03)	-4.27 (-7.12, -1.97) p=0.84	-4 (-4.32, -3.37) p=0.70	-3.72 (-4.98, -2.94) p=0.51
TEd(overshoot)	8.45 (7.4, 9)	10 (8.15, 12) p=0.60	11.7 (9.18, 14.1) p=0.07	8.15 (6.81, 10.9) p=0.96
TEd(peak)	52.2 (49.7, 53.8)	58.9 (52.5, 62.1) p=0.24	55.2 (53.2, 55.9) p=0.14	52.5 (51.2, 54.6) p=0.46
TEh(20-40 msec)	-72.2 (-74.9, -66)	-88.7 (-92.2, -84.9) **p=0.02***	-87 (-93, -84.2) **p<0.005****	-78.9 (-83, -71.8) p=0.10
TEh(slope 101-140 msec)	1.15 (0.883, 1.44)	1.81 (1.24, 2.24) p=0.30	1.56 (1.5, 1.8 n=8) **p=0.04***	1.32 (1.05, 1.51) p=0.63
TEd20(peak)	26.8 (25.5, 27.7)	32.3 (31.1, 32.9) **p=0.02***	29.5 (28.8, 31.7) **p=0.03***	28.8 (27.5, 29.2) p=0.08
TEd40(Accomodation)	6.2 (5.2, 6.97)	9.25 (8.4, 10.4) p=0.07	5.5 (4.77, 5.82) p=0.41	7.05 (5.68, 7.4) p=0.57
TEd20(10-20 msec)	24.2 (23, 25.6)	28.7 (27.6, 29.7) **p=0.04***	28 (26.8, 30 n=8) **p=0.02***	26.9 (25.5, 27.8) **p=0.03***
TEh20(10-20 msec)	-26 (-27.1, -23.8)	-32.7 (-33.8, -30.6) **p=0.01***	-29.3 (-29.9, -24.8) p=0.27	-26.9 (-27.9, -26.4) p=0.17
S2 accommodation	5.32 (4.91, 6.55)	8.52 (7.27, 9.76) **p=0.03***	5.3 (4.63, 5.5) p=0.82	7.56 (5.11, 7.98) p=0.31
Accommodation half-time	46.4 (38.9, 52.4)	51.4 (35, 62.8) p=0.73	40.9 (31.8, 46.6) p=0.36	46.1 (45.4, 47.1) p=0.90
Recovery Cycle				
Relative Refractory Period (msec)	0.377 (0.321, 0.39)	0.785 (0.687, 1.29) **p<0.005****	0.354 (0.33, 0.392) p=0.96	0.344 (0.305, 0.37) p=0.46
Refractoriness at 2msec	9.81 (1.08, 14.8)	8.03 (2.35, 64.1) p=0.87	11.7 (4.65, 39.9) p=0.73	5.53 (-0.063, 11.4) p=0.57
Refractoriness at 2.5msec	-2.66 (-8.47, -1.61)	15.3 (9.34, 36) **p=0.01***	-9.41 (-9.93, -3.65) p=0.27	-5.09 (-7.04, -2.76) p=0.70
Superexcitability (%)	-11.6 (-14.2, -9.62)	-7.84 (-13.3, -1.83) p=0.37	-14.8 (-18.8, -13.3) p=0.06	-11.8 (-12.6, -10.1) p=0.82
Subexcitability (%)	2.53 (1.68, 6.78)	5.86 (2.59, 10.3) p=0.53946	3.04 (1.79, 4.1) p=0.83	2.41 (1.29, 3.2) p=0.46
Superexcitability at 5msec	-12 (-14.4, -11.8)	-0.418 (-7.61, 6.54 n=4) **p=0.008****	-14.7 (-17.7, -13.5) p=0.20	-11.8 (-13.7, -9.83) p=0.57
Superexcitability at 7msec	-9.81 (-11.9, -8.09)	-8.24 (-14.5, 0.563) p=0.94	-12.7 (-14.3, -10.7) p=0.10	-8.88 (-10.4, -7.19) p=0.57

Figure 37. NET at the end of treatment. ***A****: I/V relationship;* ***B****: Strength-duration time constant;* ***C****: Threshold electrotonus;* ***D****: Recovery Cycle.* OHP group showed an increased superexcitability in recovery cycle, a finding that was not present in OHP+TPM and TPM groups. Compared to CTRL, all other groups showed also some statistical differences for current threshold properties and threshold electrotonus.

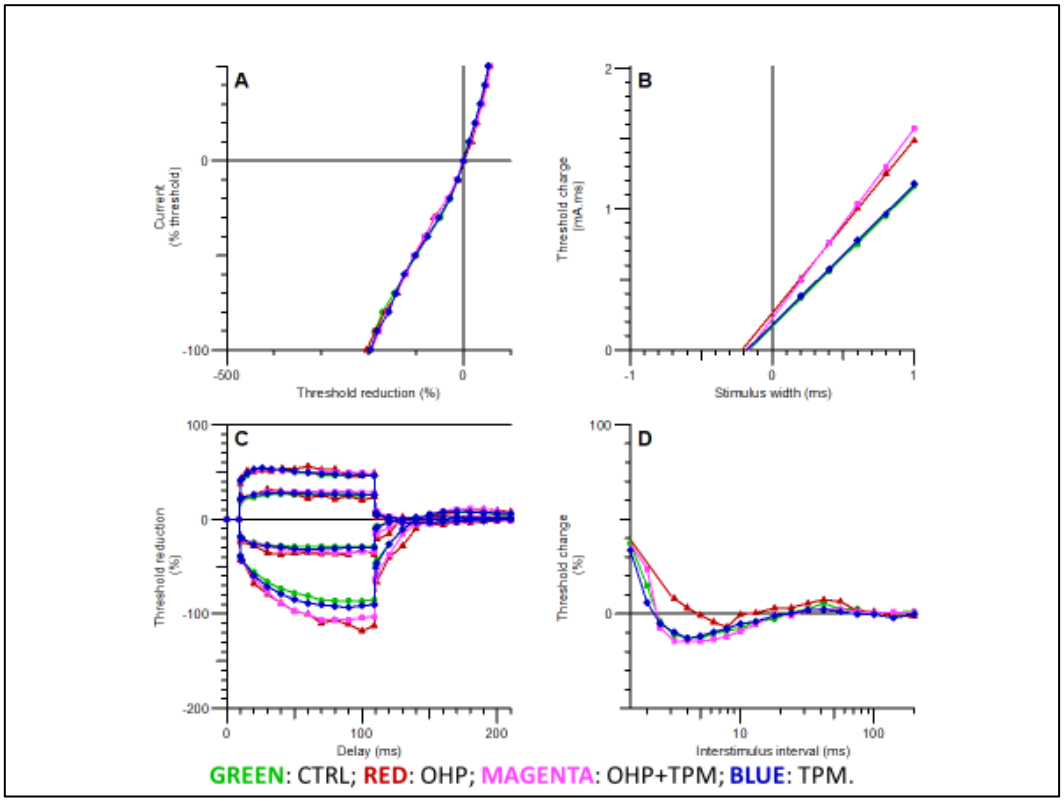

Figure 38. Caudal nerve morphology at the end of treatment (60x magnification). OHP group was the only one group showing an evident and abundant large fiber loss and fibers in degeneration.

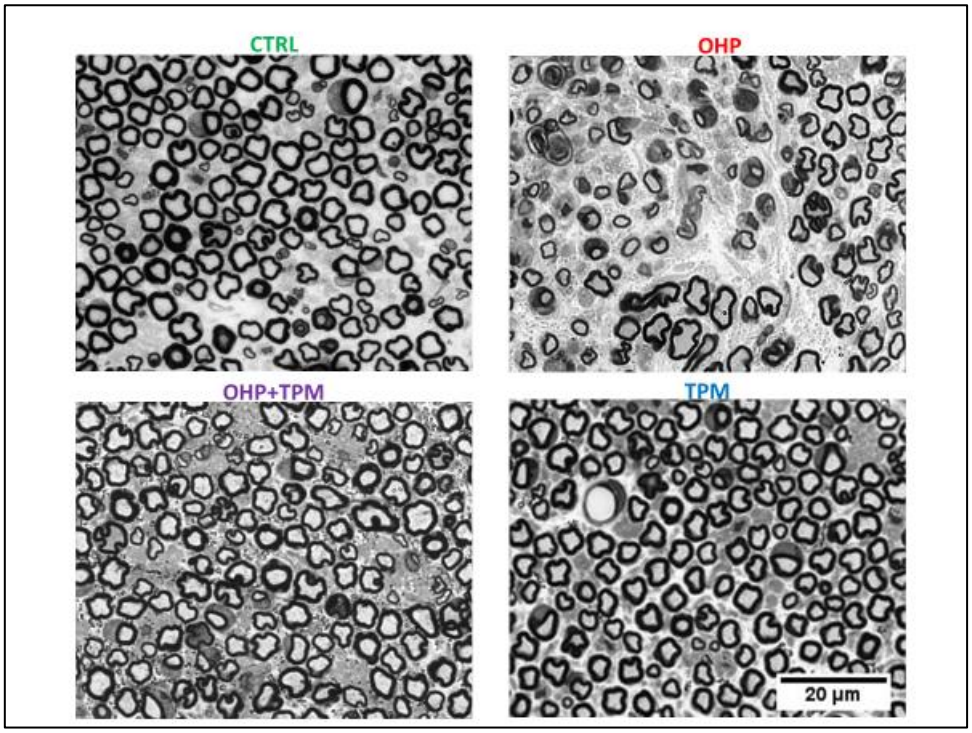

Figure 39. Fiber density (frequency graph for different diameters) for caudal nerves at the end of treatment. *X axis represents fiber diameter (µm); Y axis represents the number of fibers for each fiber caliber.* Only OHP group showed a significant decrease in fiber density (see **Table 60** below for level of significance).

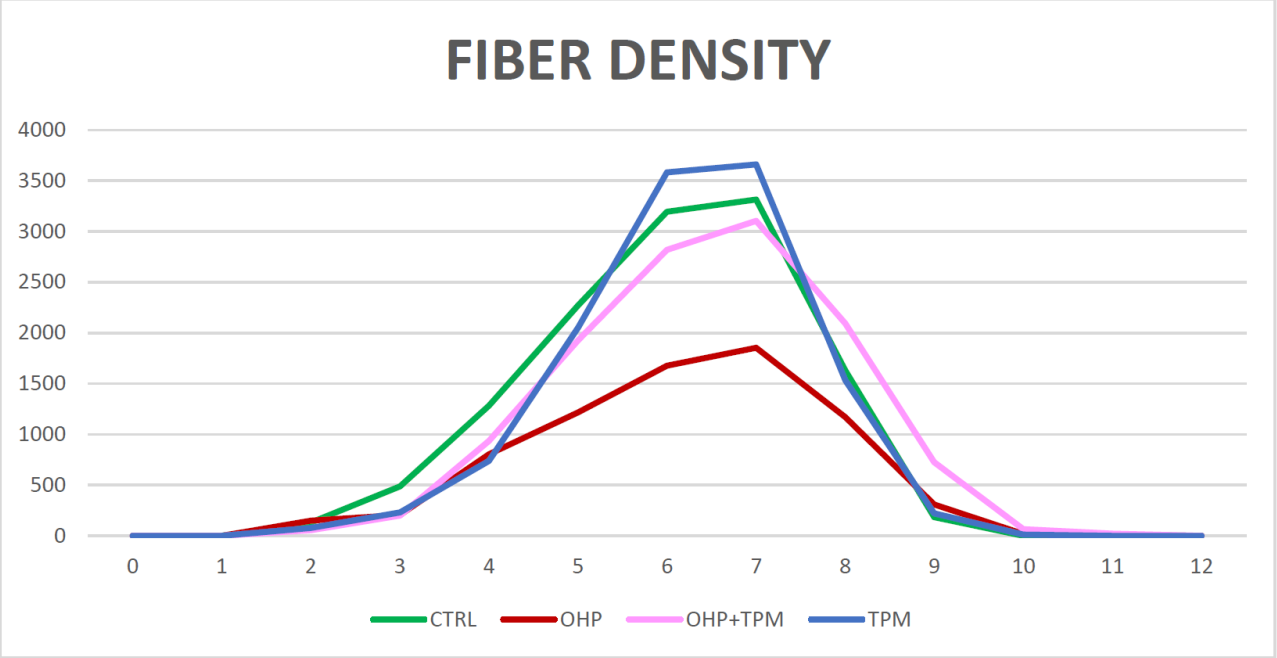

Table 60. Caudal nerve fiber density: descriptive statistics, one-way Anova and Dunnet t test. Only OHP group showed a significant decrease.

	Mean	Std. Deviation	One-way ANOVA	Dunnet t (2-sided) p-value
DENS in CTRL group	12505.02	1437.19	**p-value: 0.001**	
DENS in OHP group	**7431.31**	**282.26**		**0.001**
DENS in OHP+TPM group	11940.07	1520.52		0.87
DENS in TPM group	12103.04	623.83		0.96
DENS: caudal nerve fiber density (n/µ²)				

Figure 40. Intraepidermal nerve fibers (IENF) findings at the end of treatment (10x magnification). OHP group was the one showing an abundant loss of fibers, compared to CTRL one. See **Table 61** below for level of significance.

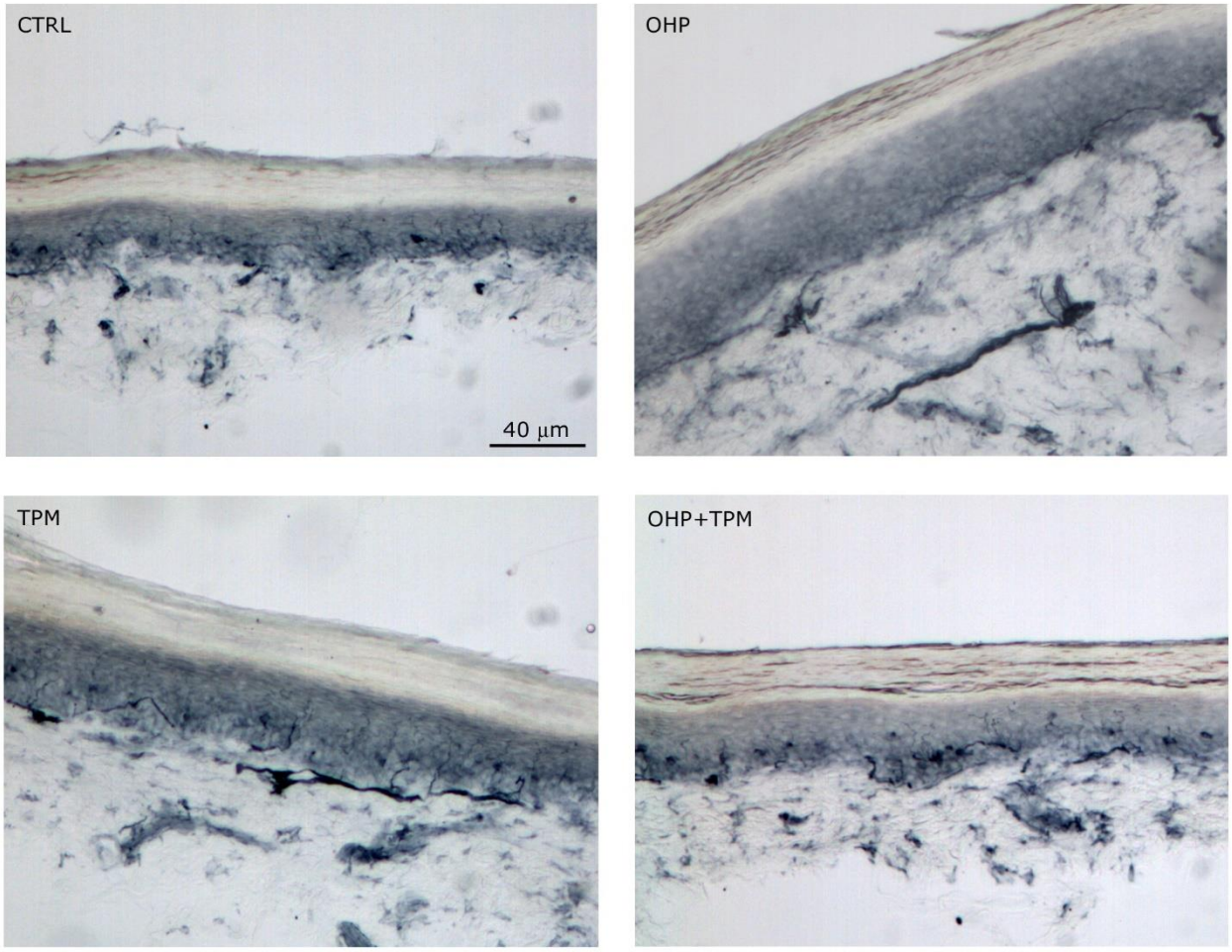

Table 61. Intraepidermal nerve fiber: descriptive statistics, one-way Anova and Dunnet t test. Only OHP group showed a significant decrease.

	Mean	Std. Deviation	One-way ANOVA	Dunnet t (2-sided) p-value
IENF in CTRL group	30.75	3.48	**p-value: <0.001**	
IENF in OHP group	**19.72**	**2.92**		**<0.001**
IENF in OHP+TPM group	32.63	3.50		0.42
IENF in TPM group	29,41	2,034		0.68
IENF: Intra-epidermal nerve fiber (n/mm)				

Figure 41. Body weight for all groups during the observational period. No group showed a severe weight loss.

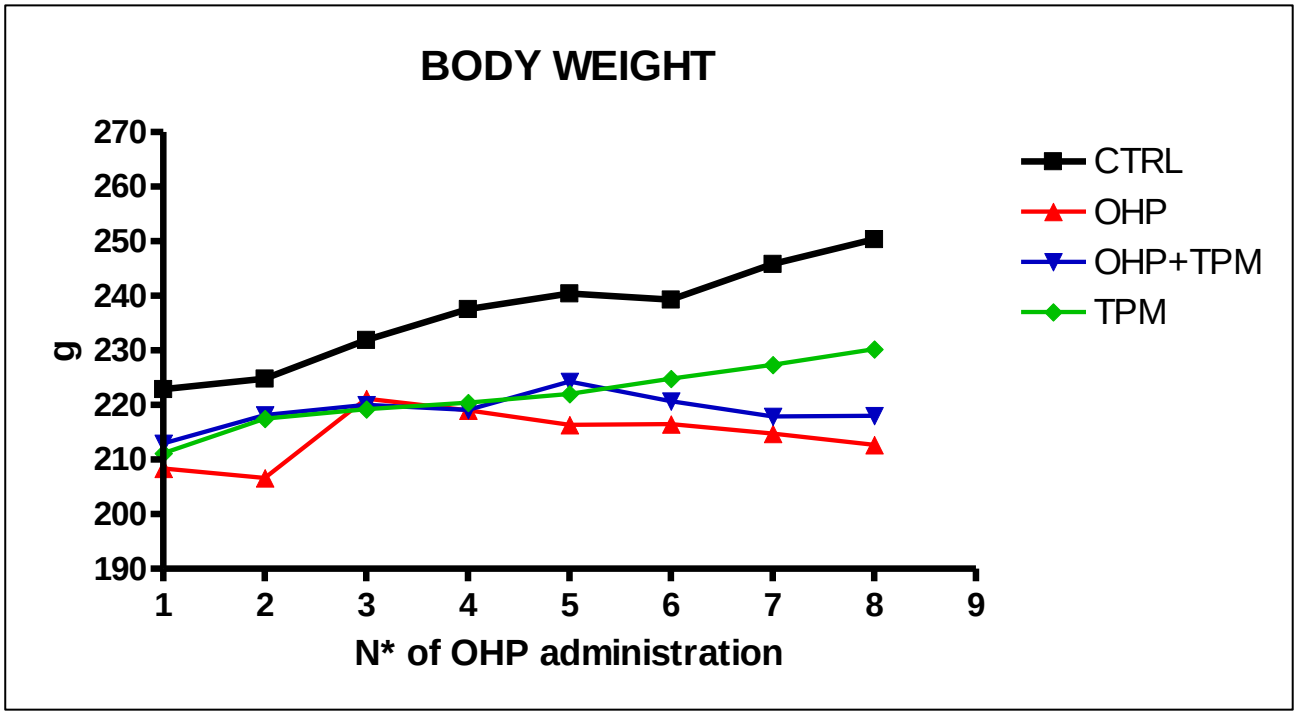

6.6.3 Summary of inferences from TASK 6

In **TASK 6** the possible role of TPM as a neuroprotectant against OIPN was investigated. As see in TASK 5, TPM was able to modify NET profile, preventing changes on recovery cycle. However, the most interesting findings were the one related to chronic OIPN. Chronic OIPN was assessed with multiple parameters: standard neurophysiology, behavioral test (Dynamic test), neuropathology (caudal nerve morphology/morphometry and IENF). All the outcome measure demonstrate a complete protective effect in the TPM+OHP group, whereas OHP showed the clear development of a relevant neurotoxicity for all tested parameters.

7 DISCUSSION

This project was divided into different TASKS to validate or refuse the working hypothesis. The aim was to test the possible causative relationship between acute and chronic OIPN, in a preclinical *in vivo* setting.

7.1 DEVISING THE APPROPRIATE ANIMAL MODEL

TASK 1 was intended to demonstrate the feasibility of acute OIPN induction and detection in the animal model. The easiest method to ascertain this was the detection of abnormal EMG findings at rest. This approach was directly translated from clinical setting. Given the peculiar report OHP treated patients gave to their health care professionals, a state of acute axonal hyperexcitability was, in fact, suspected; thus, EMG at rest was used as screening tool. In 2002, Wilson et al.[49] demonstrated in a small cohort of 13 OHP treated patients EMG findings compatible with axonal hyperexcitability, in absence of a motor polyneuropathy; the same findings were reported by Lehky et al. in 2004[50]. In 2010 Hill et al.[112] compared EMG findings among OHP, CDDP and PTX treated patients: they described alterations only in OHP treated ones. Therefore, the same technique was tested in a well-described OIPN rat model by Cavaletti et al.[46]. Changes after a single administration were tested. An increase of the standard chronic model dosage (which requires repetitive administrations over 1 month) was used aiming at eliciting acute phenomena with a higher probability[47,113,114]. Data were perfectly matching what was reported in the clinical cohorts: all and only OHP treated animals showed a striking axonal hyperexcitability profile 24 hours after the administration. These phenomena were transient, as expected: 7 days after, no altered findings were still present. However, EMG recordings were not the ideal outcome measure for acute OIPN detection, despite simplicity of the procedure and the standard equipment required because there was a subjective component in the scoring system and little information was gained on the pathophysiological mechanisms underlying. So, a more refined methodological approach was warranted.

Then again, the next step started from clinical evidence. As stated in the "Introduction", NET is the appropriate technique to investigate *in vivo* a suspected channelopathy, as acute OIPN could be; so far, no one published preclinical data regarding NET application in OIPN animal models, but there is a growing literature on its application at the "bed-side". Park et al. in 2009[36] applied NET to a cohort of 58 consecutive OHP treated patients: they found altered excitability in both sensory and motor recordings. The cohort was followed up to chemotherapy completion. A difference was seen between motor and sensory recordings, which was quite expected. Motor and sensory NET showed altered axonal hyperexcitability after the 1st administration, in the absence of an actual neuropathy. However, in the subsequent cycles, while motor findings remained unchanged (i.e., compatible with "axonal hyperexcitability"), sensory ones showed not only a functional alteration, due to the transient channelopathy, but also the hallmarks of an early sensory chronic neuropathy. Since sensory changes at NET precede changes at nerve conduction studies, the Authors

concluded that sensory NET could be suggested as a sensitive biomarker of early sensory neuropathy detection. Given this fact, NET based on the CMAP of the caudal nerve was used in the animal model. The ideal outcome measure was required to keep well separated data between acute and chronic phenomena, since the aim was to verify if a reduction of acute OIPN could consequently modify chronic OIPN natural history. Thus, in case of acute OIPN prevention in the subsequent Tasks, if there weren't also an effect on chronic OIPN too, the causative relationship between acute and chronic condition would have been questioned. Moreover, it was very recently demonstrated by Heide et al.[57], that, in OHP treated patients, motor axons at NET display more pronounced changes in excitability, compared to sensory ones; so the choice to use motor recordings was even more justified.

TASK 2 was then constructed to verify if NET, conducted as stated in "Methods", was able to detect acute OIPN after a single OHP administration at the same dosage used in Task 1 (5 mg/Kg, iv). To ensure CTRL and OHP groups were equal at base-line, they were randomized with standard neurophysiology (sensory and motor recordings) and with the Cold Plate Test. Among behavioral tests, Cold Plate Test was elected as outcome measure for acute OIPN: cold-induced paresthesia/dysesthesia reported by patients can be assimilated to cold-induced hyperalgesia in animals.[29,115]

After the single OHP administration animals were tested at 24 hours with Cold Plate Test and at 48 hours with NET. Both outcome measures showed expected results. A significant change was observed in superexcitability, after the infusion, thus significantly pulling upward the recovery cycle curve (see **Figure 21**). This finding was extremely encouraging since it was matching what has been observed with NET in clinical setting in the last 15 years[32,34,36,57,116]. Moreover, Cold Plate Test confirmed cold-hyperalgesia induction, thus, corroborating all acute OIPN key features were present. Of course, that was not enough to translate the clinical experience to the "bench side". So, in **TASK 3** it was verified if the standard chronic model was equally able to reproduce both acute and chronic OIPN alterations; the chronic model, in fact, is based on a 3 mg/Kg dosage repeated over the month of treatment (iv, 2qw4w), whereas in Task 1 and 2 the 5mg/Kg dose was used. After the 1st administration no differences were seen between CTRL and OHP groups both at NET and at Cold Plate Test. However, different findings were present at the end of treatment. NET showed OHP superexcitability parameters were significantly set at a less negative value, compared to CTRL; Cold Plate Test was instead not significant in OHP versus CTRL animals. Outcome measures to detect chronic OIPN were standard neurophysiology and Dynamic Test (mechanical nociceptive threshold; see "Methods"): nerve conduction studies, in OHP group, were compatible with a mild axonal sensory polyneuropathy (decreased SNAP amplitudes), without motor involvement, matching what known from clinical evidence[41,48]; moreover, Dynamic Test demonstrated a significant alteration in mechanical perception. Neuropathological findings of caudal nerves confirmed the modest alterations seen at standard neurophysiology (**see Figure 26**). NET was then monitored a week after the end of treatment confirming the transience of acute OIPN. All

measurements were then repeated 6 weeks after treatment: an almost complete recovery was observed for all outcome measures, apart from a modest significance at Dynamic Test. Thus, overall, OIPN induction with the 3 mg/Kg dosage was not satisfying: no acute OIPN signs were seen after the 1st administration and the chronic OIPN was very mild. A revision of the current chronic model was then warranted aiming at obtaining a better expression of whole OIPN spectrum.

TASK 4 was subsequently planned with 3 different dosages (3, 4, 5 mg/Kg iv, 2q4ws) with the primary aim to select the most adequate cumulative dose/dose intensity to be then tested in subsequent experiments; given the increase in the cumulative dosage, weight and animal welfare were closely monitored to avoid intolerable general toxicity. After the 1st administration NET, as well as Cold Plate Test, were performed at 24 hours. Cold Plate Test was not significant, but OHP5 animals were not able to complete the whole observational period due to marked intolerance to the cold surface (3 animals out of 8), thus preventing a correct completion of data collection which might have revealed increased total number of signs compared to CTRL animals. NET findings were collected at 24 hours revealing a different profile compared to TASK 2 and 3 (in which data were collected at 48 hours): current-threshold properties were different in OHP4 and OHP5 groups as well as some features in threshold electrotonus, compared to CTRL animals; in threshold electrotonus even OHP3 dosage showed some alterations. We hypothesized that this difference was due to the different time point of data acquisition (24 hours in TASK4 VS 48 hours in TASK 2 and 3). All clinical findings available for comparison were also collected at 48 hours[32,34,36,57,116]; thus, it was decided to plan a time course in TASK 5 as discussed in the corresponding paragraph. At the end of treatment, instead, Cold Plate Test was significant for cold hyperalgesia in OHP3 group. As happened after the 1st administration Cold Plate Test interpretation was quite difficult for higher dosages: OHP4 and OHP5 group data were not available for the comparison since more than 50% of animals did not complete the observational period due to intolerance to the cold surface. Findings were considered “overall positive” result compared to CTRL group. NET recordings showed alterations in a clear dose-dependent manner. OHP4 and OHP5 animals showed differences in stimulus-response curve, threshold electrotonus, recovery cycle; notably, in recovery cycle curve, more parameters were involved and a higher level of significance was reached in OHP5 group. OHP3 group, instead, showed some alterations only for threshold electrotonus. Moreover, nerve conduction studies were compatible with an axonal sensory polyneuropathy in group OHP4 and OHP5 with a more marked impairment for OHP5 animals; this was confirmed by neuropathology of caudal nerve as can be seen in **Figure 32**. As sign of general toxicity, weight monitoring did not show a perilous decrease even in the group treated with the highest OHP dosage (i.e., a decrease of the base line weight > 20%). Thus, considering findings after 1st administration and at the end of treatment, 5mg/Kg (iv, 2qw4ws) was the ideal schedule to be used in subsequent experiments.

7.2 PATHOPHYSIOLOGICAL CONSIDERATIONS THANKS TO NET

Apart from refining the model, in TASKS 2, 3 and 4, NET confirmed the presence of altered axonal properties after OHP infusion. In TASKS 2 and 3, when NET was performed at 48 hours, the key feature was a change in superexcitability. The recovery cycle curve was significantly set upwards compared to CTRL (see **Figure 21**). Heide et al.[57] published this year data from a small cohort of 12 patients who developed the same acute changes on motor NET after the 1st OHP infusion. They related NET findings to an altered function of Na+ channels, after running a mathematical simulation (MEMFIT) to test which conductance was the most likely to alter excitability as seen[57]. In TASK 4, instead, NET was performed at 24 hours after the 1st administration revealing minor alterations in threshold electrotonus (see **Figure 27**); as stated yet, this could be related to the different time points in data acquisition. The consistency of threshold electrotonus alterations were confirmed at the end of treatment, in combination with a clear upwards shift for recovery cycle: OHP4 and OHP5 showed, again, dose-dependent alterations (see **Figure 30**). This was not surprising since Park et al. in 2011[33] observed NET parameters were altered dose-dependently in a cohort of 18 OHP-treated patients. The same group observed alterations at NET in OHP treated patients, compatible with changes in Na+ channels functioning[36,116]. Given the physiological considerations reported in the Introduction and alterations in recovery cycle in TASKS described so far, data were compatible with the involvement of Na+ channels. However, a situation potentially more complex than this could also be suggested. In TASKS 3 and 4 alterations in Threshold Electrotonus, Current/Threshold Properties and in stimulus-response curve were present too. Stimulus-response curve properties are mainly related to Na+ channel function supporting again the working hypothesis of this project. In Threshold Electrotonus and Current/Threshold curves internodal and rectifying conductances are respectively tested; K+ currents are involved in these mechanisms and some role for these conductances might also be advocated. To judge these findings preclinical data (*in vitro* or *ex vivo*) were available for a comparison.

Adelsberger et al. in 2000[31] performed a combined *ex vivo*/*in vitro* study. They tested adult rat nerves in a recording chambers after stripping off the perineural sheath, for the *ex vivo* study, and tested DRG for the patch clamp recordings, in the *in vitro* part. They compared effects of OHP (250 µM) in comparisons/combination with the effects of agents able to block Na and K+ channels (i.e., tetrodotoxin [TTX] and 4-aminopyridine). The profile of alterations observed was compatible with an altered activation/inactivation of Na+ channels and no effects on K+ ones was demonstrated. In 2001 Groulleau et al.[35], applied the whole cell patch-clamp technique on central nervous system neurons of the cockroach *Periplaneta Americana*. OHP effects were compared with cisplatin and carboplatin (500 µM was the dose for each drug). Moreover, a comparison with oxalate alone and dichlorodiaminocyclohexane platinum (dach-Cl2-platin, i.e., OHP with the oxalate group) was performed. They concluded that an inhibitory effect on Na+ voltage-operated currents was present after OHP administration, while cis- and carboplatin were ineffective. Moreover, they showed that Oxalate alone was able to induce the same pattern of changes, whereas dach-

Cl2-platin was ineffective; since oxalate is a strong Ca2+ chelator they also hypothesized that OHP alters sodium kinetics, in consequence of Ca2+ chelation. Webster et al. in 2005[117] investigated effects of OHP (0.5mM) on a mouse phrenic nerve/hemidiaphragm preparation tested in a recording chamber. Data were compared with the effects of TTX, carbamazepine, β-pompilidotoxin (it slows Na+ channel inactivation) and 4-aminopyridine. Changes seen after OHP exposure were abolished by TTX and carbamazepine, as well as β-pompilidotoxin produced the same effects as OHP; 4-aminopyridine was instead unable to prevent OHP action on the preparation. So, Authors concluded that OHP was able to alter Na+ channel kinetics. Wu et al. in 2009[118] performed patch-clamp recordings on clonal strain NG108-15 cell line (i.e., Senday virus-induced fusion of the mouse neuroblastoma clone N18TG-2 and rat glioma clone C6 BV-1) to devise OHP effects (100μM) on different ion channels: peak amplitude of voltage-operated Na+ channels was reduced, even if no changes were seen in the overall current-voltage relations; no effects was observed on Ca2+ channels, whereas suppression of delayed-rectifier K+ current was seen. An effect on both Na+ and K+ current was also described by Benoit et al. in 2006[119]; they tested a frog single myelinated axon to test nodal ionic currents after exposure to different OHP dosages (1-100 μmol/l). They observed a decrease of the current for both ions, without altering their kinetics, even though effects were more evident on Na+ currents. The voltage-dependency of bot Na+ and K+ ion channels was shifted towards more negative values; therefore, at a given membrane potential the percentage of Na+ and K+ channels activated was increased. Some groups also suggested an exclusive role for K+ channels and K+ equilibrium. Kagiava et al. in 2008[120] performed recordings on isolated rat nerves to test effects of different OHP dosages (25, 100, 500 μM), observing alterations in K+ voltage operated channel, without any effects on the Na+ components. The same group also observed in 2008[120] that OHP (25 μM) had an effect on gap junction channels, lengthening their opening, with consequent excessive K+ accumulation in the perixonal space with osmotic swelling; they tested mouse sciatic nerve after dissection and preparation in a recording chamber. This hypothesis was supported by the observation that octanol co-administration (gap junction channels and hemichannels blocking agent) was able to prevent OHP effects. Sittl et al. in 2010[121] made observations on isolated rat nerve segments and on segments of human sural nerves; human specimens were obtained from a biobank and used for isolated nerve recordings (the material had been collected for clinical purposes in the diagnostic work-up for polyneuropathy). They obtained similar results in animal and human nerves. OHP (30 μM) effects on axonal excitability were compared with cooling and flupirtine (K+ channel activating agent). Cooling, as expected, enhanced OHP effects, since a decrease in temperature depolarizes axons as a consequence of Na+/K+ pump slowing[122] and K+ conductance decrease[123,124]; on the opposite site, flupirtine decreased OHP effects. Authors did not state if the *primum movens* of acute OIPN was a Na+ or K+ current alteration; they solely suggested that enhancing K+ currents could be a strategy to contain OHP effects on axons. The same group published then in 2012[125] another paper comparing data from human and animal specimens. For animal study, wild type and Scn8a^{med} mice were used; these mutated animals lack Nav1.6 channel, which is the main Na+ channel in both sensory

and motor myelinated axons. Mice were used to obtain single nerve fiber for nerve excitability testing and DRG for whole-cell patch clamp recordings. OHP concentrations was 10-100 µM for *ex vivo* studies and 30 µM for *in vitro* ones. In electrophysiological recordings of both human and wild-type mouse nerves they observed, as expected, that cooling in the presence of OHP induced bursts of action potentials; instead, no effect of cooling was seen in Scn8a^{med} mice nerves. The same discrepancy was observed at whole-cell patch clamp, performed in DRG from wild type and mutated animals: cooling had an effect only on wild type DRG. Thus, Authors suggested a pivotal role for Nav1.6 in acute OIPN.

Finally, an *in silico* experiment should be quoted. Dimitrov et al. in 2011[126] performed a simulation with a mathematical model to predict which change(s) could explain phenomena due to OHP exposure. Their modelling suggested that both Na+ and fast K+ conductances should have been altered to match findings reported in literature by *in vitro*/*ex vivo* experiments.

All the reported evidence highlights that there is no a definite answer on the exact mechanisms underlying acute OIPN. All the quoted papers are quite difficult to be compared; some of the observed discrepancies can be, in fact, partially attributed to the completely different study designs and experimental conditions. The most evident difference was OHP concentration, quite a relevant point since OHP effects are dose-dependent. Moreover, these concentrations were quite different also from the clinical setting: plasma platinum mean C_{max} in patients was reported to range from 2.59-3.22 µg/ml (i.e., 6.5-8.11 µM)[127] to 3-6 µg/ml (8-16 µM)[128].

Given this rather complex picture, a decision was to be made for the next experimental step. The most reasonable decision was to embrace a broader hypothesis, despite considering still Na+ currents as pivotal. Preclinical literature findings were more convincing for the "sodium" hypothesis and were matching the paper I co-authored, which gave the idea for this whole project: in a cohort of nearly 300 OHP treated patients, chronic OIPN was associated with a more pronounced acute OIPN (graded as clinical symptoms) and with polymorphisms in Na+ channels genes[43].

The neuroprotectant agent was then selected seeking for a broader spectrum of action: topiramate was chosen. Its pharmacodynamic profile is, in fact, pleiotropic. It has a main effect in blocking voltage-gated sodium channels. However, other mechanisms have been described: reduction of L-type calcium channel activity[95], inhibition of glutamate activity[95], enhancement of GABA-evoked curents[101], mild inhibition of carbonic anhydrase isoenzymes[96,102], and positive modulation of some types of voltage-gated K+ channels[101,104].

7.3 NEUROPROTECTION FINDINGS

In **TASK 5** changes at NET in the 72 hours after acute OHP administration were observed, comparing findings with a co-treatment group (OHP+TPM). Topiramate was administered at 100 mg/Kg dosage in comparison

to clinical practice, corresponding to the human maximum tolerated dose. However, it should be noted though that acute[129] and chronic[130] daily administration of the TPM up to the highest range in clinical practice corresponds to plasma level ranging from 4 to 10 µg/ml, i.e. a low dosage, as used in *in vitro* studies by Taverna et al.[99] in which TPM effects on Na+ currents were clearly demonstrated. To ensure a steady state in the blood stream, we started TPM administration (once daily, per os) 5 days before OHP iv injection. Drug administration timing was studied to administer OHP at the peak of TPM effect. Homogeneity among groups was secured with standard neurophysiology (sensory and motor recordings) at base line.

Figure 34, **35** and **36** allows to follow changes during the observational period for all groups as seen at NET. The main differences were seen in the *recovery cycle of excitability*. In the OHP treated group the curve was pulled upwards with a trend that reached the significance at 72 hours. In OHP+TPM group the curve was significantly pulled downwards at the start of the observational period. In the next days, the OHP+TPM recovery cycle curve was progressively pulled upwards reaching the same level as CTRL group at 72 hours. It was as if TPM effects were evident at 24 hours and then progressively decreased as OHP ones ensued, reaching at 72 hours a kind of equilibrium between the TPM tendency to pull the curve downwards and OHP tendency to pull it upwards.

Going more into details of all changes observed in OHP group, these other considerations should be made. OHP group at 24 hours showed alterations only in hyperpolarizing Threshold Electrotonus, meaning first alterations occurred at the internodal conductances. At 48 hours, again, hyperpolarizing Threshold Electrotonus showed changes as well as Stimulus/response curve and more notably increased refractoriness at recovery cycle; these 2 new changes can be directly linked to an effect on Na+ channels. Similar refractoriness changes were observed when Na+ channel function was altered through biological toxins (as in a case report after tetrodotoxin intoxication, due to puffer fish ingestion[131]), neuropathic medications (mexiletine[132]) or genetic mutation of Na+ channel[133]. At 72 hours, instead, Current/Threshold properties were different to CTRL group showing a possible effect of the cationic conductance I_H, resulting in inward rectification; hyperpolarizing Threshold Electrotonus was again altered and Recovery cycle showed superexcitability value at 7msec set at far less negative level. Collectively these data were compatible with changes mainly in Na+ channel conductances with a little contribution from the other components reported.

These results were rather encouraging since acute OIPN pattern was clearly changed with TPM concomitant administration. TPM was not able to revert all changes seen at NET: recovery cycle was the main target for TPM; thus, a modulation effect mainly related to Na+ channel was hypothesized, despite TPM broader spectrum of action. One more step was finally required to discover if this modulation was able to change the natural history of chronic OIPN.

In **TASK 6** daily TPM co-administration effects on OHP chronic treatment was ascertained. This time findings were compared not only with CTRL group but also to TPM treated animals to ensure that TPM was not

neurotoxic by itself and to rule out some other unexpected effects. Given the well-known effect of TPM to cause weight loss[134], we closely monitored animal welfare and weight, without registering any severe general toxicity. At the end of treatment recovery cycle was the most interesting curve at NET (see **Figure 37**): OHP group showed a markedly pulled upward recovery cycle curve as in previous TASKS; this pattern was not present in the OHP+TPM group. Notably, TPM group was equal to CTRL for all parameters: this was far from surprising. TPM dose of TASK 5 and 6 was in the same range used by Taverna et al.[99] in voltage clamp recordings of pyramidal neurons, derived from slices of rat dorsal fronto-pariental cortex. They showed that this (rather low) concentration was not able to modify the physiological generation of the action potential in natural state neurons; instead, TPM action ensued in case of sustained depolarizing events or high frequency discharges ("use-dependent" effect).

However, the most interesting findings were seen in chronic neuropathy detection:

- OHP group showed hallmarks of neuropathy as defined by all outcome measure: Dynamic test (mechanical allodynia), nerve conduction studies (sensory axonal polyneuropathy), caudal nerve morphological and morphometric analysis (markedly decreased fiber density in caudal nerve) and IENF (marked decrease in fiber density) as shown by **Tables 56**, **58**, **60** and **61** and **Figures 38** and **40**;
- OHP+TPM and TPM groups showed similar values to CTRL for behavioral, neurophysiological, morphological/morphometric analysis, as can be seen from the same **Tables**/**Figures**.

Thus, data showed for the first time a convincing neuroprotection effect on multiple parameters in a well-refined and translational animal model. Moreover, a protection was shown both on small (IENF) and large fibers (nerve conduction studies and caudal nerve morphometry). In clinical practice this would have meant absence of neuropathic pain and sensory loss, with preserved QoL.

Since TPM effects on NET data were more probably to be attributed to its effect on Na+ channels, our findings can be enlisted in support of the "Na+-channel centered" pathogenetic hypothesis.

But it would be intriguing to speculate a bit more on these promising results that even exceeded the expectations. The pivotal role of acute OIPN in chronic OIPN development was for sure the working hypothesis of this project; but OHP shares also all other mechanisms of peripheral nerve damage, common to all platinum drugs. So, some other TPM neuroprotective properties should be further explored. DRG are the common target for all platinum compounds in CIPN development[46,135-141]. CIPN related to platinum drugs has been linked to different mechanisms resulting in apoptosis induction: DNA tertiary structure in neurons is affected, thus causing cyclin D1 upregulation and hyperphosphorylation of retinoblastoma gene product[142]; oxidative stress and mitochondrial dysfunction[143-145]; activation of p38 and ERK1/2[146]. The more evident neurotoxic profile of OHP, compared to cis- and carboplatin, could be related to a "double" damaging action

for OHP: axonal hyperexcitability could probably be the adjunctive damage mechanism, but it cannot be the unique mechanism of nerve damage.

What if reverting the Na+ channelopathy were able to generate a virtuous domino effect on other pathways?

Persson et al.[147] suggested that Na+ channel activity (and an excess of it) may induce chronic axonal damage, reversing the flux of the Na+/Ca2+ exchanger (i.e., Ca2+ importing is the final effect). This is not a bizarre hypothesis: a particular Na+/Ca2+ isoform (isoform 2, NCX2) is expressed distally in peripheral axons along with Nav1.6, Nav1.7, Nav1.8 and Nav1.9[148]. A study from Stys et al.[149] showed that the rat optic nerve, in case of metabolic anoxia, developed a persistent Na+ influx and an impairment of Na+/K+-ATPase pump with increased intracellular Na+ concentrations, reversing the operation of Na+/Ca2+ exchanger: toxic axonal Ca2+ levels were demonstrated. The same group then replicated these data in peripheral nerves[150]. In support of the disruptive role of NCX2 reverse operation, KB-R7943 effects can be reported: it blocks the reverse of NCX2, without altering the forward operation. KB-R7943, administered *in vitro* to adult rat DRG neurites, attenuated degeneration consequent to rotenone (mitochondrial toxin)[151].

Ca2+ levels and their variations are directly related to many intracellular processes. Their importance and the necessity of a fine regulation can be inferred by the numerous and diverging protein families each cell expresses for Ca2+ homeostasis and Ca2+-related functioning: proteins that can increase or decrease Ca2+ concentrations, Ca2+ binding proteins that trap free of organelle Ca2+ and Ca2+ sensitive proteins whose activity is dependent on Ca2+ binding[152]. Ca2+ increased intracellular levels have been described as a key event in axonal degeneration[153]. Events demonstrated in transected axons exemplifies the crucial role of Ca2+ dysregulation. Knöferle et al.[154] followed early events in axonal degeneration in the rat optic nerve, adopting an *in vivo* epifluorescence imaging, demonstrating that increased postlesional autophagy is Ca2+ dependent and hypothesized a causative relationship between autophagy and Ca2+levels. In the first hours after the lesion, in fact, they demonstrated appearance of autophagosomes and a rapid increase of intra-axonal Ca2+ levels was visualized using a Ca2+-sensitive dye; Ca2+channel inhibitors prevented Ca2+increase and axonal degeneration was greatly decreased, whereas Ca2+ionophore aggravated the degeneration. However, the primary event in early axonal degeneration is cytoskeletal breakdown an alteration that can also be related to Ca2+ increase: serine-threonine protease calpain activation is, in fact, dependent on Ca2+. Once activated, this protein is responsible for the cleavage of axonal neurofilament and mictrotubule-associated elements such as tubulin and spectrin[155,156]. The role of Ca2+ increase is key also in later processes leading to Wallerian degeneration as demonstrated in neuron cultures exposed to different Ca2+ environments: a switch to low Ca2+ (below 200 μM) media or Ca2+ chelation with EGTA delayed axonal degeneration, whereas Ca2+ ionophores reverted the protective action and enhanced degeneration even in uninjured neurites[157,158]. Notably, cellular Ca2+ overload by itself can even result in a death signal[159]. Fleckenstein et al.[159] in 1974 gave first reports of excessive Ca2+ as lethal mediator: cardiac pathology after

ischemia was related to an excessive intracytosolic Ca2+ levels in injured myocardiocytes. Wyllie et al.[160] reported that excessive Ca2+ induced apoptotic DNA fragmentation in isolated thymocyte nuclei, activating Ca2+- and Mg2+-dependent endonucleases. However, Ca2+ triggers a vast number of effectors resulting in death signaling: protein kinases and phosphatses, NO synthases, endonucleases, transglutaminases, phospholipases, and proteases[159]. Calpains are quite interesting: there is a calpain family of Ca2+-activated cysteine proteases, as seen in inhibitory studies, that is involved in apoptosis and it is more prominent in certain cell types, among which there are neurons[161]. Calpain cleaves endogenous calcineurin inhibitor cain/cabin 1, resulting in calcineurin activation leading to cell[162]. Moreover, during the apoptotic process calpain and caspases crosstalk was demonstrated, thus, confirming again the perilous consequences of Ca2+ "toxicity"[159].

In support of Ca2+ dysregulation as a downstream event in OIPN development, there are findings from Kawashiri et al.[163]: they evidenced a prolonged cytosolic Ca2+ level elevation in DRG exposed to OHP (100-500 µM), which was prevented if incubation with L-type Ca2+ channel blockers (diltiazem and nifedipine) was performed. As it was yet stated, increased Ca2+ levels can then trigger a cascade of events leading to apoptosis and oxidative stress (i.e., NO synthase activation as stated above). But oxidative stress and apoptosis have been suggested to be also the final/intermediate event among the common mechanisms of damage all platinum compounds exhibit on DRG. TPM might therefore prevent chronic neurotoxicity not only as a direct consequence of Na+ channelopathy correction, but also modulating these other downstream neurotoxic events, thanks to a newly found Ca2+ and Na+ equilibrium. **Figure 42** summarizes this hypothesis.

Figure 42 shows also another intriguing role TPM might play. TPM has a well-known effect as carbon anhydrase (CA) inhibitor (specifically for isoform II and IV)[95]. This inhibition could lead to blood pH decrease, if operated on CA IV contained in red blood cells; in fact, if this effect is too pronounced, in clinical practice metabolic acidosis has been reported among adverse event due to decreased serum bicarbonate levels[98]. This is a highly relevant observation that allows some more speculations. Baker and Bostock demonstrated that persistent Na+ channel is responsive to extracellular pH lowering. They tested large DRG neurons form rats with the patch clamp technique: a lowering of the opened channels and a decrease of the conductance of the single channel was seen in response to acidification[164]. Thus, it can be suggested that TPM can decrease axonal hyperexcitability both directly – with a direct action on *transient* Na+ channels - and indirectly, modulating *persistent* Na+ channels via extracellular pH lowering. *Persistent* Na+ channels account only for a small component of Na+ current, but they operate on a wider range of potentials. Thus, they may modulate neuronal excitability: they enhance the effects of subthreshold depolarization inputs, thereby contributing to repetitive neuronal firing[165,166]. As an example, Agrawal et al.[167] induced status epilepticus in rats (via lithium-pilocarpine) and in the following weeks performed whole-cell voltage-clamp of acutely dissociated

cortical neurons. Transient Na+ currents were similar to controls, whereas persistent Na+ currents were significantly larger, confirming that increased persistent currents accentuate neuronal excitability.

Regarding pH and OHP a very recent paper from Riva et al.[168] allows even further speculation. They observed that acute OHP administration led to intracellular pH acidification both in mice DRG cultured neurons (exposed to 0.1, 1, 10 µm/mL OHP concentrations for 6 or 48 hours) and in DRG cells obtained from mice treated 24 hours before with 3.5 mg/Kg OHP iv. They also observed that pH decrease hypersensitized TRPA1 channels, known to be pH sensitive[169,170]. A mechanistic explanation for this pH alteration was not given by Authors, even though they stated that preventing this acidification might protect neurons. This is not in contrast with the reasoning made so far about extracellular pH levels and TPM. Modification of pH due to TPM should be considered from another point of view. If TPM would be able to rebalance intracellular pH lowering in DRG neurons after OHP administration, due to its role as a CA inhibitor, should be demonstrated. As discussed by Casey et al.[171], all cells possess a pH buffering capacity and TPM effects as CA inhibitor can vary greatly among different tissues, depending on the specific CA isoenzyme present and the environmental conditions; in fact, CA catalyzes the interconversion between carbon dioxide and water and the dissociated ions of carbonic acid (i.e., HCO3- and H+). This is a reversible reaction and it is catalyzed in both directions, forward and reverse. It is important to note this, since pH lowering has been demonstrated to be a mechanism associated with tumor growth[172]. So, a concern might rise considering that TPM might be able to promote extracellular acidification as stated above. However, solid cancer cells express CA IX which favors cell growth preventing intracellular acidosis associated with hypoxia[173]: it promotes alkalinisation of intracellular pH and increases metastatic activity thanks to extracellular pH lowering[174,175]. Therefore, CA IX has become a new target for cancer treatment[176,177,178]. Then in this case, CA inhibition wouldn't be detrimental, but beneficial on cancer prognosis; in fact Ma et al.[179] demonstrated in a mouse model, bearing Lewis lung carcinoma, that TPM showed antitumor and antimetastatic effects thanks to CA inhibition and VEGF down-regulation. So, in "cancer" sites, TPM should be able to contrast pH lowering, thus, dissipating concerns that might have been raised about its interference with OHP antitumoral activity; on the contrary, a synergic effect might be even suggested.

But the paper from Riva et al.[168] gives insights to a possible adjunctive link between acute and chronic toxicity, advocating again the complex relationship between OHP and Ca2+ via TRPA1 hypersensitization. TRPA1 is a part of a Ca2+ plasma membrane calcium channels family involved in the transduction of noxious stimuli: TRANSIENT RECEPTOR POTENTIAL (TRP) channels. In mammals 6 families have been described according to gene homology: TRPM, TRPV, TRPA, TRPML and TRPP[180]. TRPA1 is the more interesting among them since it is permeable both for monovalent and divalent cations, but with a higher permeability for Ca2+, compared to other families[181]. Thus, again, if TPM were to act also on upstream events leading to TRPA1

hypersensitization, it might contain another possible mechanism of Ca+ homeostasis disturbance, modulating upstream events that would lead to platinum drugs common mechanisms of neuronal damage.

A recent review by Jordan et al. is not in contradiction with hypothesis made so far attributing to Ca2+ homeostasis the possible role as link between acute and chronic OIPN[182]. They performed a systematic review of 694 clinical trials to ascertain the efficacy of Calcium and Magnesium infusions to prevent OIPN. Only 5 trials were of enough quality to be considered and none demonstrated a beneficial effect. However, there are some biases. The most relevant trial was from Loprinzi et al.[183]: 353 patients with colon cancer undergoing OHP were randomly assigned to intravenous calcium/magnesium before and after oxaliplatin, a placebo before and after, or calcium/magnesium before and placebo after. This is the first pitfall. Data from TASKS of this PhD project clearly demonstrate that OHP has prolonged effects over the days: a neuroprotection strategy should at least consider a chronic co-treatment and it can be argued that an i.v. infusion of Ca2+/Mg2+ could be able to revert all the possible pathways of damage diffusely described in this discussion; at least, the effect of that schedule and dosage should be verified on axonal excitability (for example, via NET in OHP treated patients). Last, but not least, the primary end-point to detect and grade OIPN was the sensory scale of the European Organisation for Research and Treatment of Cancer Quality of Life Questionnaire-Chemotherapy-Induced Peripheral Neuropathy 20 tool. As pointed out by Cavaletti et al.[184] and - more recently - by Jewandeter et al.[185], a solid outcome measure should be elected in a clinical trial. But in this case no formal neurological assessment was performed; the only physician-based outcome measure was NCI-CTC, a scale that doesn't require a physical examination and it was, in fact, demonstrated not to be effective in detect and grade CIPN[186].

So, the data presented in this project are a novelty both at clinical and preclinical levels. TPM has been tested in a few cases to treat OIPN. In 2014 Deuis et al.[187], investigated TPM analgesic properties after OHP administration in C57BL/6 mice. However, findings of this PhD project cannot be compared to their study which showed many limitations and differences from the model in TASKS discussed so far. First, they declared to induced neuropathy by a single intraplantar injection of OHP and they detected what they defined as "polyneuropathy", by testing mechanical threshold in the same hind-paw where OHP was given 24 hours previously. No neurophysiological or neuropathological data were acquired to verify proper neuropathy induction; moreover, it was not stated if control animals were treated with the vehicle. Thus, it was not possible to rule out the hyperalgesic effect of the puncture itself. TPM according to this paper did not show any analgesic property, but the dosage used was far lower than ours: they administered 50 mg/Kg ip; given the route of administration, the single shot it was probably under the efficacious dose. On the "bed side", there is no clinical trial for a possible comparison. Durand et al.[188] in 2005 published a single case report for TPM use in OIPN; however, they used the drug as a symptomatic treatment for neuropathic pain after neuropathy onset[188].

Despite promising data obtained thanks to all presented TASKS there are some limitations to be acknowledge. TPM dosage used in this project was equal to the maximum clinical tolerated one. Thus, it should be verified if the same results could be obtained with less amount of TPM, corresponding to the lower range of the human therapeutic dosages. Moreover, efficacy was demonstrated in a single experiment limited to a cohort of female rats. In future it would be important to replicate data in both sexes and in other species (mouse).

In conclusion, a promising new strategy to prevent OIPN onset can be derived from this project. Observations were based on highly translational outcome measures and tested a neuroprotectant agent (TPM) yet approved for clinical use: if a confirmation with further experiments will be reached, a quite rapid translation to a clinical trial can be expected. Notably, if TPM synergic action with OHP were also demonstrated, the clinical relevance of its administration in CRC patients would be even higher.

Figure 42. Possible overall pathogenetic hypothesis encompassing acute and chronic OIPN and the role of TPM neuroprotection properties.

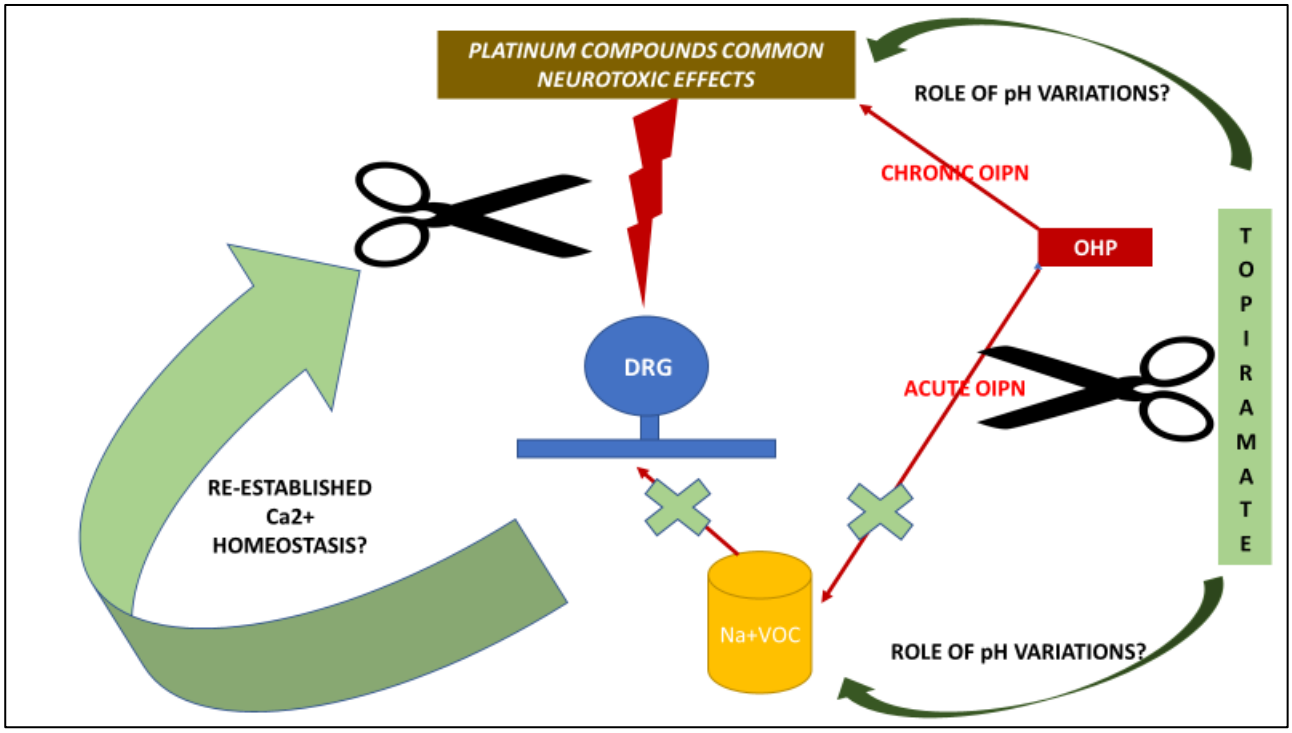

8 FUTURE DEVELOPMENTS

After the promising results obtained so far, axonal hyperexcitability modulation in OIPN will be further tested.

In the next phase the model will be switched from rats to mice. This different specie shows some advantages. Only a few cancer cell lines can induce cancer in immunocompetent rats; so, rat models are limited in usefulness for studying, at the same time, antineoplastic activity and neurotoxic effects of a given anticancer compound. Thus, when testing a compound for CIPN prevention, in immunodeficient mice also safety and interaction with chemotherapy can be ascertained [45,189].

These points will be addressed in future experiments:

- Replica of efficacy findings in another specie (mouse) and in both sexes;
- Evaluation of efficacy of lower TPM dosages to avoid adverse events, when/if data will be transferred to a clinical trial in the future;
- Verification of TPM effects on peripheral neurotoxicity on CDDP: no action should be expected if Na+ channel is the crucial element in OIPN development, since, as it was yet stated, TPM action is use-dependent. If some effects will be seen with CDDP the importance of other mechanisms of damage should be again reconsidered;
- Comparison in efficacy with other proband molecules to devise if there is/are other pivotal mechanism(s): acetazolamide will be tested to test the role of CA inhibition, oxcarbazepine to verify the role of Na+ channels and nifedipine for the role of Ca2+ ones;
- Reproduction of TPM efficacy in an immunodeficient mouse OIPN model to verify the suggested possible synergistic role of TPM on cancer treatment.

If further promising evidences will be collected in the next few years, a neuroprotective clinical trial can be not so far away in the hope to find a long-waited cure for a still unmet clinical need.

9 BIBLIOGRAPHY

1. Chau I, Cunningham D. Oxaliplatin for colorectal cancer in the United States: better late than never. *J Clin Oncol* 2003; **21**(11): 2049-51.
2. Screnci D, McKeage MJ. Platinum neurotoxicity: clinical profiles, experimental models and neuroprotective approaches. *J Inorg Biochem* 1999; **77**(1-2): 105-10.
3. Kavanagh J, Tresukosol D, Edwards C, et al. Carboplatin reinduction after taxane in patients with platinum-refractory epithelial ovarian cancer. *J Clin Oncol* 1995; **13**(7): 1584-8.
4. Nichols CR, Williams SD, Loehrer PJ, et al. Randomized study of cisplatin dose intensity in poor-risk germ cell tumors: a Southeastern Cancer Study Group and Southwest Oncology Group protocol. *J Clin Oncol* 1991; **9**(7): 1163-72.
5. Muggia FM. Dose intensity: not the only path to clinical dose optimization. *J Infus Chemother* 1996; **6**(2): 57-8.
6. André T, Boni C, Mounedji-Boudiaf L, et al. Oxaliplatin, fluorouracil, and leucovorin as adjuvant treatment for colon cancer. *N Engl J Med* 2004; **350**(23): 2343-51.
7. Fischel JL, Etienne MC, Formento P, Milano G. Search for the optimal schedule for the oxaliplatin/5-fluorouracil association modulated or not by folinic acid: preclinical data. *Clin Cancer Res* 1998; **4**(10): 2529-35.
8. Bajetta E, Celio L, Ferrario E, et al. Capecitabine plus oxaliplatin and irinotecan regimen every other week: a phase I/II study in first-line treatment of metastatic colorectal cancer. *Ann Oncol* 2007; **18**(11): 1810-6.
9. Grothey A, Goetz MP. Oxaliplatin plus oral fluoropyrimidines in colorectal cancer. *Clin Colorectal Cancer* 2004; **4 Suppl 1**: S37-42.
10. Perego P, Robert J. Oxaliplatin in the era of personalized medicine: from mechanistic studies to clinical efficacy. *Cancer Chemother Pharmacol* 2016; **77**(1): 5-18.
11. Argyriou AA, Bruna J, Marmiroli P, Cavaletti G. Chemotherapy-induced peripheral neurotoxicity (CIPN): an update. *Crit Rev Oncol Hematol* 2012; **82**(1): 51-77.
12. Cavaletti G, Alberti P, Marmiroli P. Chemotherapy-induced peripheral neurotoxicity in cancer survivors: an underdiagnosed clinical entity? *Am Soc Clin Oncol Educ Book* 2015: e553-60.
13. Cavaletti G, Marmiroli P. Chemotherapy-induced peripheral neurotoxicity. *Curr Opin Neurol* 2015; **28**(5): 500-7.
14. Bjornard KL, Gilchrist LS, Inaba H, et al. Peripheral neuropathy in children and adolescents treated for cancer. *Lancet Child Adolesc Health* 2018; **2**(10): 744-54.
15. Kandula T, Farrar MA, Cohn RJ, et al. Chemotherapy-Induced Peripheral Neuropathy in Long-term Survivors of Childhood Cancer: Clinical, Neurophysiological, Functional, and Patient-Reported Outcomes. *JAMA Neurol* 2018; **75**(8): 980-8.
16. Kandula T, Park SB, Cohn RJ, Krishnan AV, Farrar MA. Pediatric chemotherapy induced peripheral neuropathy: A systematic review of current knowledge. *Cancer Treat Rev* 2016; **50**: 118-28.
17. Miaskowski C, Mastick J, Paul SM, et al. Impact of chemotherapy-induced neurotoxicities on adult cancer survivors' symptom burden and quality of life. *J Cancer Surviv* 2018; **12**(2): 234-45.
18. Shah A, Hoffman EM, Mauermann ML, et al. Incidence and disease burden of chemotherapy-induced peripheral neuropathy in a population-based cohort. *J Neurol Neurosurg Psychiatry* 2018; **89**(6): 636-41.
19. Mols F, Beijers T, Lemmens V, van den Hurk CJ, Vreugdenhil G, van de Poll-Franse LV. Chemotherapy-induced neuropathy and its association with quality of life among 2- to 11-year colorectal cancer survivors: results from the population-based PROFILES registry. *J Clin Oncol* 2013; **31**(21): 2699-707.
20. Mols F, Beijers T, Vreugdenhil G, van de Poll-Franse L. Chemotherapy-induced peripheral neuropathy and its association with quality of life: a systematic review. *Support Care Cancer* 2014; **22**(8): 2261-9.
21. Argyriou AA, Kyritsis AP, Makatsoris T, Kalofonos HP. Chemotherapy-induced peripheral neuropathy in adults: a comprehensive update of the literature. *Cancer Manag Res* 2014; **6**: 135-47.
22. Grisold W, Cavaletti G, Windebank AJ. Peripheral neuropathies from chemotherapeutics and targeted agents: diagnosis, treatment, and prevention. *Neuro Oncol* 2012; **14 Suppl 4**: iv45-54.
23. Pachman DR, Barton DL, Swetz KM, Loprinzi CL. Troublesome symptoms in cancer survivors: fatigue, insomnia, neuropathy, and pain. *J Clin Oncol* 2012; **30**(30): 3687-96.
24. Bennion AE, Molassiotis A. Qualitative research into the symptom experiences of adult cancer patients after treatments: a systematic review and meta-synthesis. *Support Care Cancer* 2013; **21**(1): 9-25.
25. Hershman DL, Lacchetti C, Dworkin RH, et al. Prevention and management of chemotherapy-induced peripheral neuropathy in survivors of adult cancers: American Society of Clinical Oncology clinical practice guideline. *J Clin Oncol* 2014; **32**(18): 1941-67.
26. Smith EM, Pang H, Cirrincione C, et al. Effect of duloxetine on pain, function, and quality of life among patients with chemotherapy-induced painful peripheral neuropathy: a randomized clinical trial. *JAMA* 2013; **309**(13): 1359-67.
27. Cavaletti G, Marmiroli P. Pharmacotherapy options for managing chemotherapy-induced peripheral neurotoxicity. *Expert Opin Pharmacother* 2018; **19**(2): 113-21.
28. Carozzi VA, Canta A, Chiorazzi A. Chemotherapy-induced peripheral neuropathy: What do we know about mechanisms? *Neurosci Lett* 2015; **596**: 90-107.
29. Lucchetta M, Lonardi S, Bergamo F, et al. Incidence of atypical acute nerve hyperexcitability symptoms in oxaliplatin-treated patients with colorectal cancer. *Cancer Chemother Pharmacol* 2012; **70**(6): 899-902.
30. Newsom-Davis J. The emerging diversity of neuromuscular junction disorders. *Acta Myol* 2007; **26**(1): 5-10.
31. Adelsberger H, Quasthoff S, Grosskreutz J, Lepier A, Eckel F, Lersch C. The chemotherapeutic oxaliplatin alters voltage-gated Na(+) channel kinetics on rat sensory neurons. *Eur J Pharmacol* 2000; **406**(1): 25-32.

32. Krishnan AV, Goldstein D, Friedlander M, Kiernan MC. Oxaliplatin-induced neurotoxicity and the development of neuropathy. *Muscle Nerve* 2005; **32**(1): 51-60.
33. Park SB, Lin CS, Krishnan AV, Goldstein D, Friedlander ML, Kiernan MC. Dose effects of oxaliplatin on persistent and transient Na+ conductances and the development of neurotoxicity. *PLoS One* 2011; **6**(4): e18469.
34. Park SB, Lin CS, Kiernan MC. Nerve excitability assessment in chemotherapy-induced neurotoxicity. *J Vis Exp* 2012; (62).
35. Grolleau F, Gamelin L, Boisdron-Celle M, Lapied B, Pelhate M, Gamelin E. A possible explanation for a neurotoxic effect of the anticancer agent oxaliplatin on neuronal voltage-gated sodium channels. *J Neurophysiol* 2001; **85**(5): 2293-7.
36. Park SB, Lin CS, Krishnan AV, Goldstein D, Friedlander ML, Kiernan MC. Oxaliplatin-induced neurotoxicity: changes in axonal excitability precede development of neuropathy. *Brain* 2009; **132**(Pt 10): 2712-23.
37. Catterall WA, Dib-Hajj S, Meisler MH, Pietrobon D. Inherited neuronal ion channelopathies: new windows on complex neurological diseases. *J Neurosci* 2008; **28**(46): 11768-77.
38. Krishnan AV, Lin CS, Park SB, Kiernan MC. Axonal ion channels from bench to bedside: a translational neuroscience perspective. *Prog Neurobiol* 2009; **89**(3): 288-313.
39. Sugawara T, Mazaki-Miyazaki E, Ito M, et al. Nav1.1 mutations cause febrile seizures associated with afebrile partial seizures. *Neurology* 2001; **57**(4): 703-5.
40. Rossignol E, Mathieu J, Thiffault I, et al. A novel founder SCN4A mutation causes painful cold-induced myotonia in French-Canadians. *Neurology* 2007; **69**(20): 1937-41.
41. Argyriou AA, Velasco R, Briani C, et al. Peripheral neurotoxicity of oxaliplatin in combination with 5-fluorouracil (FOLFOX) or capecitabine (XELOX): a prospective evaluation of 150 colorectal cancer patients. *Ann Oncol* 2012; **23**(12): 3116-22.
42. Argyriou AA, Cavaletti G, Briani C, et al. Clinical pattern and associations of oxaliplatin acute neurotoxicity: a prospective study in 170 patients with colorectal cancer. *Cancer* 2013; **119**(2): 438-44.
43. Argyriou AA, Cavaletti G, Antonacopoulou A, et al. Voltage-gated sodium channel polymorphisms play a pivotal role in the development of oxaliplatin-induced peripheral neurotoxicity: results from a prospective multicenter study. *Cancer* 2013; **119**(19): 3570-7.
44. Alberti P. Chemotherapy-induced peripheral neurotoxicity - outcome measures: the issue. *Expert Opin Drug Metab Toxicol* 2017; **13**(3): 241-3.
45. Carozzi VA, Chiorazzi A, Canta A, et al. Chemotherapy-induced peripheral neurotoxicity in immune-deficient mice: new useful ready-to-use animal models. *Exp Neurol* 2015; **264**: 92-102.
46. Cavaletti G, Tredici G, Petruccioli MG, et al. Effects of different schedules of oxaliplatin treatment on the peripheral nervous system of the rat. *Eur J Cancer* 2001; **37**(18): 2457-63.
47. Cavaletti G, Petruccioli MG, Marmiroli P, et al. Circulating nerve growth factor level changes during oxaliplatin treatment-induced neurotoxicity in the rat. *Anticancer Res* 2002; **22**(6C): 4199-204.
48. Alberti P, Rossi E, Argyriou AA, et al. Risk stratification of oxaliplatin induced peripheral neurotoxicity applying electrophysiological testing of dorsal sural nerve. *Support Care Cancer* 2018; **26**(9): 3143-51.
49. Wilson RH, Lehky T, Thomas RR, Quinn MG, Floeter MK, Grem JL. Acute oxaliplatin-induced peripheral nerve hyperexcitability. *J Clin Oncol* 2002; **20**(7): 1767-74.
50. Lehky TJ, Leonard GD, Wilson RH, Grem JL, Floeter MK. Oxaliplatin-induced neurotoxicity: acute hyperexcitability and chronic neuropathy. *Muscle Nerve* 2004; **29**(3): 387-92.
51. Neher E, Sakmann B. Single-channel currents recorded from membrane of denervated frog muscle fibres. *Nature* 1976; **260**(5554): 799-802.
52. Burke D, Kiernan MC, Bostock H. Excitability of human axons. *Clin Neurophysiol* 2001; **112**(9): 1575-85.
53. Krishnan AV, Lin CS, Park SB, Kiernan MC. Assessment of nerve excitability in toxic and metabolic neuropathies. *J Peripher Nerv Syst* 2008; **13**(1): 7-26.
54. Bostock H, Cikurel K, Burke D. Threshold tracking techniques in the study of human peripheral nerve. *Muscle Nerve* 1998; **21**(2): 137-58.
55. Kiernan MC, Burke D, Andersen KV, Bostock H. Multiple measures of axonal excitability: a new approach in clinical testing. *Muscle Nerve* 2000; **23**(3): 399-409.
56. Tomlinson SE, Howells J, Burke D. In vivo assessment of neurological channelopathies: Application of peripheral nerve excitability studies. *Neuropharmacology* 2018; **132**: 98-107.
57. Heide R, Bostock H, Ventzel L, et al. Axonal excitability changes and acute symptoms of oxaliplatin treatment: In vivo evidence for slowed sodium channel inactivation. *Clin Neurophysiol* 2018; **129**(3): 694-706.
58. Yang Q, Kaji R, Hirota N, et al. Effect of maturation on nerve excitability in an experimental model of threshold electrotonus. *Muscle Nerve* 2000; **23**(4): 498-506.
59. George A, Bostock H. Multiple measures of axonal excitability in peripheral sensory nerves: an in vivo rat model. *Muscle Nerve* 2007; **36**(5): 628-36.
60. Arnold R, Moldovan M, Rosberg MR, Krishnan AV, Morris R, Krarup C. Nerve excitability in the rat forelimb: a technique to improve translational utility. *J Neurosci Methods* 2017; **275**: 19-24.
61. Wild BM, Morris R, Moldovan M, Krarup C, Krishnan AV, Arnold R. In Vivo Electrophysiological Measurement of the Rat Ulnar Nerve with Axonal Excitability Testing. *J Vis Exp* 2018; (132).
62. Boërio D, Greensmith L, Bostock H. Excitability properties of motor axons in the maturing mouse. *J Peripher Nerv Syst* 2009; **14**(1): 45-53.
63. Boërio D, Kalmar B, Greensmith L, Bostock H. Excitability properties of mouse motor axons in the mutant SOD1(G93A) model of amyotrophic lateral sclerosis. *Muscle Nerve* 2010; **41**(6): 774-84.

64. Kiernan MC, Lin CS, Andersen KV, Murray NM, Bostock H. Clinical evaluation of excitability measures in sensory nerve. *Muscle Nerve* 2001; **24**(7): 883-92.
65. Arroyo EJ, Scherer SS. On the molecular architecture of myelinated fibers. *Histochem Cell Biol* 2000; **113**(1): 1-18.
66. Schwarz JR, Reid G, Bostock H. Action potentials and membrane currents in the human node of Ranvier. *Pflugers Arch* 1995; **430**(2): 283-92.
67. Matthew C. Kiernan CSYL. Nerve Excitability: A Clinical Translation. In: Aminoff MJ, ed. Aminoff's Electrodiagnosis in Clinical Neurology. 6th Edition ed: Saunders; 2012: 345-65.
68. Hammond C. Ionic fluxes across the neuronal plasma membrane. In: Hammond C, ed. Cellular and Molecular Neurobiology. London.: Academic Press; 2001: 36-109.
69. Eric R. Kandel , James H. Schwartz , Jessell. TM. Principles of Neural Science. In: Medical M-H, ed. 4th edition. ed; 2000: 144-61.
70. Ritchie JM, Chiu SY. Distribution of sodium and potassium channels in mammalian myelinated nerve. *Adv Neurol* 1981; **31**: 329-42.
71. Rosenbluth J. Intramembranous particle distribution at the node of Ranvier and adjacent axolemma in myelinated axons of the frog brain. *J Neurocytol* 1976; **5**(6): 731-45.
72. Crill WE. Persistent sodium current in mammalian central neurons. *Annu Rev Physiol* 1996; **58**: 349-62.
73. Baker MD, Bostock H. Inactivation of macroscopic late Na+ current and characteristics of unitary late Na+ currents in sensory neurons. *J Neurophysiol* 1998; **80**(5): 2538-49.
74. Gutman GA, Chandy KG, Grissmer S, et al. International Union of Pharmacology. LIII. Nomenclature and molecular relationships of voltage-gated potassium channels. *Pharmacol Rev* 2005; **57**(4): 473-508.
75. Röper J, Schwarz JR. Heterogeneous distribution of fast and slow potassium channels in myelinated rat nerve fibres. *J Physiol* 1989; **416**: 93-110.
76. Devaux JJ, Kleopa KA, Cooper EC, Scherer SS. KCNQ2 is a nodal K+ channel. *J Neurosci* 2004; **24**(5): 1236-44.
77. Pape HC. Queer current and pacemaker: the hyperpolarization-activated cation current in neurons. *Annu Rev Physiol* 1996; **58**: 299-327.
78. HODGKIN AL, HUXLEY AF. A quantitative description of membrane current and its application to conduction and excitation in nerve. *J Physiol* 1952; **117**(4): 500-44.
79. Rakowski RF, Gadsby DC, De Weer P. Stoichiometry and voltage dependence of the sodium pump in voltage-clamped, internally dialyzed squid giant axon. *J Gen Physiol* 1989; **93**(5): 903-41.
80. Bostock H. The strength-duration relationship for excitation of myelinated nerve: computed dependence on membrane parameters. *J Physiol* 1983; **341**: 59-74.
81. Mogyoros I, Kiernan MC, Burke D. Strength-duration properties of human peripheral nerve. *Brain* 1996; **119 (Pt 2)**: 439-47.
82. Irnich W. Georges Weiss' fundamental law of electrostimulation is 100 years old. *Pacing Clin Electrophysiol* 2002; **25**(2): 245-8.
83. G. W. On the possibility to make mutually comparable devices serving for electrical excitation" (Sur la possibilité de rendre comparables entre eux les appareils servant à l'excitation électrique). *Archives Italiennes de Biologie* 1901; **35**: 413-46.
84. Bostock H, Rothwell JC. Latent addition in motor and sensory fibres of human peripheral nerve. *J Physiol* 1997; **498 (Pt 1)**: 277-94.
85. Burke D, Mogyoros I, Vagg R, Kiernan MC. Quantitative description of the voltage dependence of axonal excitability in human cutaneous afferents. *Brain* 1998; **121 (Pt 10)**: 1975-83.
86. Barrett EF, Barrett JN. Intracellular recording from vertebrate myelinated axons: mechanism of the depolarizing afterpotential. *J Physiol* 1982; **323**: 117-44.
87. David C. Preston BES. Electromyography and Neuromuscular Disorders: Clinical-Electrophysiologic Correlations. 3rd ed; 2012.
88. David G, Modney B, Scappaticci KA, Barrett JN, Barrett EF. Electrical and morphological factors influencing the depolarizing after-potential in rat and lizard myelinated axons. *J Physiol* 1995; **489 (Pt 1)**: 141-57.
89. Baker M, Bostock H, Grafe P, Martius P. Function and distribution of three types of rectifying channel in rat spinal root myelinated axons. *J Physiol* 1987; **383**: 45-67.
90. Miller TA, Kiernan MC, Mogyoros I, Burke D. Activity-dependent changes in impulse conduction in normal human cutaneous axons. *Brain* 1995; **118 (Pt 5)**: 1217-24.
91. Taylor JL, Burke D, Heywood J. Physiological evidence for a slow K+ conductance in human cutaneous afferents. *J Physiol* 1992; **453**: 575-89.
92. Kiernan MC, Bostock H. Effects of membrane polarization and ischaemia on the excitability properties of human motor axons. *Brain* 2000; **123 Pt 12**: 2542-51.
93. Baker MD. Axonal flip-flops and oscillators. *Trends Neurosci* 2000; **23**(11): 514-9.
94. Bostock H, Baker M. Evidence for two types of potassium channel in human motor axons in vivo. *Brain Res* 1988; **462**(2): 354-8.
95. Shank RP, Maryanoff BE. Molecular pharmacodynamics, clinical therapeutics, and pharmacokinetics of topiramate. *CNS Neurosci Ther* 2008; **14**(2): 120-42.
96. Shank RP, Gardocki JF, Vaught JL, et al. Topiramate: preclinical evaluation of structurally novel anticonvulsant. *Epilepsia* 1994; **35**(2): 450-60.
97. Maryanoff BE, Nortey SO, Gardocki JF, Shank RP, Dodgson SP. Anticonvulsant O-alkyl sulfamates. 2,3:4,5-Bis-O-(1-methylethylidene)-beta-D-fructopyranose sulfamate and related compounds. *J Med Chem* 1987; **30**(5): 880-7.

98. Lyseng-Williamson KA, Yang LP. Topiramate: a review of its use in the treatment of epilepsy. *Drugs* 2007; **67**(15): 2231-56.
99. Taverna S, Sancini G, Mantegazza M, Franceschetti S, Avanzini G. Inhibition of transient and persistent Na+ current fractions by the new anticonvulsant topiramate. *J Pharmacol Exp Ther* 1999; **288**(3): 960-8.
100. Zhang X, Velumian AA, Jones OT, Carlen PL. Modulation of high-voltage-activated calcium channels in dentate granule cells by topiramate. *Epilepsia* 2000; **41 Suppl 1**: S52-60.
101. Herrero AI, Del Olmo N, González-Escalada JR, Solís JM. Two new actions of topiramate: inhibition of depolarizing GABA(A)-mediated responses and activation of a potassium conductance. *Neuropharmacology* 2002; **42**(2): 210-20.
102. Angehagen M, Ben-Menachem E, Rönnbäck L, Hansson E. Novel mechanisms of action of three antiepileptic drugs, vigabatrin, tiagabine, and topiramate. *Neurochem Res* 2003; **28**(2): 333-40.
103. Dodgson SJ, Shank RP, Maryanoff BE. Topiramate as an inhibitor of carbonic anhydrase isoenzymes. *Epilepsia* 2000; **41 Suppl 1**: S35-9.
104. Russo E, Constanti A. Topiramate hyperpolarizes and modulates the slow poststimulus AHP of rat olfactory cortical neurones in vitro. *Br J Pharmacol* 2004; **141**(2): 285-301.
105. Kagiava A, Kosmidis EK, Theophilidis G. Oxaliplatin-induced hyperexcitation of rat sciatic nerve fibers: an intra-axonal study. *Anticancer Agents Med Chem* 2013; **13**(2): 373-9.
106. Reagan-Shaw S, Nihal M, Ahmad N. Dose translation from animal to human studies revisited. *FASEB J* 2008; **22**(3): 659-61.
107. Sarangi SC, Kakkar AK, Kumar R, Gupta YK. Effect of lamotrigine, levetiracetam & topiramate on neurobehavioural parameters & oxidative stress in comparison with valproate in rats. *Indian J Med Res* 2016; **144**(1): 104-11.
108. Chiorazzi A, Wozniak KM, Rais R, et al. Ghrelin agonist HM01 attenuates chemotherapy-induced neurotoxicity in rodent models. *Eur J Pharmacol* 2018.
109. Meregalli C, Fumagalli G, Alberti P, et al. Neurofilament light chain as disease biomarker in a rodent model of chemotherapy induced peripheral neuropathy. *Exp Neurol* 2018; **307**: 129-32.
110. Meregalli C, Marjanovic I, Scali C, et al. High-dose intravenous immunoglobulins reduce nerve macrophage infiltration and the severity of bortezomib-induced peripheral neurotoxicity in rats. *J Neuroinflammation* 2018; **15**(1): 232.
111. Auger RG. AAEM minimonograph #44: diseases associated with excess motor unit activity. *Muscle Nerve* 1994; **17**(11): 1250-63.
112. Hill A, Bergin P, Hanning F, et al. Detecting acute neurotoxicity during platinum chemotherapy by neurophysiological assessment of motor nerve hyperexcitability. *BMC Cancer* 2010; **10**: 451.
113. Pisano C, Pratesi G, Laccabue D, et al. Paclitaxel and Cisplatin-induced neurotoxicity: a protective role of acetyl-L-carnitine. *Clin Cancer Res* 2003; **9**(15): 5756-67.
114. Carozzi V, Chiorazzi A, Canta A, et al. Effect of the chronic combined administration of cisplatin and paclitaxel in a rat model of peripheral neurotoxicity. *Eur J Cancer* 2009; **45**(4): 656-65.
115. Sakurai M, Egashira N, Kawashiri T, Yano T, Ikesue H, Oishi R. Oxaliplatin-induced neuropathy in the rat: involvement of oxalate in cold hyperalgesia but not mechanical allodynia. *Pain* 2009; **147**(1-3): 165-74.
116. Krishnan AV, Goldstein D, Friedlander M, Kiernan MC. Oxaliplatin and axonal Na+ channel function in vivo. *Clin Cancer Res* 2006; **12**(15): 4481-4.
117. Webster RG, Brain KL, Wilson RH, Grem JL, Vincent A. Oxaliplatin induces hyperexcitability at motor and autonomic neuromuscular junctions through effects on voltage-gated sodium channels. *Br J Pharmacol* 2005; **146**(7): 1027-39.
118. Wu SN, Chen BS, Wu YH, Peng H, Chen LT. The mechanism of the actions of oxaliplatin on ion currents and action potentials in differentiated NG108-15 neuronal cells. *Neurotoxicology* 2009; **30**(4): 677-85.
119. Benoit E, Brienza S, Dubois JM. Oxaliplatin, an anticancer agent that affects both Na+ and K+ channels in frog peripheral myelinated axons. *Gen Physiol Biophys* 2006; **25**(3): 263-76.
120. Kagiava A, Tsingotjidou A, Emmanouilides C, Theophilidis G. The effects of oxaliplatin, an anticancer drug, on potassium channels of the peripheral myelinated nerve fibres of the adult rat. *Neurotoxicology* 2008; **29**(6): 1100-6.
121. Sittl R, Carr RW, Fleckenstein J, Grafe P. Enhancement of axonal potassium conductance reduces nerve hyperexcitability in an in vitro model of oxaliplatin-induced acute neuropathy. *Neurotoxicology* 2010; **31**(6): 694-700.
122. Thomas RC. Electrogenic sodium pump in nerve and muscle cells. *Physiol Rev* 1972; **52**(3): 563-94.
123. Maingret F, Lauritzen I, Patel AJ, et al. TREK-1 is a heat-activated background K(+) channel. *EMBO J* 2000; **19**(11): 2483-91.
124. Kang D, Choe C, Kim D. Thermosensitivity of the two-pore domain K+ channels TREK-2 and TRAAK. *J Physiol* 2005; **564**(Pt 1): 103-16.
125. Sittl R, Lampert A, Huth T, et al. Anticancer drug oxaliplatin induces acute cooling-aggravated neuropathy via sodium channel subtype Na(V)1.6-resurgent and persistent current. *Proc Natl Acad Sci U S A* 2012; **109**(17): 6704-9.
126. Dimitrov AG, Dimitrova NA. A possible link of oxaliplatin-induced neuropathy with potassium channel deficit. *Muscle Nerve* 2012; **45**(3): 403-11.
127. Graham MA, Lockwood GF, Greenslade D, Brienza S, Bayssas M, Gamelin E. Clinical pharmacokinetics of oxaliplatin: a critical review. *Clin Cancer Res* 2000; **6**(4): 1205-18.
128. Eckel F, Schmelz R, Adelsberger H, Erdmann J, Quasthoff S, Lersch C. [Prevention of oxaliplatin-induced neuropathy by carbamazepine. A pilot study]. *Dtsch Med Wochenschr* 2002; **127**(3): 78-82.
129. Johannessen SI. Pharmacokinetics and interaction profile of topiramate: review and comparison with other newer antiepileptic drugs. *Epilepsia* 1997; **38 Suppl 1**: S18-23.
130. Perucca E. A pharmacological and clinical review on topiramate, a new antiepileptic drug. *Pharmacol Res* 1997; **35**(4): 241-56.
131. Kiernan MC, Isbister GK, Lin CS, Burke D, Bostock H. Acute tetrodotoxin-induced neurotoxicity after ingestion of puffer fish. *Ann Neurol* 2005; **57**(3): 339-48.

132. Kuwabara S, Misawa S, Tamura N, et al. The effects of mexiletine on excitability properties of human median motor axons. *Clin Neurophysiol* 2005; **116**(2): 284-9.
133. Kiernan MC, Krishnan AV, Lin CS, Burke D, Berkovic SF. Mutation in the Na+ channel subunit SCN1B produces paradoxical changes in peripheral nerve excitability. *Brain* 2005; **128**(Pt 8): 1841-6.
134. Grootens KP, Meijer A, Hartong EG, et al. Weight changes associated with antiepileptic mood stabilizers in the treatment of bipolar disorder. *Eur J Clin Pharmacol* 2018; **74**(11): 1485-9.
135. Thompson SW, Davis LE, Kornfeld M, Hilgers RD, Standefer JC. Cisplatin neuropathy. Clinical, electrophysiologic, morphologic, and toxicologic studies. *Cancer* 1984; **54**(7): 1269-75.
136. Krarup-Hansen A, Rietz B, Krarup C, Heydorn K, Rørth M, Schmalbruch H. Histology and platinum content of sensory ganglia and sural nerves in patients treated with cisplatin and carboplatin: an autopsy study. *Neuropathol Appl Neurobiol* 1999; **25**(1): 29-40.
137. Gregg RW, Molepo JM, Monpetit VJ, et al. Cisplatin neurotoxicity: the relationship between dosage, time, and platinum concentration in neurologic tissues, and morphologic evidence of toxicity. *J Clin Oncol* 1992; **10**(5): 795-803.
138. Meijer C, de Vries EG, Marmiroli P, Tredici G, Frattola L, Cavaletti G. Cisplatin-induced DNA-platination in experimental dorsal root ganglia neuronopathy. *Neurotoxicology* 1999; **20**(6): 883-7.
139. Tredici G, Braga M, Nicolini G, et al. Effect of recombinant human nerve growth factor on cisplatin neurotoxicity in rats. *Exp Neurol* 1999; **159**(2): 551-8.
140. Cavaletti G, Pezzoni G, Pisano C, et al. Cisplatin-induced peripheral neurotoxicity in rats reduces the circulating levels of nerve growth factor. *Neurosci Lett* 2002; **322**(2): 103-6.
141. Cavaletti G, Fabbrica D, Minoia C, Frattola L, Tredici G. Carboplatin toxic effects on the peripheral nervous system of the rat. *Ann Oncol* 1998; **9**(4): 443-7.
142. Gill JS, Windebank AJ. Cisplatin-induced apoptosis in rat dorsal root ganglion neurons is associated with attempted entry into the cell cycle. *J Clin Invest* 1998; **101**(12): 2842-50.
143. Zhang H, Mizumachi T, Carcel-Trullols J, et al. Targeting human 8-oxoguanine DNA glycosylase (hOGG1) to mitochondria enhances cisplatin cytotoxicity in hepatoma cells. *Carcinogenesis* 2007; **28**(8): 1629-37.
144. Jiang Y, Guo C, Vasko MR, Kelley MR. Implications of apurinic/apyrimidinic endonuclease in reactive oxygen signaling response after cisplatin treatment of dorsal root ganglion neurons. *Cancer Res* 2008; **68**(15): 6425-34.
145. McDonald ES, Windebank AJ. Cisplatin-induced apoptosis of DRG neurons involves bax redistribution and cytochrome c release but not fas receptor signaling. *Neurobiol Dis* 2002; **9**(2): 220-33.
146. Scuteri A, Galimberti A, Maggioni D, et al. Role of MAPKs in platinum-induced neuronal apoptosis. *Neurotoxicology* 2009; **30**(2): 312-9.
147. Persson AK, Hoeijmakers JGJ, Estacion M, Black JA, Waxman SG. Sodium Channels, Mitochondria, and Axonal Degeneration in Peripheral Neuropathy. *Trends Mol Med* 2016; **22**(5): 377-90.
148. Persson AK, Black JA, Gasser A, Cheng X, Fischer TZ, Waxman SG. Sodium-calcium exchanger and multiple sodium channel isoforms in intra-epidermal nerve terminals. *Mol Pain* 2010; **6**: 84.
149. Stys PK, Waxman SG, Ransom BR. Ionic mechanisms of anoxic injury in mammalian CNS white matter: role of Na+ channels and Na(+)-Ca2+ exchanger. *J Neurosci* 1992; **12**(2): 430-9.
150. Lehning EJ, Doshi R, Isaksson N, Stys PK, LoPachin RM. Mechanisms of injury-induced calcium entry into peripheral nerve myelinated axons: role of reverse sodium-calcium exchange. *J Neurochem* 1996; **66**(2): 493-500.
151. Persson AK, Kim I, Zhao P, Estacion M, Black JA, Waxman SG. Sodium channels contribute to degeneration of dorsal root ganglion neurites induced by mitochondrial dysfunction in an in vitro model of axonal injury. *J Neurosci* 2013; **33**(49): 19250-61.
152. Berridge MJ, Bootman MD, Roderick HL. Calcium signalling: dynamics, homeostasis and remodelling. *Nat Rev Mol Cell Biol* 2003; **4**(7): 517-29.
153. Fernyhough P, Calcutt NA. Abnormal calcium homeostasis in peripheral neuropathies. *Cell Calcium* 2010; **47**(2): 130-9.
154. Knöferle J, Koch JC, Ostendorf T, et al. Mechanisms of acute axonal degeneration in the optic nerve in vivo. *Proc Natl Acad Sci U S A* 2010; **107**(13): 6064-9.
155. Billger M, Wallin M, Karlsson JO. Proteolysis of tubulin and microtubule-associated proteins 1 and 2 by calpain I and II. Difference in sensitivity of assembled and disassembled microtubules. *Cell Calcium* 1988; **9**(1): 33-44.
156. Johnson GV, Litersky JM, Jope RS. Degradation of microtubule-associated protein 2 and brain spectrin by calpain: a comparative study. *J Neurochem* 1991; **56**(5): 1630-8.
157. Schlaepfer WW, Bunge RP. Effects of calcium ion concentration on the degeneration of amputated axons in tissue culture. *J Cell Biol* 1973; **59**(2 Pt 1): 456-70.
158. George EB, Glass JD, Griffin JW. Axotomy-induced axonal degeneration is mediated by calcium influx through ion-specific channels. *J Neurosci* 1995; **15**(10): 6445-52.
159. Zhivotovsky B, Orrenius S. Calcium and cell death mechanisms: a perspective from the cell death community. *Cell Calcium* 2011; **50**(3): 211-21.
160. Wyllie AH. Glucocorticoid-induced thymocyte apoptosis is associated with endogenous endonuclease activation. *Nature* 1980; **284**(5756): 555-6.
161. Vanags DM, Pörn-Ares MI, Coppola S, Burgess DH, Orrenius S. Protease involvement in fodrin cleavage and phosphatidylserine exposure in apoptosis. *J Biol Chem* 1996; **271**(49): 31075-85.
162. Kim MJ, Jo DG, Hong GS, et al. Calpain-dependent cleavage of cain/cabin1 activates calcineurin to mediate calcium-triggered cell death. *Proc Natl Acad Sci U S A* 2002; **99**(15): 9870-5.
163. Kawashiri T, Egashira N, Kurobe K, et al. L type Ca^{2}+ channel blockers prevent oxaliplatin-induced cold hyperalgesia and TRPM8 overexpression in rats. *Mol Pain* 2012; **8**: 7.

164. Baker MD, Bostock H. The pH dependence of late sodium current in large sensory neurons. *Neuroscience* 1999; **92**(3): 1119-30.
165. Taddese A, Bean BP. Subthreshold sodium current from rapidly inactivating sodium channels drives spontaneous firing of tuberomammillary neurons. *Neuron* 2002; **33**(4): 587-600.
166. Tokuno HA, Kocsis JD, Waxman SG. Noninactivating, tetrodotoxin-sensitive Na+ conductance in peripheral axons. *Muscle Nerve* 2003; **28**(2): 212-7.
167. Agrawal N, Alonso A, Ragsdale DS. Increased persistent sodium currents in rat entorhinal cortex layer V neurons in a post-status epilepticus model of temporal lobe epilepsy. *Epilepsia* 2003; **44**(12): 1601-4.
168. Riva B, Dionisi M, Potenzieri A, et al. Oxaliplatin induces pH acidification in dorsal root ganglia neurons. *Sci Rep* 2018; **8**(1): 15084.
169. Miyake T, Nakamura S, Zhao M, et al. Cold sensitivity of TRPA1 is unveiled by the prolyl hydroxylation blockade-induced sensitization to ROS. *Nat Commun* 2016; **7**: 12840.
170. Wang YY, Chang RB, Liman ER. TRPA1 is a component of the nociceptive response to CO2. *J Neurosci* 2010; **30**(39): 12958-63.
171. Casey JR, Grinstein S, Orlowski J. Sensors and regulators of intracellular pH. *Nat Rev Mol Cell Biol* 2010; **11**(1): 50-61.
172. Stock C, Schwab A. Protons make tumor cells move like clockwork. *Pflugers Arch* 2009; **458**(5): 981-92.
173. Koyuncu I, Gonel A, Kocyigit A, Temiz E, Durgun M, Supuran CT. Selective inhibition of carbonic anhydrase-IX by sulphonamide derivatives induces pH and reactive oxygen species-mediated apoptosis in cervical cancer HeLa cells. *J Enzyme Inhib Med Chem* 2018; **33**(1): 1137-49.
174. Chen R, Zou Y, Mao D, et al. The general amino acid control pathway regulates mTOR and autophagy during serum/glutamine starvation. *J Cell Biol* 2014; **206**(2): 173-82.
175. Chiche J, Ilc K, Laferriere J, et al. Hypoxia-inducible carbonic anhydrase IX and XII promote tumor cell growth by counteracting acidosis through the regulation of the intracellular pH. *Cancer Res* 2009; **69**(1): 358-68.
176. Supuran CT, Alterio V, Di Fiore A, et al. Inhibition of carbonic anhydrase IX targets primary tumors, metastases, and cancer stem cells: Three for the price of one. *Med Res Rev* 2018; **38**(6): 1799-836.
177. Supuran CT. Inhibition of carbonic anhydrase IX as a novel anticancer mechanism. *World J Clin Oncol* 2012; **3**(7): 98-103.
178. McDonald PC, Winum JY, Supuran CT, Dedhar S. Recent developments in targeting carbonic anhydrase IX for cancer therapeutics. *Oncotarget* 2012; **3**(1): 84-97.
179. Ma B, Pan Y, Song Q, et al. The effect of topiramate on tumor-related angiogenesis and on the serum proteome of mice bearing Lewis lung carcinoma. *Eur J Pharmacol* 2011; **663**(1-3): 9-16.
180. Nilius B, Szallasi A. Transient receptor potential channels as drug targets: from the science of basic research to the art of medicine. *Pharmacol Rev* 2014; **66**(3): 676-814.
181. Marmiroli P, Cavaletti G, Carozzi V, Riva B, Lim D, Genazzani AA. Calcium-related neurotoxicity of oxaliplatin: understanding the mechanisms to drive therapy. *Curr Med Chem* 2015; **22**(32): 3682-94.
182. Jordan B, Jahn F, Beckmann J, Unverzagt S, Müller-Tidow C, Jordan K. Calcium and Magnesium Infusions for the Prevention of Oxaliplatin-Induced Peripheral Neurotoxicity: A Systematic Review. *Oncology* 2016; **90**(6): 299-306.
183. Loprinzi CL, Qin R, Dakhil SR, et al. Phase III randomized, placebo-controlled, double-blind study of intravenous calcium and magnesium to prevent oxaliplatin-induced sensory neurotoxicity (N08CB/Alliance). *J Clin Oncol* 2014; **32**(10): 997-1005.
184. Cavaletti G, Frigeni B, Lanzani F, et al. Chemotherapy-Induced Peripheral Neurotoxicity assessment: a critical revision of the currently available tools. *Eur J Cancer* 2010; **46**(3): 479-94.
185. Gewandter JS, Brell J, Cavaletti G, et al. Trial designs for chemotherapy-induced peripheral neuropathy prevention: ACTTION recommendations. *Neurology* 2018; **91**(9): 403-13.
186. Frigeni B, Piatti M, Lanzani F, et al. Chemotherapy-induced peripheral neurotoxicity can be misdiagnosed by the National Cancer Institute Common Toxicity scale. *J Peripher Nerv Syst* 2011; **16**(3): 228-36.
187. Deuis JR, Lim YL, Rodrigues de Sousa S, et al. Analgesic effects of clinically used compounds in novel mouse models of polyneuropathy induced by oxaliplatin and cisplatin. *Neuro Oncol* 2014; **16**(10): 1324-32.
188. Durand JP, Alexandre J, Guillevin L, Goldwasser F. Clinical activity of venlafaxine and topiramate against oxaliplatin-induced disabling permanent neuropathy. *Anticancer Drugs* 2005; **16**(5): 587-91.
189. Meregalli C, Carozzi VA, Sala B, et al. Bortezomib-induced peripheral neurotoxicity in human multiple myeloma-bearing mice. *J Biol Regul Homeost Agents* 2015; **29**(1): 115-24.

10 ACKNOWLEDGEMENTS

I thankfully acknowledge all precious contributions to the finalization of the whole project.

Drugs administration: University of Milano-Bicocca Experimental Neurology Unit (ENU) *in vivo* group (Annalisa Canta, PhD; Alessia Chiorazzi, PhD; Giulia Fumagalli, MSc; Cristina Meregalli, PhD; Laura Monza, MSc; Norberto Oggioni; Eleonora Pozzi, MSc).

Behavioral test execution: Annalisa Canta, PhD; Eleonora Pozzi, MSc.

Peripheral nerves and skin specimen harvesting: ENU *in vivo* group.

Peripheral nerves and skin specimen processing: ENU *histology* group (Elisa Ballarini, PhD; Virginia Rodriguez-Menendez, PhD; Mario Bossi).

Project revision and supervision: Professor G. Cavaletti, MD (Head of ENU).

Manuscript revision: Professor G. Cavaletti, MD (Head of ENU), Professor P. Marmiroli, MD (ENU).

NET analysis support: Professor H. Bostock, PhD (UCL, London).